Evaluations of synthetic glycolipid antigens (GGPLs and GGLs) towards diagnosis of Mycoplasma infectious diseases (MIDs)

July 2015

MENGFEI YUAN

Graduate School of

Advanced Integration Science

CHIBA UNIVERSITY

（千葉大学審査学位論文）

Evaluations of synthetic glycolipid antigens (GGPLs and GGLs) towards diagnosis of Mycoplasma infectious diseases (MIDs)

July 2015

MENGFEI YUAN

Graduate School of

Advanced Integration Science

CHIBA UNIVERSITY

Contents

Chapter 1 General Introduction

1-1 "Mycoplasma Infectious Diseases, MIDs"

Mycoplasmas, the smallest free-living organisms known, are prokaryotes that are bounded only by a plasma membrane. （**Figure 1-1**）. Their lack of a cell wall provides for direct and intimate contact of plasma membrane with the cell surface of the host cell. Therefore, under appropriate conditions, it may cause cell fusion and then infect host cell. （**Figure 1-2**）. This special structure is associated with cellular pleomorphism and resistance to cell wall-active antimicrobial agents such as penicillins and cephalosporins.. The organisms' small genomes limit biosynthesis and explain the difficulties encountered with *in vitro* cultivation.

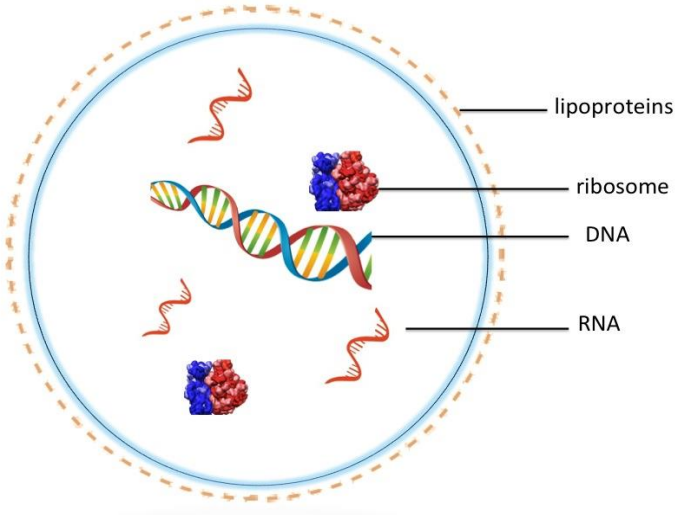

Figure 1-1. Mycoplasma is a "plasma"-like form without cell wall.

Mycoplasmas typically colonize mucosal surfaces of the respiratory and urogenital tracts of many animal species. Sixteen species of mycoplasmas have been recovered from human *M. pneumoniae* causes upper and lower respiratory infections. *M. genitalium* and *Ureaplasma urealyticum* are established causes of urethritis and have been implicated in other genital conditions[1].

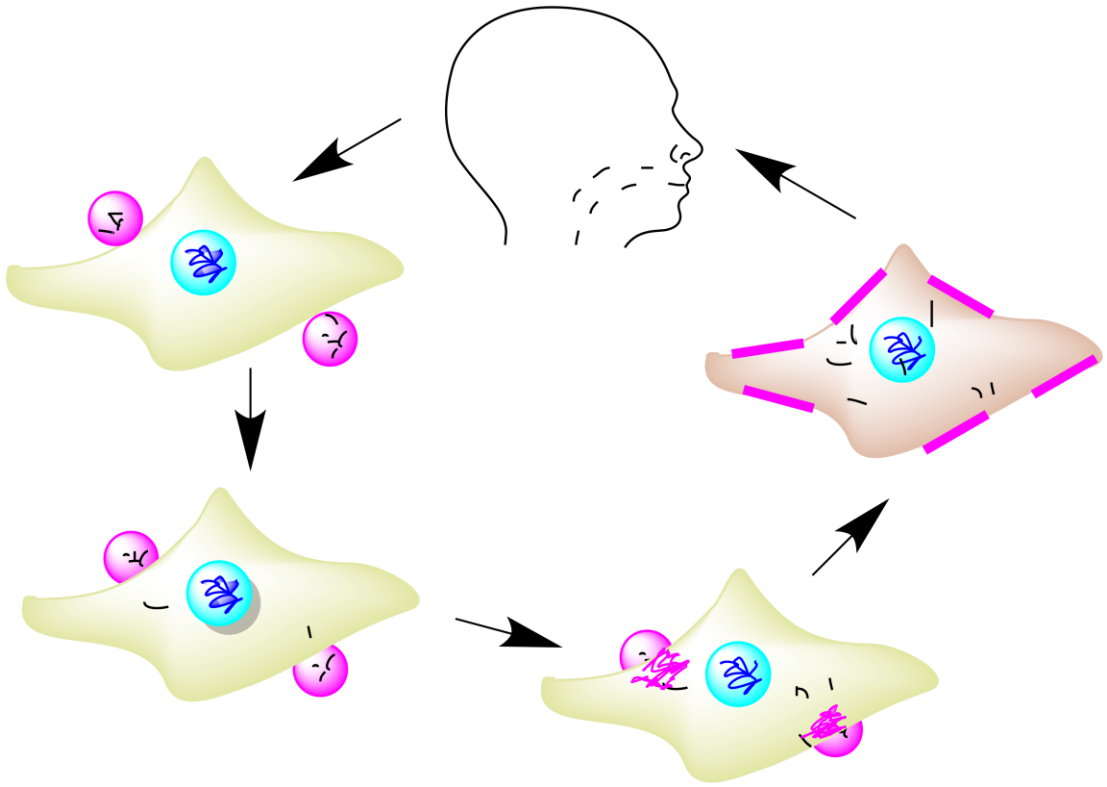

Figure 1-2. The fusion of mycoplasma with eukaryotic host cell and it may causes mycoplasma infectious diseases (MIDs) .

Mycoplasmas are well known as the pathogens of

mycoplasma pneumonia, and have also come to be recognized as causative bacterias in asthma, rheumatic diseases and neurological disorders [2-5]. Also it is suspected that mycoplasmas are related to atherosclerosis and tumours (including leukaemia) [6.7]. The concept of mycoplasma-caused infectious diseases has changed to include not only pneumonia but also other serious illness, now termed mycoplasma-related disorders.

Mycoplasma Infectious Diseases (MID) are systemic illnesses that cause vasculitis and neuritis. MID not only includes pneumonia but also diseases such as asthma, arthritis, nephritis, meningitis, encephalitis, dermatitis, pancreatitis, hepatitis, and hematologic illnesses. The broader concept of MID encompasses acute to chronic phases with diverse symptoms. Therefore, it is often confusing and difficult to identify Mycoplasma-infected patients among those with incurable diseases, such as autoimmune diseases, rheumatic diseases, nervous system disorders, and hematological disorders. (Table1-1)

In brief , it is confusing and difficult to identify the mycoplasma-infected patient among those of incurable diseases,

such as autoimmune diseases, a rheumatic disease, a nervous system disorder, and hematological disorders.

Therefore, it is important to know the cause of it as early as possible to avoid it. In the case of the new diagnostics for mycoplasma enable it to see the state of infection at the time of asymptomatic infection. Incubation periods can be decades before symptoms appear. It is very important issue, the control and prevention for infection from mothers to infants.

Table1-1. Species that infect humans and associated diseases

Species	Associated Diseases
M.amohoriforme	*Chronic bronchopneumonia*[8]
M. fermentans	*Respiratory, genital and rheumatoid diseases* [9] *and AIDs*[10]
M. genitalium	*Male urethritis*[10]
M. pirum	*Isolated from a few AIDs patients*[10]
M. pneumonia	*Subclinical infection, upper respiratory disease, bronchopneumonia*[10] *and central nervous system diseases*[11]
M. salivarium	*Periodontal diseases*[12]
M. hominis	*Genital infections in the adult*[13]

1-2 Antigenic properties of mycoplasma out-member

Mycoplasmas have surface antigens such as membrane proteins, lipoproteins, lipoglycans and glycolipids.(**Figure1-3**) Membrane proteins have several different topologies and perform a variety of fuctions vital to the survival of organism, such as relay signals between the cell's internal and external environments , oxidoreductase , transferase or allow cells to identify each other. Lipoproteins serve to emulsify the lipid molecules. Lipoglycans can determine cell-environment interactions.

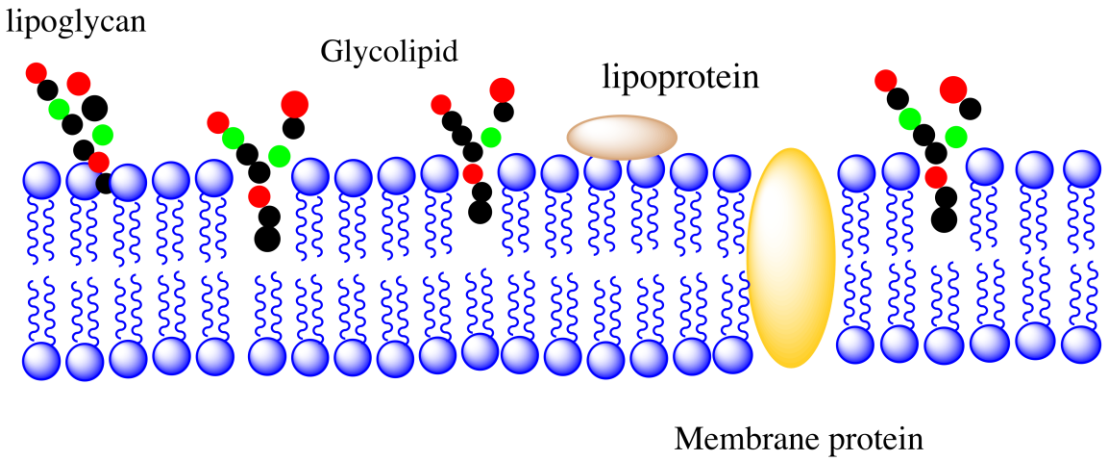

Figure1-3. Antigenic properties of Mycoplasma out-member

Glycolipids constitute a significant portion of membrane lipid in several mycoplasmas. Some studies had indicated that

monoglycosyldiacylglycerol and diglycosyldiacylglycerol are two majoy glycolipids on the surface of mycoplasma member, where their nonbilayer-bilayer balance contributes to membrane properties such as curvature and stability, as shown in *Acholeplasma laidlawii*, one of the best investigated bacteria with regard to the function of glycolipids in biological membranes. In addition, free glycoglycerolipids (GGLs) isolated form Mycoplasma out-member as structural elements play a fundamental role in membrane properties and stability. [14-16] GGLs are not only key structural components of the plasma membrane in mycoplasmas, but also active lipid components of M.*pneumoniae*. (**Figure 1-4**)

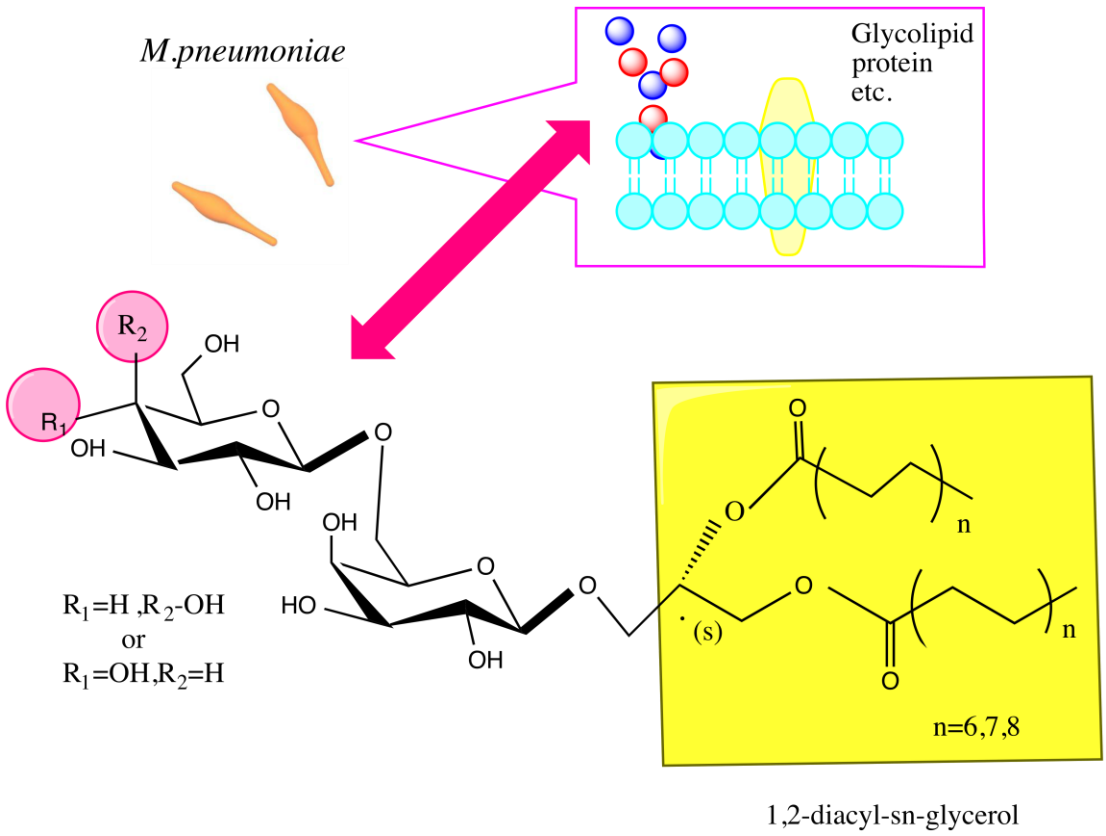

Figure 1-4. GGL glycolipid antigens isolated from *M.pneumoniae*

1-3 Glycolipids and Innate Immunity

Glycolipids are reported that they are closed related to immune responses. The human immune system is constantly exposed to a great variety of microorganisms and other antigenic substances. Microorganisms invading the body are attacked by primary immune responses (such as the complement system) or phagocytosis by macrophages or neutrophils.

Bacterial cell walls are major targets of host immune

responses. Lipids are major components of biomembranes. Microbial lipopolysaccharides are located on the surface of biomembranes and are important in the host recognition of microbial infections and subsequent immune responses.

Until recently, it had been the paradigm that T cells recognize peptide antigens that are presented by major histocompatibility complex (MHC) class I or I molecules. It has now been demonstrated that lipids can be presented by antigen -presenting cells (APC) through the CD1 family of molecules. The structures of the CD1 family of molecules are similar to those of MHC class I and II molecules.

Lipid and glycolipid antigens include naturally occurring foreign glycolipids from intracellular pathogens and synthetic glycolipids that are related in structure to mammalian glycolipids. The portals and pockets of CD1 antigen-binding grooves influence ligand specificity and facilitate presentation of a surprisingly diverse set of antigenic lipids, glycolipids, lipopeptides and even some small, non-lipidic molecules. Presentation of antigens by CD1 proteins requires uptake and intracellular processing by APCs. There is evidence for the existence of cellular pathways that lead to presentation of both

exogenous and endogenous lipid antigens. [17-19]

αGalCer-α-glycolipids have been identified and its commonly used form comprises an α-linked galactose head group and a ceramide base (consisting of an 18-carbon phyto-sphingosine chain and a 26-carbon acyl chain). Subsequently, hydrophobic tail of αGalCer was shown to bind to human and mouse CD1d and potently activate type I NKT cells. [20] In addition to this, hydrophilic head of glycolipids can be recognized by NKT cell and activate them to release Th1 and Th2 .(**Figure 1-5**)

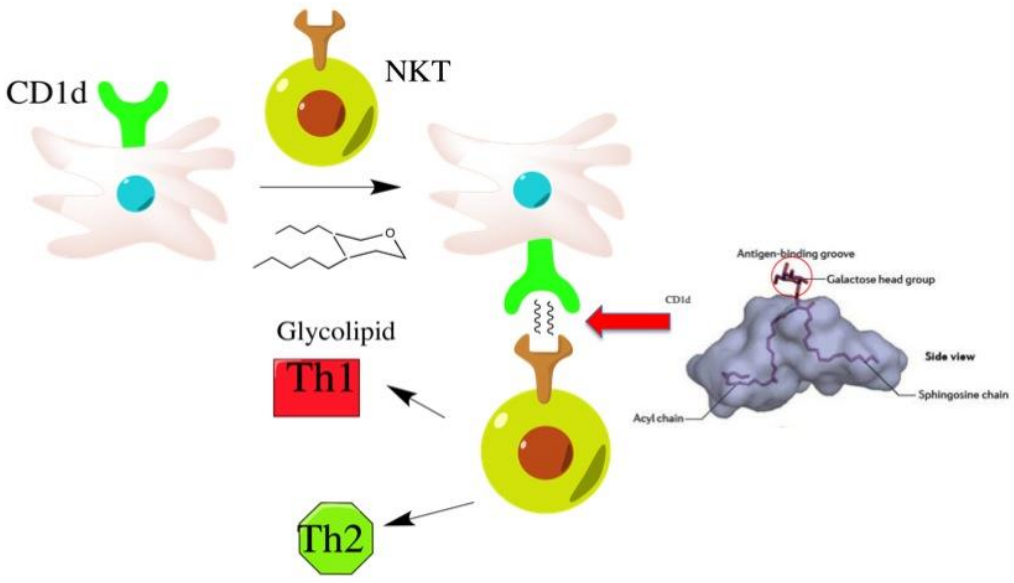

Figure 1-5. CD1d mediate glycolipids antigen (αGalCer) presentation.

1-4 Glycolipids and "MIDs"

It is thought that the lipid antigens of the cell membrane of mycoplasmas play an important role in the immune response, and that the cell membrane is in direct contact with the external world. The proteins and lipids of mycoplasma membranes are the main immunogens and antigens that are recognized by anti-mycoplasma sera. Both proteins and lipids play a major role in growth and metabolic inhibition tests for mycoplasmas. Glycolipids play a main role in the assay for the *M. pneumoniae* and *M. fermentans* complement binding assays. [21]

As a solution to the problem of a lack of antigen, small antigenic molecules of mycoplasmas have been found to be lipid-antigens. The structures of the mycoplasma lipid-antigens were then determined and chemically synthesized. *M. fermentans* has specific lipid-antigens called GGPL-I and GGPL-III, and *M. pneumoniae* also has specific lipid-antigen GGL moieties. [22-26] The complete structures of the immunodeterminants of glycolipid antigens have been determined using instrumental analyses including nuclear

magnetic resonance, mass spectrometry and chemical syntheses.

1-4.1 *M. fermentans* lipid-antigens phosphocholine-containing glycoglycerolipids (GGPLs)

Recently, evidence has accumulated that *M. fermentans* is a pathogen of rheumatoid arthritis (RA). *M. fermentans* has frequently been isolated from the synovial fluid of patients with rheumatoid arthritis, and exhibits agglutinating activity towards erythrocytes. Moreover, *M. fermentans* has been shown to induce experimental arthritis in rabbits following inoculation of the trachea and knee joint. [27]

GGPLs, which have strong antigenicity and are species-specific immunological determinants of *M. fermentan* [28], surprisingly have characteristic phosphocholine-containing glycoglycerolipids and can be clearly distinguished from other human related mycoplasma species through lipid analysis. Phylogenetic data strongly support the notion that mycoplasma species evolved from ancestors that are common to Gram-positive bacteria. This potential relationship suggests that it would be interesting to examine the distribution of GGPL

in other microorganisms, as these lipid antigens are synthesized with specific enzymes [29,30].

A monoclonal antibody that specifically recognizes GGPL-III could detect the existence of the GGPL-III antigens in synovial tissues from RA patients. GGPL-III antigens were detected in 38.1% (32/84) of RA synovial tissues, but not in osteoarthritis (OA) or normal synovial tissues[31]. Interestingly, GGPL-III antigens were detected on the surface of the endoplasmic reticulum by electron microscopic analysis in the GGPL-III antigen positive synovial tissue. Since it has been reported that lipid-antigens are presented by CD1 molecules through the endoplasmic reticulum, the mycoplasma lipid-antigen might be presented by such a mechanism.

1-4.2 *M.pneumoniae* lipid-antigens GGLs (GGL Gal-type and GGL Glc-type)

M. pneumoniae is a leading pathogen of both upper and lower human respiratory infections. Mycoplasma pneumonia, known as the cause of “primary atypical pneumonia”, is sometimes accompanied by other clinical syndromes:

Stevens-Johnson syndrome, nephritis (including IgA nephritis), autoimmune haemolytic anaemia, meningoencephalitis, GBS and acute psychosis. Cold agglutinin anti-I antibodies are found in the serum of as many as 70% of patients with mycoplasma pneumonia. The immunogenicity of *M. pneumoniae* is thought to be mainly due to membrane glycolipids. Mycoplasma lipid-antigens are useful biomarkers for induced levels of antibodies, and are superior in specificity and sensitivity to conventional biomarkers.

1-5 Purposes of this research

Today, diagnosis of mycoplasma infectous diseases（MIDs） is carried out by X-ray radiograph, culture, antigen-amplification(PCR), direct antigen detection by immunofluorescence or detection of cold agglutinin. However, there is no straightforward method that is valid at an early stage in infection and appearance of the pneumonia symptoms.

Among various mycoplasma surface antigens, glycolipid is closely related to pathology of mycoplasma. Just recently, Matsuda et al. [32].found out the presence of a pair of β-glycolipid

antigens in the cell-membrane components of the *M. pneumoniae*. One is β-D-galactopyranosyl-(1→6)-β-D -galactopyranoside (β-Gal-type**1**) and another β-D-glucopyranosyl -(1→6)-β- D-galactopyranoside(β-Glc-type**2**). Miyachi et al. [26] have already performed stereoselective syntheses of each β-glycolipid antigens. ($C_{16:0}$ fatty acid homologues)

Structural analysis of synthetic glycolipid antigens is critical for understanding the mechanisms of molecular interactions involved in the pathogenesis of immune abnormalities, and for devising strategies surrounding immune system regulation and drug discovery.

This study aims at developing an effective diagnostic methodology of mycoplasma infectious diseases (MIDs). Present study has already tried to utilize synthetic glycolipid antigens. In this thesis, two different species of mycoplasma synthetic glycolipid antigens have been chemically synthesized and fully characterized with proton NMR spectroscopy , respectively. Every diastereomeric proton (HproR and HproS protons) was discriminated and subjected to conformational analysis based on Karplus equations.

1-6 Synthesis of mycoplasma glycolipid antigens

Glycolipids are present in outer surface of plasma membrane in forms of either glycerolglycolipids or sphingoglycolipids. Glyceroglycolipids consist of a mono- or oligosaccharide moiety linked glycosidically to the hydroxyl group of glycerol. Sphingoglycolipids are formed by head group to ceramide. Glycolipids are amphiphilic, meaning they may serve as important building blocks of biomembranes. Natural glycolipids are lipids with a carbohydrate attached and usually occur as complex mixtures, so it is very difficult to separation of a homogeneous molecular species. Thus, chemical synthesis of glycolipids play an important role in study of their biological functions. Recently, a lots of synthetic studies are reported for glycolipids. Base on purpose of this study, syntheic mycoplasma glycolipid antigens have much attracted a strong attention.

Regarding chemical syntheses, for GGLs , it contains formation of glucose ,galatose and glycerols .(**Figure 1-6**) Miyachi et al. [31] have accomplished stereoselective synthesis *M. pneumoniae* β-glycolipids by using non-malodorous thio-glycosylation method. The synthetic products confirm the absolute stuctures of the natural products. (**Figure 1-7**)

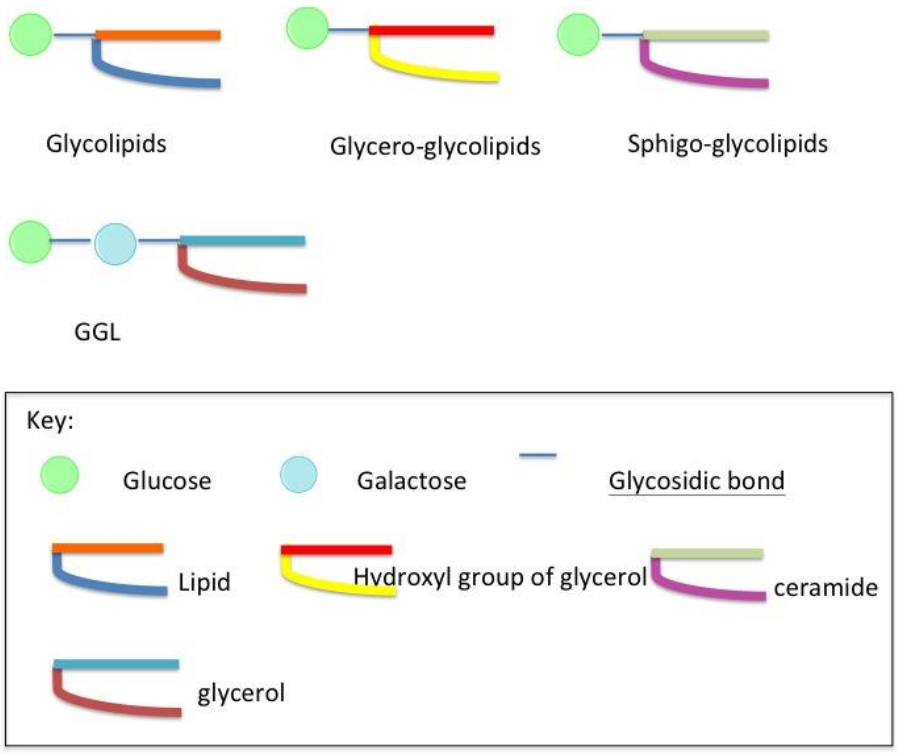

Figure 1-6. Synthesis of glycolipids starts with the different formations led to a glucose or galactose residue, respectively.

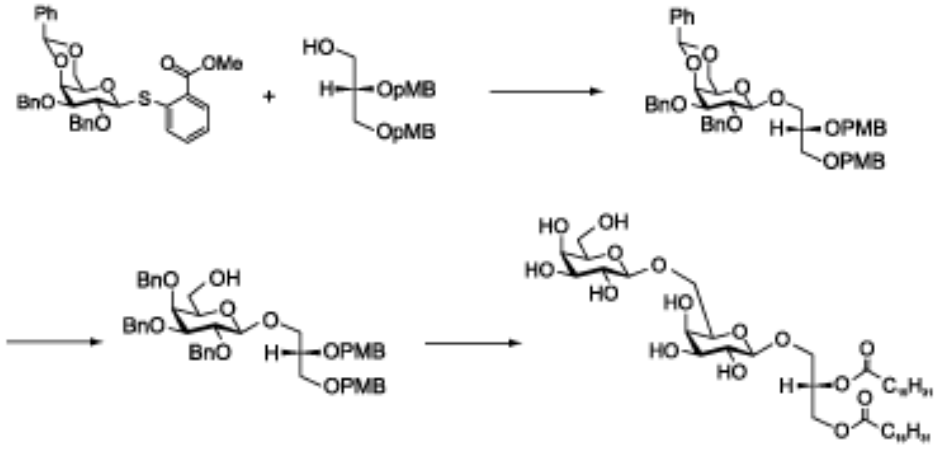

Figure 1-7. Synthesis *M. pneumoniae* β-glycolipids by using non-malodorous thio-glycosylation method.

1-7 Synthetic glycolipid antigens for diagnosis of MIDs by ELISA

Early diagnosis of *M.pneumonie* infection is important to prevent because of the appearance of antibiotics resistant mycoplasma, and also from the viewpoint of medical economics

New ELISA which utilize chemically synthesized mycoplasma species-specific lipid-antigen (anti- GGL Glc-type ELISAs) are superior to conventional methods.

In child patients, the anti-GGL Glc-type ELISA (IgM) is much more suitable for the rapid early diagnosis of M pneumoniae infection than currently available conventional serological methods, and also anti-GGL Glc-type ELISA (IgG) reflect the status of infection.

In adult patients, the anti-GGL Glc-type ELISAs (IgM /IgG/IgA) are available to diagnose *M. pneumoniae* infection suitable for the early diagnosis of *M.pneumoniae* infection and follow the clinical course quantitatively

The anti-GGL Glc-type ELISAs enable the studies for the links to chronic diseases, extrapulmonary diseases, and possibly

M. pneumoniae infection-related disease, such as asthma rheumatoid arthritis.

1-8 Summary of this thesis

Anti-lipid antigen antibodies are specific and quantitative markers of mycoplasma infection. Mycoplasma infected and non-infected patients among each disordes, such as asthma, multiple sclerosis, could be selected , and estimated the effect of each drug. Mycoplasma lipid-antigens are a useful tool for the understanding molecular mechanism of chronic inflammatory diseases, and for devising strategies for regulation of the immune system and for drug discovery.

In chapter 2 described a practical synthetic pathway to GGPL-I homologue ($C_{16:0}$) and its diastereomer, in which our one-pot α-glycosylation method was effectively applied. A common conformational property of GGPL-I and DPPC. The tail lipid moiety favors two *gauche* conformers of *gt* and *gg* (*gt* > *gg* >> *tg*), while the head moiety takes three conformers in averaged populations (*gt* = *gg* = *tg*).

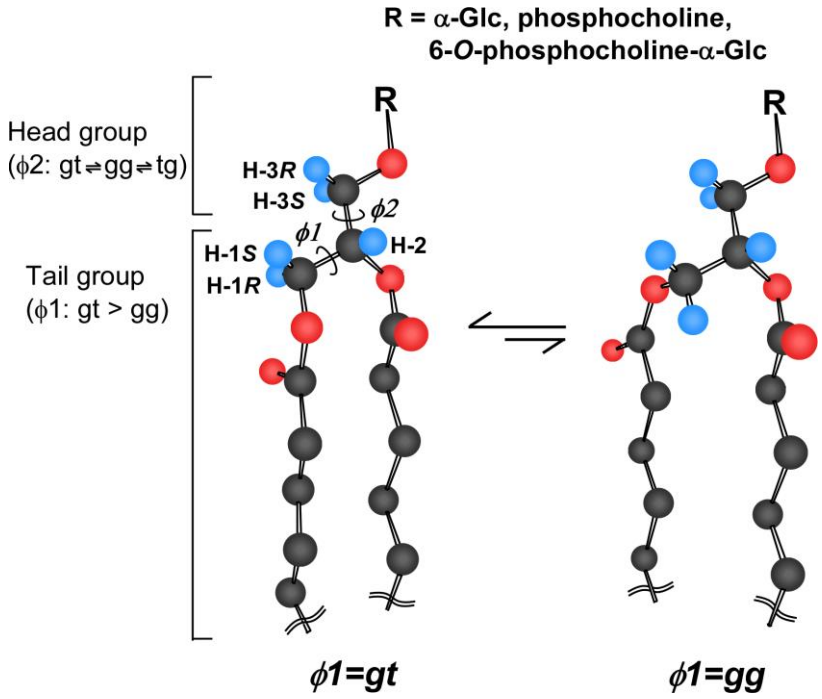

In chapter 3 described comparative analyses of helical property in asymmetric 1,2-di-O-acyl-sn-glycerols by means of ^{1}H NMR and circular dichroic (CD) spectroscopy: Notable effects of substituting groups at sn-3 position.

In chapter 4 described a conformational analysis for a series of 1,2-di-*O*-palmitoyl-*sn*-glycerols carrying different functional groups at the *sn*-3 position.

1-9 References and Notes

1.Haggerty CL. *Curr Opin Infect Dis.* 2008, 21: 65-69.

2.K.B. Waites, D.F. Talkington. *Clin. Microbiol. Rev.* **2004,**17 : 697-728.

3.Atkinson TP, Duffy LB, Pendley D, Dai Y, Cassell GH. *Allergy Asthma Proc* .**2009**,30: 158-165.

4.Gil C, Rivera A, Bañuelos D, Salinas S, García-Latorre E, Cedillo L. *BMC Musculoskelet Disord* .**2009**,10: 97-114.

5.Y. Kawahito, S. Ichinose, H. Sano, Y. Tsubouchi, M. Kohno, T. Yoswhikawa, D. Tokunaga, T. Hojo, R.Harawsawa, T. Nakano, K. Matsuda. *Biophys. Res. Com.* **2008**,369 : 561-566 .

6.Alviar CL, Echeverri JG, Jaramillo NI, Figueroa CJ, Cordova JP, Korniyenko A, Suh J, Paniz-Mondolfi A.*Med Hypotheses* **2011**,76: 517-521,.

7.Nussinovitch U. *Isr Med Assoc J* **2010**,12: 439-440.

8.Pitcher DG1, Windsor D, Windsor H, Bradbury JM, Yavari C, Jensen JS, Ling C, Webster D. *Int J Syst Evol Microbiol.* **2005**,Nov;55(Pt 6):2589-94.

9.Yáñez A1, Martínez-Ramos A, Calixto T, González-Matus FJ, Rivera-Tapia JA, Giono S, Gil C, Cedillo L.*BMC Res* Notes. **2013** Jan 8;6:9.

doi: 10.1186/1756-0500-6-9.

10. Shmuel Razin. *Medical Microbiology. 4th edition,* **1996.**

11. Daxboeck F. *Curr Opin Neurol.* **2006** Aug; 19(4):374-8,

12. Forest N. *J Biol Buccale*. 1979Dec;7(4):321-30.

13. Andres Pascual，Marie-Helene Perez, Katia Jaton, Gaudenz Hafen, Stefano Di Bernardo, Jacques Cotting, Gilbert Greub and Bernard Vaudaux，*BMC Infectious Diseases* **2010**, **10**:335

14. Lindblom G, Brentel I, Sjölund M, Wikander G, Wieslander. *Biochemistry* .1986 ,25: 7502-7510.

15.Dahlqvist A, Nordström S, Karlsson OP, Mannock DA, McElhaney RN et al. *Biochemistry.***1995** 34: 13381-13389.

16.Vikström S, Li L, Karlsson OP, Wieslander A . *Biochemistry* .**1999**,38: 5511-5520.

17. Bricard G, Porcelli SA. *Cell Mol Life Sci* . **2007**,64:1824-1840.

18. Salio M, Silk JD, Cerundolo V. *Opin Immunol*. **2010 Feb**; 22(1):81-8.

19. Cohen NR, Garg S, Brenner MB , *Adv Immunol.* **2009,** 102: 1-94.

20. Jamie Rossjohn, Daniel G. Pellicci, Onisha Patel, Laurent Gapin and Dale I. Godfrey，*Immunology*，**2012**,12：845-855

21. Razin S, Prescott B, James WD, Caldes G, Valdesuso J, Chanock RM. *Infect Immun*. **1971** Mar; 3(3):420-3.

22 Matsuda K, Kasama T, Ishizuka , Handa S, Yamamoto N, Taki T. *J Biol Chem*. **1994** Dec 30;269(52):33123-8.

23. Matsuda K, Ishizuka I, Kasama T, Handa S, Yamamoto N, Taki T.*Biochim Biophys Acta*. **1997** Nov 8;1349(1):1-12.

24. Nishida .Y, Ohrui .H et al, *Tetrahedron Lett.***1994,**35, 5465.

25. Nishida.Y, Ohrui .Het al., *Tetrahedron Lett.*, **1999,**40, 2371-2374.

26. Miyachi. A., Dohi. H. Matsuda.K, Nishida. Y, *Carbohydr Res*. **2009** Jan, 5;344(1):36-43.

27. Rivera A, Yáñez A, León-Tello G, Gil C, Giono S, Barba E, Cedillo L.*BMC Musculoskelet Disord*. **2002** Jun ,3;3:15.

28. Matsuda K1, Li JL, Harasawa R, Yamamoto N. *Biochem Biophys Res Commun*. **1997** Apr 28;233(3):644-9.

29. M. Fujiwara, N Ishida, K. Asano, K. Matsuda, N. Nomura, Y. Nishida, R. Harasawa. *J. Vet. Med. Sci.* 2010,72: 805–808 .

30. N. Ishida, D. Irikura, K. Matsuda, S. Sato, T. Sone, M. Tanaka, K. Asano. *Curr.Microbiol*. **2009**,58: 535–540.

31. Kawahito Y, Ichinose S, Sano H, Tsubouchi Y, Kohno M, Yoshikawa T, Tokunaga D, Hojo T, Harasawa R, Nakano T, Matsuda K. *Biochem Biophys Res Commun*. 2008 May 2; 369 (2):561-6.

32. Matsuda, K., Tadano-Aritomi, K., Ide-Tanaka, N., Tomiyama, T., Harasawa, R., Shingu, Y., Morita, D., Kusunoki, S. *Jap. J. Mycoplasmology* 2007.

Chapter2

Study on stereochemistry of synthetic *M. fermentans* α-glycolipid antigens (GGPLs)

2-1 Introduction

Mycoplasmas constitute a family of gram-positive microbes lacking rigid cell walls. They are suspected to associate with human immune diseases in either direct or indirect ways, though the molecular mechanism is not fully understood[1]. In recent biochemical studies, *Mycoplasma* outer-membrane lipoproteins[2,3] and glycolipids[4-6] are thought to serve not only as the main antigens but also as probable pathogens. Also in our research team, Matsuda *et al.* [7-10] has isolated a new class of α-glycolipid antigens (GGPL-I and GGPL-III, **Figure 2-1**) from *M. fermentans*. Another α-glycolipid (Mf GL-II), which has a chemical structure very close to GGPL-III, was identified and characterized by other groups [12-14].

Absolute chemical structures of GGPL-I [15] and GGPL–III [16] have already been established by chemical syntheses of stereoisomers; these α-glycolipids have a common chemical backbone of 3-*O*-(α-D-glucopyranosyl) -*sn*-glycerol carrying phosphophocholine at the sugar primary (6-OH) position. The fatty acids at the glycerol moiety are saturated [palmitic acid ($C_{16:0}$) and stearic acid ($C_{18:0}$)]. GGPL-I has a structural feature.

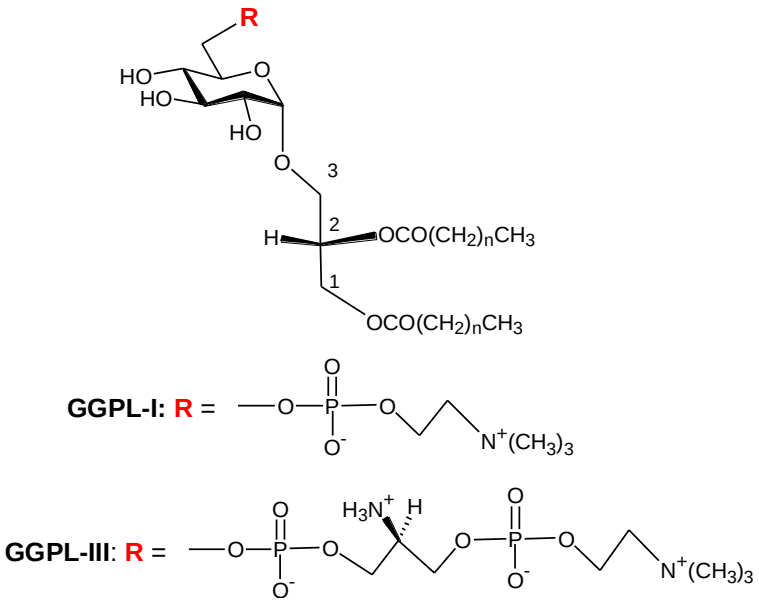

Figure 2-1: Absolute chemical structures of *M. fermentans* α-glycolipid antigens, GGPL-I and GGPl-III (GGPL: Glycosyl-*sn*-glycerophospholipid).

analogous to 1,2-di-*O*-palmitoyl phosphatidylcholine (DPPC) as a ubiquitous cell membrane phospholipid. Apparently, GGPLs are of amphiphilic compounds which can form certain self-assembled structures under physiological conditions[12,13] and may give physicochemical stress on the host immune cell systems [17]. Actually, our research team has proven that these α-glycolipid antigens have certain pathogenic functions[18,19].

In order to exploit their biological functions in detail, it is necessary to obtain these α-glycolipids in sufficient amounts. Thus, both genetic [20-22] and chemical synthetic approaches [23,24] are being undertaken, whereas no practical way has been established yet. In this paper, we report a chemical access to both natural GGPL-I homologue ($C_{16:0}$) and its diastereomer (**I-a**

and **I-b** in **Scheme2-1**), in which our one-pot α-glycosylation methodology [25,26] is effectively applied. The two GGPL-I isomers prepared thereby were characterized with ^{1}H NMR spectroscopy in terms of configuration and conformation at the asymmetric glycerol moiety.

2-2 Result and Discussion

A practical synthetic access to GGPL-I homologues

GGPL-I provides two key asymmetric centers to be controlled literally in the synthetic pathway. One is the configuration at the chiral glycerol moiety, and another is the sugar α-glycoside linkage. In former synthetic works on 3-*O*-(α-D-glycopyranosyl)-*sn*-glycerol [27-30], chiral 1,2-*O*-isopropylidene-*sn*-glycerol is often employed [29,30] as the acceptor substrate of different α-glycosylation reactions. In this case, however, an attention should be paid to the acid catalyzed migration of the dimethylketal group [23,29,30,31]. In our synthetic pathway, chiral (*S*)- or (*R*)-glycidol is employed as an alternative source of the chiral glycerol to circumvent this problem.

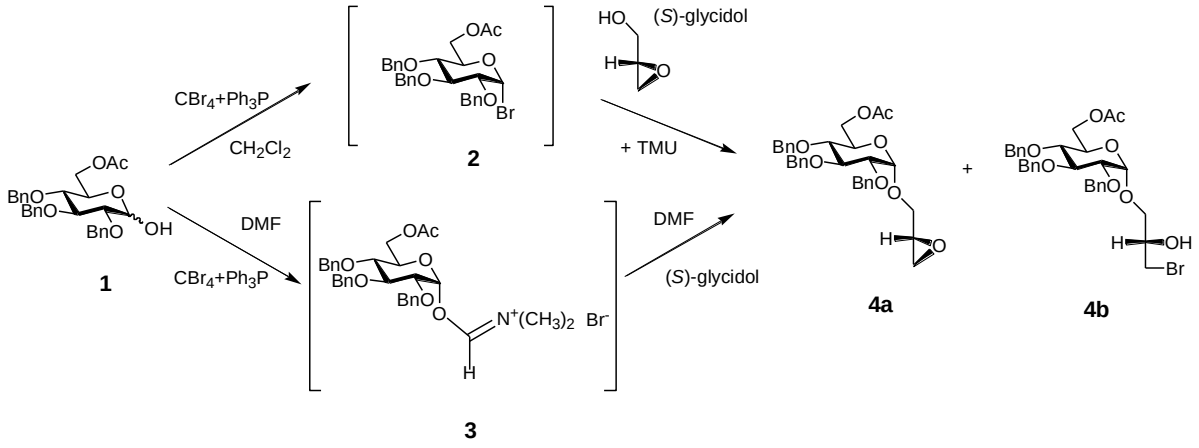

Scheme 2-1. An established synthetic pathway to □-glycosyl-*sn*-glycerols 4a and 5a. A reagent combination of CBr_4 and Ph_3P (Appel-Lee reagent) is utilized in either CH_2Cl_2 or DMF solvent.

In an established synthetic approach, 6-*O*-acetyl-2,3,4-tri-*O*-benzyl protected sugar **1** [23] is used as the donor and treated with a reagent combination of CBr_4 and Ph_3P (Appel-Lee reagent) in either CH_2Cl_2 or DMF solvent (or their mixture). For the reaction in CH_2Cl_2, *N,N,N',N'*-tetramethylurea (TMU) is added after *in situ* formation of α-glycosyl bromide **2** which equilibrates with a more reactive β-glycosyl bromide species [32]. In the pathway using DMF, the α-glycosylation is routed by α-glycosyl cationic imidate **3** which was predicted in formers studies [33] and evidenced in our preceding NMR and MS study [25,26].

The reaction between **1** and (*S*)-glycidol in CH_2Cl_2 (+TMU) gave a mixture of epoxy compound **4a** (60~70%) and bromide **5a** (30-40%). In **5a**, the oxirane ring was opened by nucleophilic Br^- ions produced by Ph_3P and CBr_4. Also in the DMF-promoted reaction, a mixture of **4a** (70~90%) and **5a**

(10~30%) was derived. In both reaction pathways, however, the glycosylation was α-selective (α:β = >90:10, yields >80%) and not accompanied by isomerization at the glycerol moiety.

A mixture of **4a** and **5a** was used in the following chemical transformation (**Scheme 2**). First, a *lyso*-glycolipid **6a** was derived after de-protection at the sugar hydroxymethyl position and S_N2 substitution with cesium palmitate at the glycerol *sn*-1 position. Then, this compound was converted to glycolipid **8a** after the sequential reactions of temporary protection at the sugar primary position with *t*-butyldimethylsilyl group (TBDMS), *O*-acylation at the glycerol 2-OH position to give **7a**, and then removal of the TBDMS group.

For introducing phosphocholine group at the sugar 6-OH position, we employed a phosphoroamidite method using 1*H*-tetrazole as promoter[34]. First, **8a** was treated with 2-cyanoethyl-*N,N,N',N'*-tetraisopropyl phosphorodiamidite in the presence of 1*H*-tetrazole and then with choline tosylate to give **9a**. After de-protection of the sugar *O*-benzyl group by catalytic hydrogenolysis, GGPL-I homologue **I-a** was obtained. In the same way, the GGPL-I *sn*-isomer **I-b** was derived from a mixture of **4b** and **5b** available in the reaction between **1** and (*R*)-glycidol (**Schemes 2-1 and 2-2b**).

Scheme2-2: Syntheses of GGPL-I homologue I-a and its isomer I-b. Conditions: Conditions: a) K_2CO_3, CH_3OH; b) cesium palmitate in DMF; c) TBDMS chloride then palmitoyl chloride in pyridine + DMAP; d) TFA in CH_3OH; e) i) 2-cyanoethyl-*N,N,N',N'*-tetraisopropyl phosphorodiamidite, *1H*-tetrazole and MS-4A in CH_2Cl_2; ii) choline tosylate, 1*H*-tetrazole, iii) mCPBA, iv) aq. NH_3 in CH_3OH, f) H_2, $Pd(OH)_2/C$ in CH_3OH.

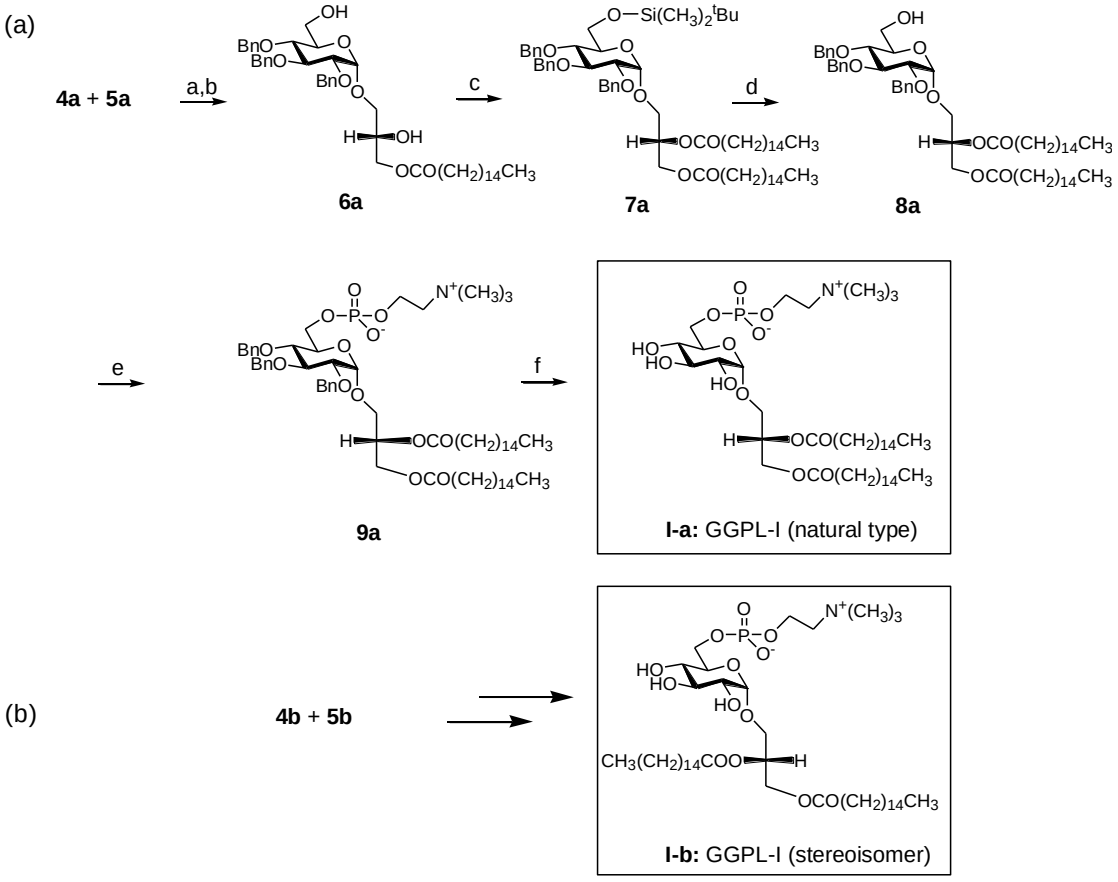

^{1}H NMR characterization of I-a, I-b and the related glycerolipids

^{1}H NMR spectroscopy provides a useful tool for discriminating between the two GGPL-I isomers as shown in **Figure 2**: A clear difference was observed in chemical shifts of glycerol methylene protons as designated with "**a**" and "**b**". Conversely, little difference was observed

between the *sn*-isomers at the sugar H-1 signal as well as at the glycerol H-2 (**Table 2-1**). Natural GGPL-I and GGPL-III gave ^{1}H NMR data very close to those of **I-a**, indicating that both have a common skeleton of 3-*O*-(α-D-glucopyranosyl)-*sn*-glycerol [15,16].

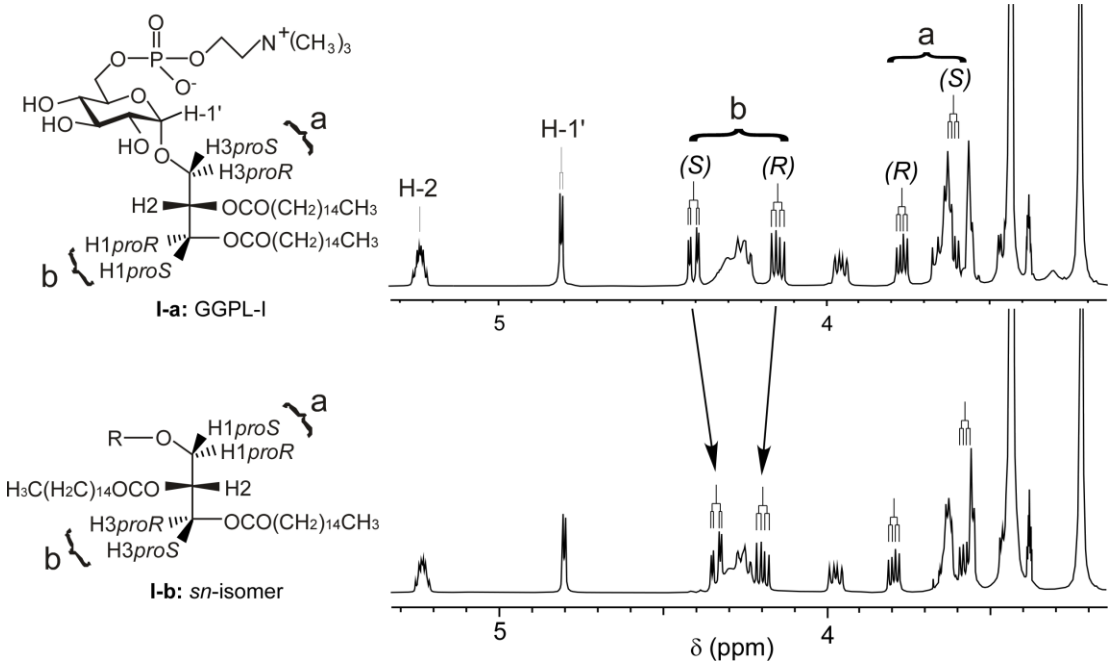

Figure2-2: ^{1}H-NMR spectra of I-a and I-b (500MHz, 25℃, $CDCl_3$:CD_3OD=10:1).

Assignment of *sn*-glycerol methylene protons (H_{proR} and H_{proS}) was performed on the basis of our preceding studies on deuterium-labeled glycerols [35-37] and □(1-6)-linked disaccharides[38-40]

Table2-1. ^{1}H-NMR data (500MHz) of I-a, I-b, and their precursors (9a and 9b).

Comp.	δppm (^{3}J and ^{2}JHz)					
	glucose	*sn*-glycerol moiety				
	H-1'	H-1		H-2	H-3	
		proR	*proS*		proR	*proS*
I-a	4.80 (3.5)	4.14 (6.5)	4.40 (3.5,12.0)	5.24	3.76 (5.5)	3.61 (5.5,11.0)
9a	4.70 (3.5)	4.17 (6.5)	4.38 (3.0,12.0)	5.22	3.72 (5.5)	3.52 (6.0,11.0)
I-b	4.80 (3.5)	3.80 (6.0)	3.57 (5.5,11.0)	5.23	4.34 (3.5)	4.20 (6.5,12.0)
9b	4.74 (3.5)	3.76 (5.5)	3.57 (5.5,11.0)	5.23	4.37 (3.0)	4.19 (6.5,12.0)

These α-glycolipids were dissolved in a mixture of $CDCl_3$ and CD_3OD (10:1) at 11.2mM concentration.

The glycerol moiety has two C-C single bonds. By free rotation, each of them is allowed to have three staggered conformers of *gg* (*gauche-gauche*), *gt* (*gauche-trans*) and *tg* (*trans-gauche*) (**Figure 2-3**). In solution and also in self-contacting liquid crystalline states, these conformers are thought to equilibrate each other. In this study, we calculated time-averaged populations of the three conformers by means of ^{1}H NMR spectroscopy. As we reported in a preceding paper [41], the Karplus-type equation proposed

by Haasnoot *et al.*[42] was adapted for the formulation of *Equation-1*:

Equation-1

$$2.8gg + 3.1gt + 10.7tg = {}^{3}J_{H2,H1S} \quad (\text{or} \quad {}^{3}J_{H2,H3R})$$

$$0.9gg + 10.7gt + 5.0tg = {}^{3}J_{H2,H1R} \quad (\text{or } {}^{3}J_{H2,H3S})$$

$$gg + gt + tg = 1$$

In this equation, a perfect staggering ($\phi 1$ and $\phi 2$ = +60, -60 or 180 degree) is assumed for every conformer. **Figure 3** summarizes the results for a series of 3-substituted 1,2-di-*O*-palmitoyl-*sn*-glycerols, which involve tripalmitin (entry 1), DPPC (1,2-di-*O*-palmitoylphosphatidylcholine) (entry 2), and GGPL-I homologues (entries 3-5). In a solution state using a mixture of $CDCl_3$ and CD_3OD (10:1) as the solvent and concentration at 11.2mM, tripalmitin adopts the three conformers in ratio of *gt*(45%), *gg*(37%) and *tg*(17%). In comparison with this symmetric lipid, the asymmetric phospholipid (DPPC) favors *gt*-conformer more strongly around the tail lipid moiety along *sn*-1,2 position, while disfavoring *tg*-conformer in the ratio of *gt*(59%), *gg*(34%) and *tg*(7%). The head phosphate moiety along *sn*-2,3 position adopts the three conformers in averaged populations (*gg*=*gt*=*tg*).

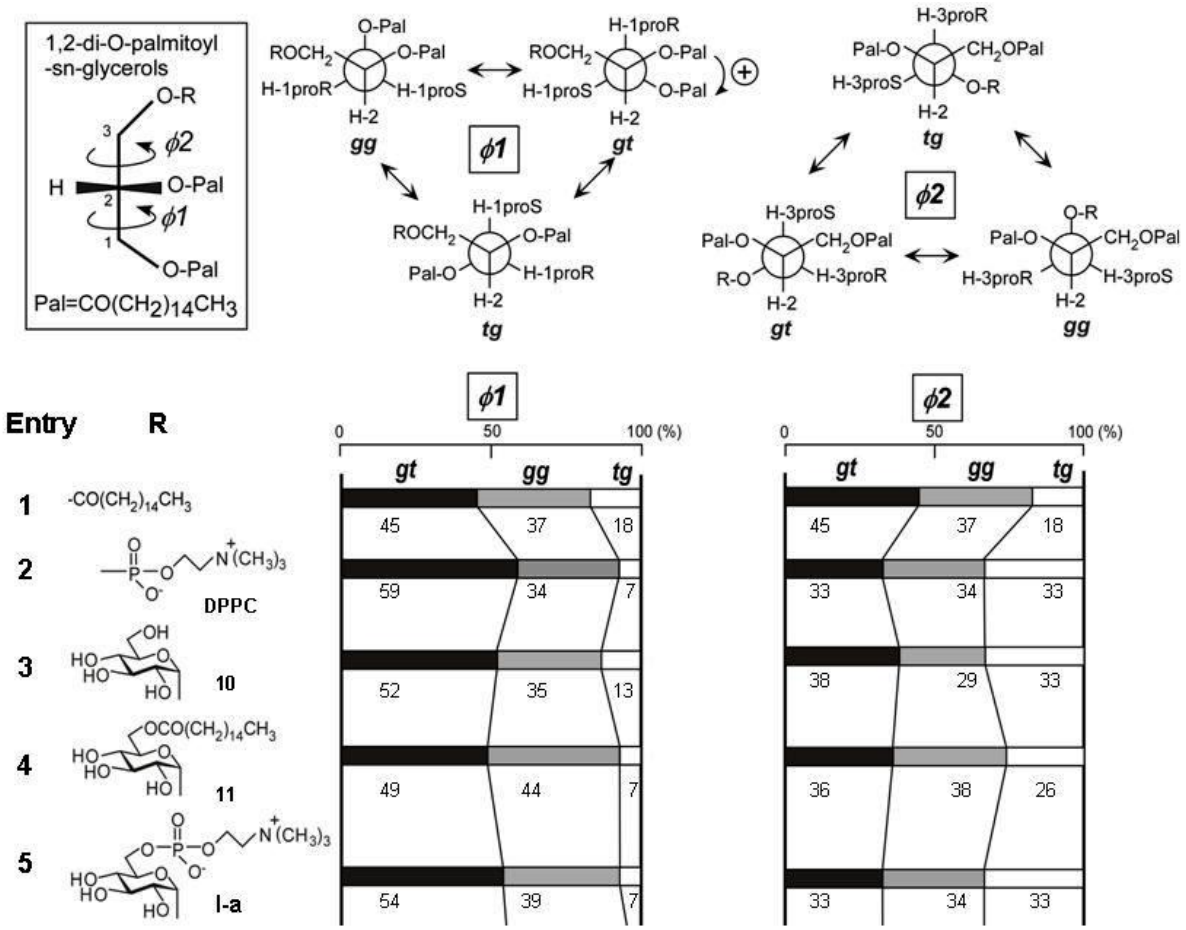

Figure 2-3. Distributions of *gg*, *gt* and *tg*-conformers in 3-substituted *sn*-glycerols at 11 mM solutions in $CDCl_3$ and CD_3OD (10:1) at 298K.

3-*O*-(α-D-glucopyranosyl)-*sn*-glycerolipids **10** and **11** (entries 3 and 4) were found to have a conformational property very similar to DPPC; the lipid tail moiety prefers the *gauche* conformations (*gt* and *gg*), while the sugar moiety allows a random conformation. Here, it should be mentioned that the conformer distribution coincidences between **I-a** (entry 5) and DPPC (entry 1) at the tail moiety [*gt*(33%), *gg*(34%) and *tg*(33%)].

The above analysis was carried out also for the stereoisomer **I-b** and

the related glycolipids (entries 6-8, **Figure 2-4**). The isomer (entry 8) showed an overall conformational property similar to **I-a** and DPPC, though a small difference was observed in the conformer distribution at the sugar head moiety. However, it should be recognized here that the helical direction (helicity) of *gt* conformer in **I-b** is reversed (anti-clockwise) from the case of DPPC and GGPL-I (clockwise) as depicted in **Figures 3** and **5**.

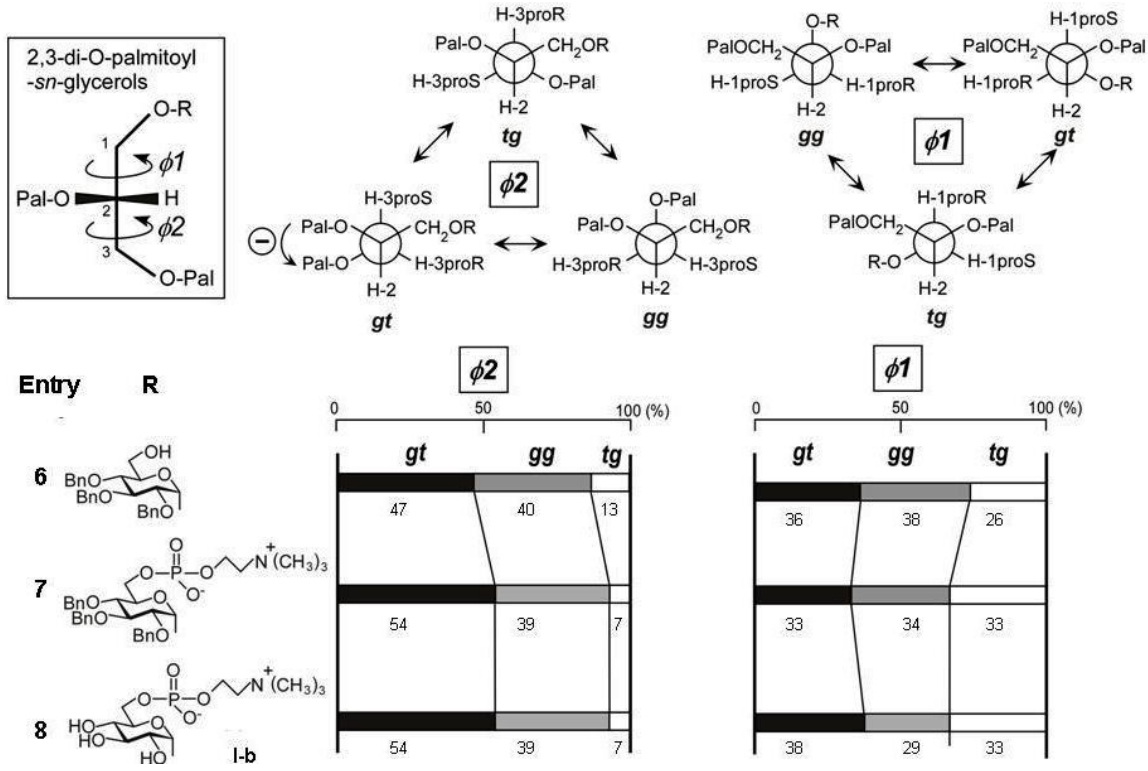

Figure 2-4. Distributions of *gg*, *gt* and *tg*-conformers in 1-substituted *sn*-glycerols. In these *sn*-isomers, ϕ1 and ϕ2 represent dihedral angles around C-C single bond at the glycerol *sn*-2,3 and 1,2 position, respectively.

2-3 Conclusion

We have proposed an established synthetic pathway to GGPL-I homologue and its stereoisomer, in which our one-pot α-glycosylation methodology was effectively applied. We envisage that the simple method will allow us to prepare a variety of α-glycolipid antigens other than GGPLs and prove their biological significance [43]. By the ^{1}H NMR conformational analysis, which was based on our former studies on deuterium-labeled *sn*-glycerols and sugars, we have proven that GGPL-I and other 3-*O*-(α-D-glucopyranosyl)-*sn*-glycerolipids have a common conformational property at the chiral glycerol moiety: The lipid tail moiety prefers two *gauche*-conformations (*gg* and *gt*) in the order as *gt* > *gg* >> *tg*; while the sugar head moiety adopts three conformers in an averaged population (*gg*=*gt*=*tg*). At the lipid tail position, the *gt*-conformer with clock-wise helicity is predominated over the anti-clockwise *gg*-conformer. The observed conformation was very close to what we have seen in DPPC (**Figure 2-5**). Although these results were based on the solution state in a solvent mixture of $CHCl_3$ and CH_3OH (10:1), it may be possible to assume that the Mycoplasma GGPLs and the related 3-*O*-(α-D-glycopyranosyl)-*sn*-glycerolipids can constitute cytoplasm membranes in good cooperation with ubiquitous phospholipids without

inducing stereochemical stress at the membrane.

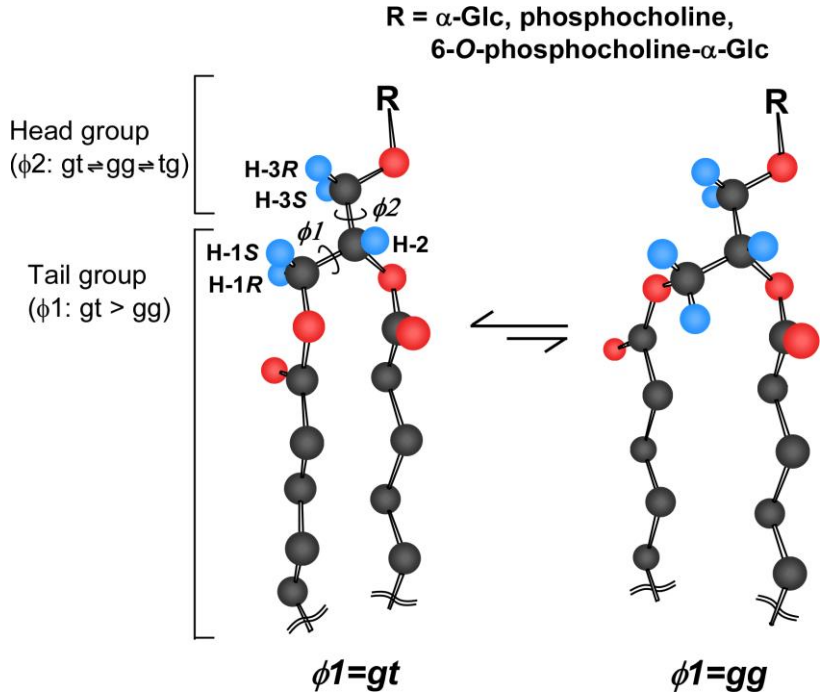

Figure 2-5. A common conformational property of GGPL-I and DPPC. The tail lipid moiety favors two *gauche* conformers of *gt* and *gg* (*gt* > *gg* >> *tg*), while the head moiety takes three conformers in averaged populations (*gt* = *gg* = *tg*).

The GGPL-I isomer (**I-b**) showed an overall conformational property similar to the natural isomer (**I-a**) and DPPC. However, it should be mentioned here that the chiral helicity of *gt* conformers in **I-b** is reversed (anti-clockwise) from the clockwise helicity of DPPC and GGPL-I. The difference in chirality seems critical in biological recognition events and also in physicochemical contact with other chiral constituents in cell membranes [44,45].

2-4 Experimental Section

General Methods

Infrared (IR) spectra were recorded on a JASCO FT/IR-230 Fourier transform infrared spectrometer on the form of KBr disks. All ^1H NMR (500 MHz) spectra were recorded using Varian INOVA-500 or Varian Gemini 200. ^1H chemical shifts are expressed in parts per million (δ ppm) by using an internal standard of tetramethylsilane (TMS = 0.000 ppm). Mass spectra were recorded with a JEOL JMS 700 spectrometer for fast atom bombardment (FAB) spectra. Silica gel column chromatography was performed on silica gel 60 (Merck 0.063-0.200 mm and 0.040-0.063 mm) and eluted with a mixture of toluene and ethyl acetate or a mixture of $CHCl_3$ and CH_3OH in gradient modes (100:0 to 80:20). For purification of phosphocholine containing products, a column chromatography packed with Iatrobeads (IATRON LABORATORIES INC., 6RS-8060) was applied and euluted with a mixture of CH_3OH and $CHCl_3$ in gradient modes. For thin layer chromatography (TLC) analysis, Merck pre-coated TLC plates (silica gel 60 F_{254}, layer thickness 0.25mm) and Merck TLC aluminum roles (silica gel 60 F_{254}, layer thickness 0.2mm) were used. All other chemicals were purchased from Tokyo Kasei Kogyo Co., Ltd., Kishida

Chemical Co., Ltd., and Sigma Aldrich Chemical Company Co, Int., and were used without further purification.

A typical procedure for the one-pot α-glycosylation: CBr_4 (1.6 g, 6.09 mmol) and Ph_3P (2.02 g, 6.09 mmol) were added to a solution of 6-*O*-acetyl-2,3,4-tri-*O*-benzyl-D-glucose**1** (1.0 g, 2.03 mmol) in 10 mL of DMF and stirred for 3 h at room temperature. Then, (*S*)-glycidol (301 mg, 4.06 mmol) was added to the reaction mixture and stirred for 14 h at room temperature. Products were diluted with a mixture of toluene and ethyl acetate (10:1), and the solution washed with saturated aq. $NaHCO_3$ and aq. NaCl solution, dried and concentrated. The residue was purified by silica gel column chromatography in toluene and ethyl acetate to give a mixture of **4a** and **5a** (the ratio changed with reaction time) as colorless syrup. The total yield of **4a** and **5**a was between 80% and 90%.

3-*O*-(2,3,4-tri-*O*-benzyl-α-D-glucopyranosyl)-1,2-di-*O*-palmitoyl-*sn*-glycerols (8a and 8b): K_2CO_3 (379mg, 2.74 mmol) was added to the mixture of **4a** and **5a** (1 g, 1.83 mmol based on **4a**) in CH_3OH (20 mL) and stirred for 1 h at room temperature. The reaction mixture was neutralized, washed with water, dried, and concentrated. The residue was dried under diminished pressure and subjected to the next reaction. A mixture of the crude residue **6a** and cesium palmitate (2.7 g, 7.3 mmol) in DMF (40 mL) was heated at

100~110 ˚C, to which the DMF solution of the residue was added slowly. The reaction mixture was stirred for 2 h at 110 ˚C, cooled to room temperature, and then, filtered with a pad of Celite powder and ethyl acetate. The filtrate was washed with saturated aq. NaCl solution, dried, and concentrated. The residue was purified by silica gel column chromatography to give **6a** as a colorless syrup (830 mg, 60% yield). To a solution of **6a** (300 mg, 0.39 mmol) in pyridine (20 mL) was added TBDMS chloride (107 mg, 0.71 mmol) and 4-*N,N*-dimethylaminopyridine (cat.) were added. The reaction mixture was stirred for 12 h at room temperature, treated with methanol (2 mL) for 3 h and concentrated. The residue was purified by silica gel column chromatography in a mixture of toluene and ethyl acetate. The main product was dissolved in pyridine (20 mL) and then reacted with palmitoyl chloride (162 mg, 0.59 mmol) for 3 h at room temperature. The reaction mixture was mixed with methanol (2mL) and then concentrated with toluene. The residue was dissolved in a mixture of CH_3OH and CH_2Cl_2 (1:1, 20 mL) and treated with trifluoroacetic acid (1 mL) for 2 h at room temperature. After concentration, the residue was purified by silica gel column chromatography in a mixture of tolune and ethyl acetate to give **8a** as a white waxy solid (0.32 g, 81 % yield from **6a**). $[\alpha]_D^{30}$ = +21.1 (c 1.0, $CHCl_3$); IR (KBr film): 3413, 2923, 2853,

1736, 1630, 1457, 1361, 1158, 1069, 736 cm^{-1}; ^{1}H-NMR (500 MHz, $CDCl_3$): δ_H 7.40~7.23 (m, 5Hx3, -$CH_2C_6H_5$), 5.23 (m, 1H, glycerol H-2), 4.96~4.64 (d, 2Hx3,-$CH_2C_6H_5$), 4.70 (d, 1H, J=3.5Hz, H-1), 4.40 (dd, 1H, J=4.0 and 12.0Hz, glycerol H-1_{proS}), 4.19 (dd, 1H, J=6.0 and 12.0Hz, glycerol H-1_{proR}), 3.96 (dd, 1H, J=9.5 and 9.5Hz, H-3), 3.72 (dd, 1H, J=5.5 and 10.5Hz, glycerol H-3_{proR}), 3.72 and 3.66 (b, 2H, H-6_{ProR} and H-6_{proS}), 3.65 (m, 1H, H-5), 3.54 (dd, 1H, J=5.5 and 10.5Hz, glycerol H-3_{proS}), 3.50 (dd, 1H, J=9.5 and 10.0Hz, H-4), 3.49 (dd, 1H, J=3.5 and 9.5Hz, H-2), 2.29 (m, 2Hx2, -OCOC$H_2$$CH_2(CH_2)_{12}CH_3$), 1.58 (b, 2Hx2, -$OCOCH_2CH_2$$(CH_2)_{12}CH_3$), 1.25 (b, 24Hx2,-$OCOCH_2CH_2(CH_2)_{12}$$CH_3$), 0.88 (t, 3Hx2, J=7.0Hz, -$OCOCH_2CH_2(CH_2)_{12}CH_3$); MS (FAB):cald for $C_{62}H_{96}O_{10}Na$([M+Na]$^+$) 1023.69; found 1023.7.

In the same way as derived for the synthesis of **8a**, (*R*)-glycidol and **6b** (0.30 g, 0.39 mmol) was used for the synthesis of **8b** (0.30 g, 77 % yield) $[\alpha]_D^{32}$= +18.5 (c 1.0, $CHCl_3$); IR (KBr film): 3452, 2924, 2854, 1739, 1586, 1455, 1296, 1159, 1095, 710 cm^{-1}; ^{1}H-NMR (500 MHz, $CDCl_3$): □$_H$ 7.40~7.23 (m, 5Hx3, -$CH_2C_6H_5$), 5.23 (b, 1H, glycerol H-2), 4.96~4.63 (d, 2Hx3,-$CH_2C_6H_5$), 4.75 (d, 1H, J=3.5Hz, H-1), 4.38 (dd, 1H, J=3.5 and 12.0Hz, glycerol H-3_{proR}), 4.21 (dd, 1H, J=6.5 and 12.0Hz, glycerol H-3_{proS}), 3.96 (dd, 1H, J=9.5 and 9.5Hz, H-3), 3.73 (dd, 1H, J=6.0 and 11.0Hz, glycerol H-1_{proS}), 3.76 and 3.66 (b, 2H, H-6_{ProR} and H-6_{proS}), 3.65 (m, 1H, H-5),

3.57 (dd, 1H, J=5.5 and 11.0Hz, glycerol H-1_{proR}), 3.51 (dd, 1H, J=9.5 and 10.0Hz, H-4), 3.50 (dd, 1H, J=3.5 and 9.5Hz, H-2), 2.29 (b, 2Hx2, -OCOC*H*$_2$CH$_2$(CH$_2$)$_{12}$CH$_3$), 1.59 (b, 2Hx2, -OCOCH$_2$C*H*$_2$(CH$_2$)$_{12}$CH$_3$), 1.25 (b, 24Hx2, -OCOCH$_2$CH$_2$(C*H*$_2$)$_{12}$CH$_3$), 0.88 (t, 3Hx2, J=7.0Hz, -OCOCH$_2$CH$_2$(CH$_2$)$_{12}$C*H*$_3$); MS (FAB): m/z calcd for $C_{62}H_{96}O_{10}Na$([M+Na]$^+$) 1023.69; found 1023.7.

A phosphorodiamidite method for the synthesis of I-a:

a) Reaction vessel was kept anhydrous condition with Ar gas in the presence of molecular sieves (50%w/w), and a solution of **8a** (0.20 g, 0.20 mmol) and 2-cyanoethyl-*N,N,N',N'*-tetraisopropyl phosphorodiamidite (90.4 mg, 0.30mmol) in 10 mL of CH_2Cl_2 was injected. 1*H*-tetrazole (28.4 mg, 0.40 mmol) was added and stirred for 2 h at room temperature. Then 1H-tetrazole (42.6 mg, 0.60 mmol, 3.0equiv) and choline tosylate (220.3 mg, 0.8 mmol: thoroughly dried overnight under vacuum) were added to a reaction mixture and stirred for 1.5 h at room temperature. Reaction was quenched by the addition of water (1 mL), then *m*-chloroperbenzoic acid (51.8 mg, 0.3 mmol) was added at 0°C and stirred for 10 min at room temperature. Reaction mixture was washed with 10 % aq. Na_2SO_3 solution, saturated aq. $NaHCO_3$ solution, water and saturated aq. NaCl solution,

dried and concentrated. The residue was dissolved in a mixture of CH_3OH (10 mL) and of 30% aq. NH_3 (1 mL) and stirred for 15 min at room temperature. The reaction mixture was concentrated, and the residue was purified by column chromatography (IATROBEADS in a mixture of $CHCl_3$ and CH_3OH) to give **9a** (186 mg, 80% yield). $[\alpha]_D^{26}$ +13.0 (c 0.45, $CHCl_3$); IR (KBr film): 3301, 2929, 2856, 2537, 1731, 1577, 1419, 1216, 1093, 925, 788, 746; ^{1}H-NMR (500 MHz, $CDCl_3$): δ_H 7.35~7.25 (m, 5Hx3, -$CH_2C_6H_5$), 5.22 (m, 1H, glycerol H-2), 4.93~4.61 (d, 2Hx3, -$CH_2C_6H_5$), 4.70 (d, 1H, J=3.5Hz, H-1), 4.38 (dd, 1H, J=3.0 and 12.0Hz, glycerol H-1_{proS}), 4.19 (b, 2H, choline –$CH_2CH_2N^+(CH_3)_3$), 4.17 (dd, 1H, J=6.5 and 12.0Hz, glycerol H-1_{proR}), 4.15 and 4.02 (mx2, 2H, H-6_{ProR} and H-6_{proS}), 3.93 (dd, 1H, J=9.0 and 9.5Hz, H-3), 3.72 (dd, 1H, J=5.5 and 11.0Hz, glycerol H-3_{proR}), 3.71 (b, 1H, H-5), 3.62 (t, 1H, H-4), 3.58 (b, 2H, choline –$CH_2CH_2N^+(CH_3)_3$), 3.52 (dd, 1H, J=6.0 and 11.0Hz, glycerol H-3_{proS}), 3.46 (dd, 1H, J=3.5 and 9.5Hz, H-2), 3.15 (s, 9H, -$POCH_2CH_2N^+(CH_3)_3$), 2.28 (m, 2Hx2, -$OCOCH_2CH_2(CH_2)_{12}CH_3$), 1.58 (b, 2Hx2, -$OCOCH_2CH_2(CH_2)_{12}CH_3$), 1.25 (b, 24Hx2, -$OCOCH_2CH_2(CH_2)_{12}CH_3$), 0.88 (t, 3Hx2, J=7.0Hz, -$OCOCH_2CH_2(CH_2)_{12}CH_3$); MS (FAB): m/z calcd for $C_{67}H_{108}NO_{13}PNa$([M+Na]$^+$) 1188.75; found 1188.7.

b) Compound **9a** (0.18 g, 0.15 mmol) was hydrogenated with $Pd(OH)_2$/C

(8mg) under atmospheric pressure in a mixture of CH_3OH (10 ml) and acetic acid (0.1 mL) for 7 h (room temperature). The reaction mixture was neutralized by addition of Et_3N, filtered and concentrated. The residue was purified by column chromatography with IATROBEADS (CH_3OH and $CHCl_3$) to give **I-a** (101 mg, 75 % yield). $[\alpha]_D^{31}$= +18.7 (c 1.0, $CHCl_3$:CH_3OH=10:1); IR (KBr film): 3372, 2927, 2852, 1731, 1573, 1469, 1112, 975, 727; ^{1}H-NMR (500 MHz, $CDCl_3$:CD_3OD=10:1): δ_H 5.23 (m, 1H, glycerol H-2), 4.80 (d, 1H, J=3.5Hz, H-1), 4.39 (dd, 1H, J=3.5 and 12.0Hz, glycerol H-1_{proS}), 4.30 (b, 2H, –C*H*$_2$$CH_2N^+(CH_3)_3$), 4.24 and 3.95 (b, 2H, H-6_{ProR} and H-6_{proS}), 4.14 (dd, 1H, J=6.5 and 12.0Hz, glycerol H-1_{proR}), 3.75 (dd, 1H, J=5.5 and 11.0Hz, glycerol H-3_{proR}), 3.67 (b, 2H, choline –CH_2C*H*$_2$$N^+(CH_3)_3$), ~3.65 (b, 1Hx2, H-3 and H-5), 3.61 (dd, 1H, J=5.5 and 11.0Hz, glycerol H-3_{proS}), 3.56 (b, 1H, H-4) 3.46 (b, 1H, H-2), 3.22 (s, 9H, -POC$H_2$$CH_2N^+$(C*H*$_3$)$_3$), 2.31 (m, 2Hx2, -OCOC*H*$_2$$CH_2(CH_2)_{12}CH_3$), 1.60 (b, 2Hx2, -OCOC$H_2$C*H*$_2$$(CH_2)_{12}CH_3$), 1.25 (b, 24Hx2, -OCOC$H_2CH_2$(C*H*$_2$)$_{12}$$CH_3$), 0.88 (t, 3Hx2, J=7.0Hz, -OCOCH_2C$H_2$$(CH_2)_{12}$C*H*$_3$); HRMS (FAB): m/z calcd for $C_{46}H_{90}NO_{13}PNa$ ([M+Na]$^+$);918.6048, found; 918.6028.

In the same way as described above, **9b** (180 mg) was derived from **8b** (200 mg, 0.20 mmol) in 76 % yield and converted to the GGPL-I isomer **I-b** [70 mg, 81 % yield from **9b** (120 mg)]. **9b:**

$[\alpha]_D^{26}$= +8.1 (c 0.62, $CHCl_3$); IR (KBr film): 3413, 2923, 2857, 1735, 1461, 1241, 1097, 744, 495, 445; ^{1}H-NMR (500 MHz, $CDCl_3$): δ_H 7.35~7.23 (m, 5Hx3, -$CH_2C_6H_5$), 5.23 (b, 1H, glycerol H-2), 4.94~4.64 (d, 2Hx3,-$CH_2C_6H_5$), 4.74 (d, 1H, J=3.5Hz, H-1), 4.37 (dd, 1H, J=3.0 and 12.0Hz, glycerol H-3_{proR}), 4.23 (b, 2H, choline –$CH_2CH_2N^+(CH_3)_3$), 4.19 (dd, 1H, J=6.5 and 12.0Hz, glycerol H-3_{proS}), 4.16 and 4.09 (b, 2H, H-6_{proR} and H-6_{proS}), 3.94 (dd, 1H, J=9.5 and 9.5Hz, H-3), 3.76 (dd, 1H, J=5.5 and 11.0Hz, glycerol H-1_{proS}), 3.72 (m, 1H, H-5), 3.61 (dd, 1H, J=9.0 and 9.5Hz, H-4), 3.60 (b, 2H, choline –$CH_2CH_2N^+(CH_3)_3$), 3.57 (dd, 1H, J=5.5 and 11.0Hz, glycerol H-1_{proR}), 3.49 (dd, 1H, J=3.5 and 9.5Hz, H-2), 3.20 (s, 9H, choline –$CH_2CH_2N^+(CH_3)_3$), 2.28 (dd, 2Hx2, J=7.5 and 15Hz, -$OCOCH_2CH_2(CH_2)_{12}CH_3$), 1.58 (b, 2Hx2, -$OCOCH_2CH_2(CH_2)_{12}CH_3$), 1.25 (b, 24Hx2, -$OCOCH_2CH_2(CH_2)_{12}CH_3$), 0.88 (t, 3Hx2, J=7.0Hz, -$OCOCH_2CH_2(CH_2)_{12}CH_3$); MS (FAB): m/z calcd for $C_{67}H_{108}NO_{13}PNa$ ($[M+Na]^+$) 1188.75; found 1188.7.

I-b: $[\alpha]_D^{31}$= +10.7 (c 1.0, $CHCl_3$:CH_3OH=10:1); IR (KBr film): 3390, 2919, 2856, 1731, 1463, 1228, 1074, 964, 711; ^{1}H-NMR (500 MHz, $CDCl_3$:CD_3OD=10:1): δ_H 5.24 (m, 1H, glycerol H-2), 4.80 (d, 1H, J=3.5Hz, H-1), 4.34 (dd, 1H, J=3.5 and 12.0Hz, glycerol H-3_{proR}), 4.28 (b, 2H, choline –$CH_2CH_2N^+(CH_3)_3$), 4.25 and 3.97 (b, 2H, H-6_{ProR} and H-6_{proS}), 4.20 (dd, 1H, J=7.0 and 12.0Hz, glycerol H-3_{proS}), 3.80 (dd, 1H, J=6.0 and 11.0Hz, glycerol

H-1_{proS}), ~3.63 (b, 1Hx2, H-3 and H-5), 3.63 (b, 2H, choline –$CH_2CH_2N^+(CH_3)_3$), 3.58 (dd, 1H, J=5.5 and 11.0Hz, glycerol H-1_{proR}), 3.55 (b, 1H, H-4) 3.46 (dd, 1H, H-2), 3.22 (s, 9H, choline –$CH_2CH_2N^+(CH_3)_3$), 2.31 (dd, 2Hx2, J=7.5 and 15Hz, -$OCOCH_2CH_2(CH_2)_{12}CH_3$), 1.60 (b, 2Hx2, -$OCOCH_2CH_2(CH_2)_{12}CH_3$), 1.26 (b, 24Hx2, -$OCOCH_2CH_2(CH_2)_{12}CH_3$), 0.88 (t, 3Hx2, J=7.0Hz, -$OCOCH_2CH_2(CH_2)_{12}CH_3$); HRMS (FAB): m/z calcd for $C_{46}H_{90}NO_{13}PNa$ ($[M+Na]^+$) 918.6048; found 918.6078.

3-*O*-(α-D-glucopyranosyl)-1,2-di-*O*-palmitoyl-*sn*-glycerol (**10** in Entry 3): Compound **10** was obtained as a waxy solid (73 mg, 83% yield) from **8a** (120mg,0.12mmol) by catalytic hydrogenation under the same reaction conditions as those described above in the preparation of **I-a**. $[\alpha]_D^{30}$= +27.2 (c 1.0, $CHCl_3$:CH_3OH=10:1); IR (KBr film): 3411, 2919, 2851, 1739, 1587, 1465, 1158, 1053, 720 cm^{-1}; ^{1}H-NMR (500 MHz, $CDCl_3$:CD_3OD=10:1): δ_H 5.25 (m, 1H, glycerol H-2), 4.83 (d, 1H, J=3.5Hz, H-1), 4.40 (dd, 1H, J=3.5 and 12.0Hz, glycerol H-1_{proS}), 4.16 (dd, 1H, J=6.5 and 12.0Hz, glycerol H-1_{proR}), 3.82 (dd, 1H, J=5.5 and 10.5Hz, glycerol H-3_{proR}), 3.78 (d, 2H, J=3.5Hz, H-6_{proR} and H-6_{proS}), 3.65 (t, 1H, H=9.5 and 9.5Hz, H-3), 3.62 (dd, 1H, J=6.0 and 10.5Hz, glycerol H-3_{proS}), 3,56 (dt, 1H, H-5), 3.44 (dd,

1H, J=3.5 and 9.5Hz, H-2), 3.42 (dd, 1H, J=8.5 and 10.0, H-4), 2.32 (dt, 2Hx2, -OCOC*H*$_2$CH$_2$(CH$_2$)$_{12}$CH$_3$), 1.61 (b, 2Hx2, -OCOCH$_2$C*H*$_2$(CH$_2$)$_{12}$CH$_3$), 1.26 (b, 24Hx2, -OCOCH$_2$CH$_2$(C*H*$_2$)$_{12}$ CH$_3$), 0.88 (t, 3Hx2, J=7.0Hz, -OCOCH$_2$CH$_2$(CH$_2$)$_{12}$C*H*$_3$); HRMS (FAB): m/z calcd for $C_{41}H_{78}O_{10}Na$ ([M+Na]$^+$) 753.5493;found 753.5519.

3-*O*-(6-*O*-palmitoyl-α-D-glucopyranosyl)-1,2-di-*O*-palmitoyl-*sn*-glycerol (11 in Entry 4): A mixture of **8a** (120 mg, 0.12 mmol) and palmitoyl chloride (165 mg, 0.6 mmol) in pyridine was stirred at room temperature for 3 h and then treated with CH_3OH (1 mL) for 3 h. After concentration *in vacuo*, the residue was purified on silica gel (toluene + ethyl acetate). The main product (138 mg) was dissolved in a mixture of cyclohexene and ethanol (1:4) and subjected to catalytic hydrogenation at atmospheric pressure in the presence of $Pd(OH)_2$/C (50 mg). The product was purified by silica gel column chromatography (CH_3OH+$CHCl_3$) to afford **11** (99 mg, 85% yield from **8a**). $[\alpha]_D^{30}$= +20.9 (c 1.0, $CHCl_3$:CH_3OH=10:1); IR (KBr film): 3414, 2919, 2851, 1739, 1605, 1465, 1375, 1176, 1054, 720 cm^{-1}; ^{1}H-NMR (500 MHz, $CDCl_3$:CD_3OD=10:1): δ_H 5.25 (m, 1H, glycerol H-2), 4.82 (d, 1H, J=4.0Hz, H-1), 4.40 (dd, 1H, J=3.5 and 12.0Hz, glycerol H-1$_{proS}$), 4.34 and 4.30 (ddx2, 2H,

J=5.0 and 12.0, 2.5 and 12.0Hz, H-6_{proR} and H-6_{proS}), 4.16 (dd, 1H, J=6.5 and 12.0Hz, glycerol H-1_{proR}), 3.82 (dd, 1H, J=5.0 and 10.5Hz, glycerol H-3_{proR}), 3.73 (m, 1H, H-5), 3.65 (dd, 1H, H=9.0 and 9.5Hz, H-3), 3.61 (dd, 1H, J=5.5 and 10.5Hz, glycerol H-3_{proS}), 3.45 (dd, 1H, J=4.0 and 9.5Hz, H-2), 3.33 (dd, 1H, J=9.0 and 10.0, H-4), ~2.33 (m, 2Hx3, -OCOC*H*$_2$$CH_2(CH_2)_{12}CH_3$), 1.61 (b, 2Hx3, -$OCOCH_2C$*H*$_2$$(CH_2)_{12}CH_3$), 1.26 (b, 24Hx3, -$OCOCH_2CH_2(C$*H*$_2$$)_{12}CH_3$), 0.88 (t, 3Hx3, J=7.0Hz, -$OCOCH_2$ $CH_2(CH_2)_{12}C$*H*$_3$); HRMS (FAB): m/z calcd for $C_{57}H_{108}O_{11}Na$ ($[M+Na]^+$) 991.7789; found 991.7832.

2-5 Reference and Notes

1. Rawadi, G. *Microbes and infection*, **2000**, *2*, 955-964.

2. Shimizu, T.; Kida, Y.; Kuwano, K. *Immunology* **2004**, *113*, 121-129.

3. Francisco, R.; Encarnacion, M.; Alfonso, R.-B.; Maria, J.-V. *Current Microbiol.* **2004**, *48*, 237-239.

4. Rottem, S. *Biochem. Biophys. Acta* **1980**, *604*, 65-90.

5. Boggs, I. M. *Biochim. Biophys. Acta* **1987**, *906*, 353-404.

6. Toujima, S.; Kuwano, K.; Zhang, Y.; Fujimoto, N.; Hirama, M.; Oisi, T.; Fukuda, S.; Nagumo, Y.; Imai, H.; Kikuchi, T.; Arai, S. *Microbiology* **2000**, *146*, 2317-2323.

7. Matsuda, K.; Kasama, T.; Ishizuka, I.; Handa, S.; Yamamoto, N.; Taki, T. *J. Biol. Chem.* **1994**, *269*, 33123-33128.

8. Matsuda, K.; Li, J.-L.; Harasawa, R.; Yamamoto, N. *Biochim. Biophys. Res. Commun.* **1997**, *233*, 644-649.

9. Li, J.-L.; Matsuda, K.; Takagi, M.; Yamamoto N. *J. Immunol. Methods* **1997**, *208*, 103-113.

10. Matsuda, K.; Li, J. L.; Ichinose, S.; Harasawa, R.; Saito, M.; Yamamoto, N. *Microbiol. Immunol.* **2000**, *44*, 695-702.

11. Zaehringer, U.; Wanger, F.; Rietschel, E. T.; Ben-Menachem, G.; Deutsch, J.; Rottem, S. *J. Biol. Chem.* **1997**, *272*, 26262-26270.

12. Ben-Menachem, G.; Bystrom, T.; Rechnitzer, H.; Rottem, S.; Filfors, L.; Lindblom, G. *Eur. J. Biochem.* **2001**, *268*, 3694-3701.

13. Brandenburg, K.; Wagner, F.; Mueller, M.; Heine, H.; Andrae, J.; Koch, M. H. J.; Zaehringer, U.; Seydel, U. *Eur. J. Biochem.* **2003**, *270*, 3271-3279.

14. Yavlovich, A.; Katzenell, A.; Tarshis, M.; Higazi, A. A.-R.; Rottem, S. *Infect. Immunity* **2004**, *72*, 5004-5011.

15. Nishida, Y.; Ohrui, H.; Meguro, H.; Ishizawa, M.; Matsuda, K.; Taki, T.; Handa, S.; Yamamoto, N., *Tetrahedron Lett.* **1994**, *35*, 5465-5468.

16. Nishida, Y.; Takamori, Y.; Ohrui, H.; Ishizaka, I.; Matsuda, K.; Kobayashi, K. *Tetrahedron Lett.* **1999**, *40*, 2371-2374.

17. Matsuda, K. *Recent Res. Devel. Neurosci.* **2004**, *1*, 15-23.

18. Kawahito, Y.; Ichinose, S.; Sano, H.; Tsubouchi, Y.; Kohno, M.; Yoshikawa, T.; Tokunaga, D.; Hojo, T.; Harawsawa, R.; Nakano, T.; Matsuda、K. *Biochem. Biophys. Commun.* **2008**,*369*,561-566.

19. Sato, N.; Oizumi, T.; Kinbara, M.; Sato, T.; Funayama, H.; Sato, S.; Matsuda, K.; Takada, H.; Sugawara, S.; Endo, Y. *FEMS Immunol. Med. Microbiol.* **2010**, *59*,33-41.

20. Fujiwara, M.; Ishida, N.; Asano, K.; Matsuda, K.; Nomura, N.; Nishida, Y.; Harasawa, R. *J. Vet. Med. Sci.* **2010**, *72*, 805–808.

21. Ishida, N.; Irikura, D.; Matsuda, K.; Sato,S.; Sone, T.; Tanaka, M.; Asano, K. *Curr. Microbiol.* **2009**, *58*, 535-540.

22. Ishida, N.; Irikura, D.; Matsuda, K.; Sato, S.; Sono, T.; Tanaka, M.; Asano, K. *J. Biosci. Bioeng.* **2010**, *109*,341-345.

23. Shingu, Y.; Nishida, Y.; Dohi, H.; Matsuda, K.; Kobayashi, K. *J. Carbohydr. Chem.* **2002**, *21*, 605-611.

24. Shingu, Y.; Nishida, Y.; Dohi, H.; Kobayashi, K. *Org. Biomol. Chem.* **2003**, *1*, 1-5.

25. Nishida, Y.; Shingu, Y.; Dohi, H.; Kobayashi, K. *Org. Lett.* **2003**, *5*, 2377-2380.

26. Shingu, Y.; Miyachi, A.; Miura, Y.; Kobayashi, K.; Nishida, Y. *Carbohydr. Res.* **2005**, *340*, 2236-2244.

27. Gigg, R.; Penglis, A. A. E.; Conant, R. *J. Chem. Soc. Perkin I*, **1977**, 2014-2017.

28. Mannock, D. A.; Lewis, R. N.; McElhaney, R. N. *Chem. Phys. Lipids* **1990**, *55*, 309-321.

29. Gordon, D. M.; Danishefsky, S. J. *J. Am. Chem. Soc.* **1992**, *114*, 659-663.

30. Imai, H.; Oishi, T.; Kikuchi, T.; Hirama, M. *Tetrahedron* **2000**, *56*, 8451-8459.

31. Shvets, V. I.; Bashkatova, A. I.; Evstigneeva, R. P. Chem. Phys. Lipids, **1973**, *10*, 267-285, and the related references cited therein.

32. Lemieux, R. U.; Hendriks, K. B.; Stick, R. V.; James, K. *J. Am. Chem.*

Soc. **1975**, *97*, 4056-4062.

33. Lu, S. –R.; Lai, Y.-H.; Chen, J.-H.; Liu, C.-Y.; Mong, K.-K. T. *Angew. Chem.,* **2011**, 123, 7453-7458, and the related references cited therein.

34. Y. Hayakawa, M. Kataoka, *J. Am. Chem. Soc.* **1997**, *119*, 11758-11762.

35. Nishida, Y.; Uzawa, H.; Hanada, S.; Ohrui, H.; Meguro, H. *Agric. Biol. Chem.* **1989**, *53*, 2319-2323.

36. Uzawa, H.; Nishida, Y.; Hanada, S.; Ohrui, H.; Meguro, H. *Chem. Commun.* **1989**,862.

37. Uzawa, H.; Nishida, Y.; Ohrui, H.; Meguro, H. *J. Org. Chem.* **1990**, *55*, 116-122.

38. Ohrui, H.; Nishida, Y.; Watanabe, M.; Hori, H.; Meguro, H. *Tetrahedron Lett.* **1985**, *26*, 3251-3254.

39. Nishida, Y.; Hori, H.; Ohrui, H.; Meguro, H.; Uzawa, J.; Reimer, D.; Sinnwell, V.; Paulsen, H. *Tetrahedron Lett.* **1988**, *29*, 4461-4464.

40. Hori, H.; Nishida, Y.; Ohrui, H.; Meguro, H.; Uzawa, J. *Tetrahedron Lett.* **1988**, *29*, 4457-4460.

41. Nishida, Y.; Hori, H.; Ohrui, H.; Meguro, H. *J. Carbohydr. Chem.* **1988**, *7*, 239-250.

42. Haasnoot, C. A. G.; Leew, F. A. A.; Altona, C., *Tetrahedron* **1980**, *36*, 2783-2790.

43. Matsuda, K.; Saito, M.; Yamamoto, N.; *"Lipid antigen" in Encyclopedia*

of Life Science, Nature publishing group, vol.1 pp748-755. **2002**.

44. Koynova, R. D.; Kuttenreich, H. L.; Tenchov, B. G.; Hinz, H. J. *Biochemistry* **1988**, *27*, 4612–4619.

45. Mannock, D. A.; Lewis, R. N.; McElhaney, R. N.; Akiyama, M.; Yamada, H.; Turner, D. C.; Gruner, S. M. *Biophys J.* **1992**, 63, 1355–1368.

Chapter 3

Comparative analyses of helical property in asymmetric 1,2-di-O-acyl-sn-glycerols

3-1 Introduction

Glycerol is a naturally occurring symmetric compound, and the prochiral positions are defined as sn-glycerol according to the IUPAC rule of stereospecific numbering.[1] An important part of stereochemistry in the sn-glycerol arises from the fact that it is a “prochiral compound.” This means that when either the sn-1 or sn-3 position is modified in either a chemical or a biological pathway,[2] the glycerol derivative becomes optically active. Actually, both naturally occurring phospholipids and glycolipids in cytoplasm membranes are chiral and optically active. They possess polar substituent groups usually at sn-3 position to have the common asymmetric skeleton of 1,2-di-O-acyl-sn-glycerol. Another important stereochemical factor arises from that fact that they are the acyclic compounds allowing free rotation at each C-C single bond. Assumed that there are three staggering conformers at each of the sn-1 and sn-3 positions, the asymmetric sn-glycerol skeleton can give nine different conformers.[3]

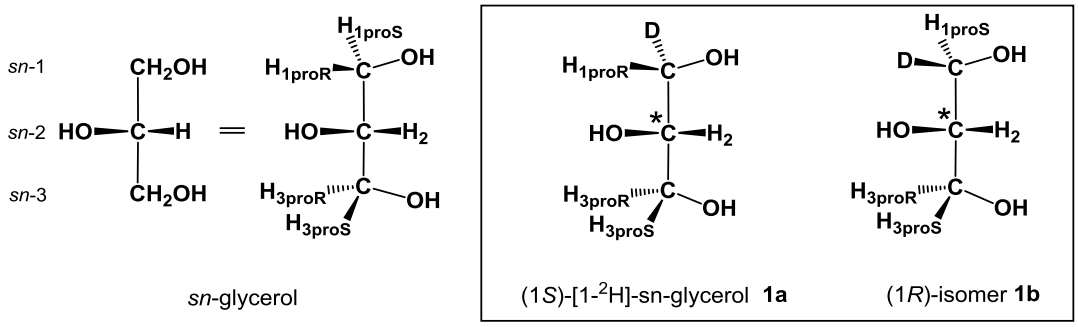

Figure 3-1

In our preceding studies,[4,5] we reported the synthesis and ^{1}H NMR characterization of chirally ^{2}H-labelled sn-glycerols **1a** and **1b** (**Figure 3-1**) and their esters (acetate, benzoate and palmitate). These ^{2}H-labelled compounds served as probes useful for discriminating each of diastereomeric protons in the prochiral sn-glycerol skeleton with ^{1}H NMR spectroscopy and have enabled us to examine conformational behaviors in both symmetric and asymmetric sn-glycerols[5,6] including Mycoplasma α-glycolipids.[7]

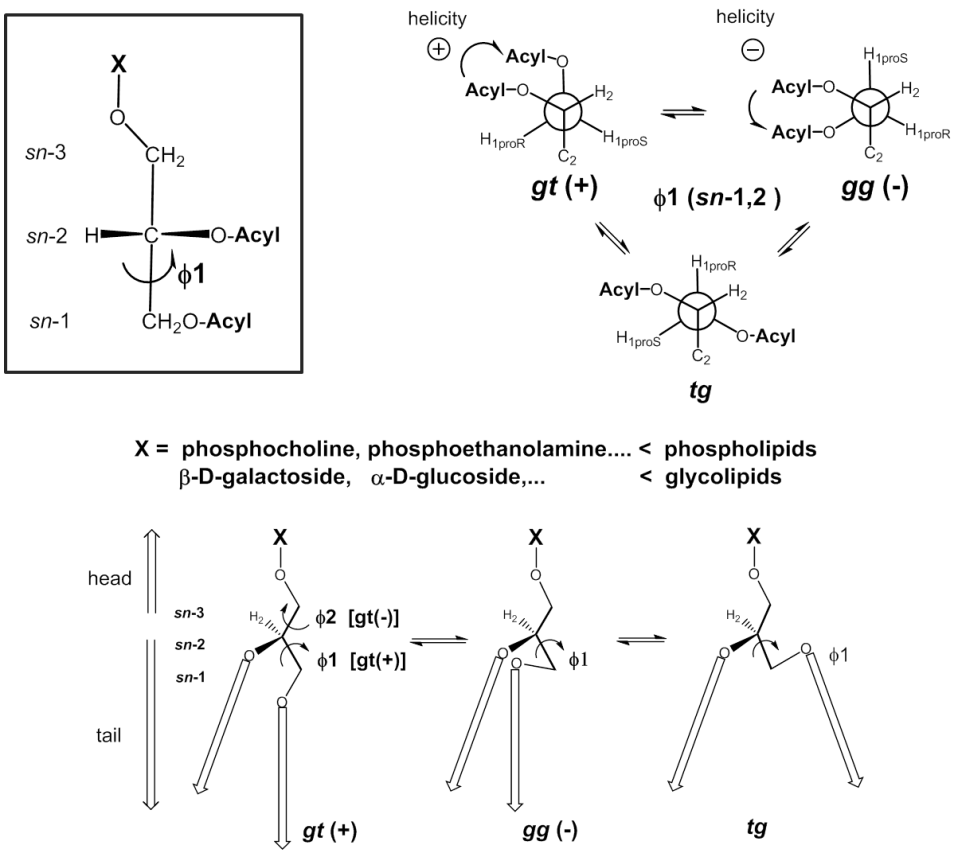

Figure 3-2

Extensive studies have been directed to the analysis of thermodynamic behaviors of cell-membrane phospholipids.[8-12] Along these studies, it has become widely accepted that phospholipids adopt two *gauche* conformers (gg and tg) at the tail in such a way of allowing stacking interaction (**Figure 3-2**). Hauser et al. [13] reported ^{1}H and ^{31}P NMR analyses for a series of phospholipids in both solution and semi-solution states that the lipid tail favored the two *gauche* conformers irrespectively of the solvents used and the functional groups attached to the head group. In our preceding study, we observed an analogous

behavior in conformational properties also in *Mycoplasma fermentans* α-glycolipids (GGPLs).[7] Here, we can see in **Figure 3-2** that the *gauche*-conformers [gt-(+) and gg-(-)] have helicity with sign reversed each other. It is obvious that the helicity around sn-1,2 di-O-acyl groups can become one of important stereochemical factors for characterizing 1,2-di-O-acyl-sn-glycerols as asymmetric biomaterials responsible for formation of cytoplasm membranes.

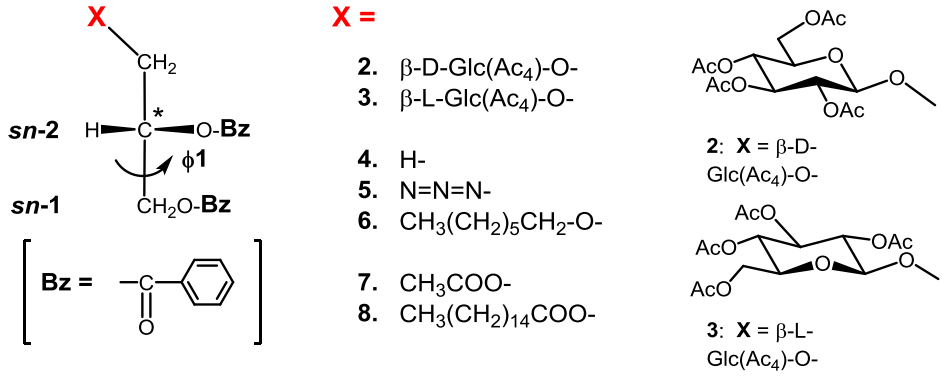

Figure 3-3

A few decades ago, we reported chiroptical properties of various 1,2-di-O-benzoyl-sn-glycerols (**Figure 3-3**) and the related chiral sn-glycerols by means of optical rotatory dispersion (ORD) and circular dichroism (CD).[6,14] During these studies, we recognized that intensity of their CD bands varied extensively among compounds **2~8**.[6] It was possible that helical property around the sn-1,2 di-O-acyl groups could be influenced

largely by sn-3 substituting groups besides the absolute sn-configuration. Since these chiral sn-glycerols are thought to serve as good models for studies on phospholipids and glycolipids, we examined conformational properties of in **2~8** in methanol solutions by means of CD and ^{1}H NMR spectroscopy as independent approaches. In this paper, we reported the results in terms of comparative analyses of helical property and notable effects of sn-3 substituting groups in the asymmetric 1,2-di-O-acyl-sn-glycerols in a solution state.

3-2 Materials and Methods

Model compounds: All compounds studied here including tri-O-benzoyl derivatives of **1a** and **1b**[5] and model compounds **2~8**[6] were prepared in our former studies, and both of their absolute configuration and optical purity were already established. For compound **3** with 3-O-β-L-Glc linkage, an optical isomer **3a** with β-D-Glc linkage at sn-1 [2,3-di-O-benzoyl-1-O-(2,3,4-tetra-O-acetyl-β-D-glucopyranosyl)-sn-glycerol] was prepared[14] and is being handled in the present

study as β-L-Glc isomer **3**. This was made to simplify discussion.

^{1}H NMR and CD analyses: All compounds **2~8** were dissolved in either methanol (10 μM) or methanol-d_4 (ca. 10 mM) for ^{1}H NMR (400 and 500 MHz) and CD analysis respectively. ^{1}H NMR data [chemical shift (δ ppm), coupling constants (Hz) in **Table 1-3**] as well as the CD and UV data [molecular ellipticity ([θ]max) of band 1 and band 2 and ε values (λmax) in **Table 1-1**) were assembled from our original data[6] and analyzed with Karplus equations to obtain information on helicity indexes (sign, intensity, disparity and volume). Three Karplus equations (**eq. B-1**, **eq. B-2** and **eq. B-3, equation 2**) were derived from a general equation (**equation 1**) of Haasnoot[15] and used for calculation of three helical conformers with a PC soft (free in e-mail contact with Yuan Mengfei, Chiba University). For this analysis, ^{1}H NMR coupling constants were collected from expanded spectra in first order analysis and checked with second order analysis in case of AMX spin system. Discrimination of diastereomeric protons (H_{1proR} and H1proS) was conducted on the basis of NMR data of tri-O-benzoates derivatives **1a** and **1b** as we described previously.[6]

3-3 Results and Discussion

1. Analysis of helical property by means of circular dichroism (CD) spectroscopy

As shown in **Figure 3-4**, the CD spectra of both **2** and **3** gave typical exciton coupling CD bands with a positive peak at ca. 235 nm (band 1) and a negative one at ca. 220 nm (band 2). All these model compounds **4~8** gave couplet CD bands with (+)-sign as summarized in **Table 3-1**, and this result allowed us to conclude in a preceding paper[6] that "CD di-benzoate chirality rule" by Nakanishi and Harada[16,17] provides us with a general tool useful for assignment of glycerol sn-configurations. At the same time, it had become obvious that these 1,2-di-O-benzoyl-sn-glycerols adopt the gt-(+) conformer with right-handed helicity more than the antipodal gg-(-) one in conformation equilibrium among three staggered conformers and hold a persistent order of gg-(+) > gg-(-) > tg (**Figure 3-2**).

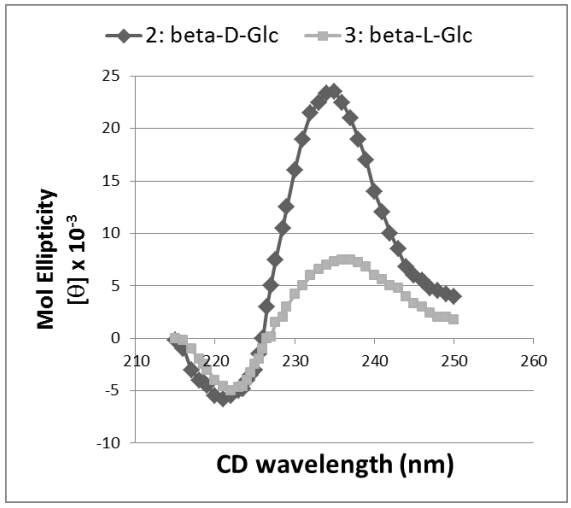

Figure 3-4 CD spetra of **2** and **3** in MeOH

On the other hand, it was notable that intensity of the exciton coupling bands varied widely between the two β-glycosylated derivatives (**2** and **3**) and also among the compounds studied here. This result has disclosed that position of the conformation equilibrium can vary more extensively than what we could expect for the two glycosyl isomers. This consideration prompted us to reinvestigate conformation behaviors of **2~8** in terms of helical property and elucidate possible effects of the sn-3 substituting group.

To correlate between CD and ^{1}H NMR data, we introduced "helicity index" as given in **Table 3-1** and **Table 3-2**. The helicity index (CD) covers information on the sign and intensity of helicity at sn-1,2 di-O-benzoate which can be determined by the exciton coupling CD bands on the basis of the "di-benzoate

chirality method" of Nakanishi and Harada.[16] There, the intensity (CD) was defined as sum of peak intensity (Δε or [θ]max) of the two couplet CD bands (band 1 and band 2) which is considered proportional to the intensity of di-benzoate exciton coupling interactions.

Table 3-1 CD and UV data of compounds **2~8** in methanol solution and "helicity index (CD)" derived from di-benzoate exciton coupling CD bands (band 1 and band 2)

Compounds		CD data (CH_3OH) $[\theta]_{max}$ x 10^{-3} (λ_{max} nm)		UV data (CH_3OH)	Helicity Index (CD)	
No	X =	band 1 (first band)	band 2 (second band)	$\varepsilon x10^{-1}$ (λmax nm)	sign	intensity (CD) [band 1+band 2]
2	β-D-Glc(Ac_4)-O-	+21.6 (234)	- 5.6 (220)	2.0 (229)	+	27
3	β-L-Glc(Ac_4)-O-	+7.6 (237)	-4.8 (222)	2.3 (229)	+	12
4	H-	+25.2 (235)	-6.9 (222)	2.1 (229)	+	32
5	N=N=N-	+10.2 (236)	-9.0 (222)	1.9 (230)	+	19
6	$CH_3(CH_2)_5CH_2$-O-	+13.6 (236)	-8.4 (220)	1.8 (230)	+	22
7	CH_3COO-	+3.0 (239)	-4.9 (226)	2.0 (230)	+	8
8	$CH_3(CH_2)_{14}COO$-	+1.4 (236)	-2.5 (226)	2.1 (230)	+	4

The helical index (CD) gives us precise information on conformation equilibrium among the three helical conformers as depicted in **Figure 3-2**. For example, the (+)-sign was indicative of predominance of the gt-(+) conformer with right-handed helicity in this equilibrium in an order as gt-(+) > gg-(-) in the equilibrium. This relation was maintained in all compounds

studied here irrespective of the sn-substituting groups. The intensity (CD) is considered to vary among them depending on degree of disparity between the two *gauche*-conformers [gt-(+) and gg-(-)] with revered helicity sign. The sn-3 substituting groups can contribute to this disparity while keeping the persistent order of gt-(+) > gg-(-). Apparently, it is integrated in the compound **2** with β-D-Glc linkage rather than in **3** with β-L-Glc isomer since the intensity (CD) of **2** was more than two times higher than that of **3**. The sn-3 acyl groups in **7** and **8** are thought to a notable effect which averages the disparity between the two *gauche*-conformers.

2. Analysis of helical property by means of ^{1}H NMR spectroscopy

For the purpose of analyzing the conformational equilibrium, we have conveniently applied a general Karplus equation (**Equation 1**). The following equation was originally proposed by Haasnoot el. al.[15] who extensively examined roles of electron substituting groups on vicinal ^{1}H-^{1}H coupling constants (^{3}J Hz). This equation is useful for analysis of those compounds having a tri-substituted C-C single bond like sn-glycerols the

tri-substituted system at sn-1,2 position and hexoses at C5-C6 position.[18]

A general Karplus equation of Haasnoot et al (lit. 15):

$$^{3}J_{H\text{-}1,H\text{-}2}\,(Hz) = 13.22 \times \cos^{2}\Phi - 0.99 \times \cos\Phi + R$$

ϕ = dihedral angle (degree) around sn-1,2 oxygen atoms

R = effects of neighboring electron negative groups (O-1, O-2 and C-3) as given by sum of $\Delta Xi \times [0.87\text{-}2.46 \times \cos^{2}(r\Phi + 19.9 \times ABS(\Delta Xi))]$

ΔXi = electron negativity of each substituting group (i) : ΔX =1.3 (O-1 and O-2) and 0.4 (C-3)

r = +1 or -1 (helical direction of the dihedral angles)

Equation 1

Here, above equation was extended to the following three equations (**eq. B-1**, **eq. B-2** and **eq. B-3** (**Equation 2**), each of which enables us to calculate time-averaged populations (%) of the three conformers. In the present ^{1}H NMR analysis, a set of vicinal coupling constants of H-1*proR* and H-1*proS* is applied. The two diastereomeric protons were discriminated with benzoyl derivatives of the chirally deuterium-labelled compounds **1a** and **1b** (**Figure 3-1**). Equation **B-1** is a basic equation which has been commonly used in our analyses of sn-glycerols.[3-7]

In **eq. B-2** and **eq. B-3**, possible deviations from perfect

staggering are taken into accounts in each of the rotamers. This is because there was a clear tendency in X-ray data that dihedral angles (ϕ1) of vicinal oxygens tended to allow deviations from perfect staggered angle (ϕ1 = ± 60°) by ca. ± 5°.[18,19]

Equations (Φ1 in each rotamer)	^3J values (Hz)	gt-(+)	gg-(-)	tg
eq. B-1 (+60, -60, 180)	$^3J_{H1proS,H2}$ =	2.8	3.1	10.7
	$^3J_{H1proR,H2}$ =	0.9	10.7	5.0
eq. B-2 (+65, -65, 180)	$^3J_{H1proS,H2}$ =	2.3	2.5	10.7
	$^3J_{H1proR,H2}$ =	1.3	10.2	5.0
eq. B-3 (+65, -65, 185)	$^3J_{H1proS,H2}$ =	2.3	2.5	10.6
	$^3J_{H1proR,H2}$ =	1.3	10.2	5.8

Equation 2

Table 3-2 ^{1}H NMR data of 1,2-di-O-benzoyl-sn-glycerols (**2~8**) in CD_3OD solution and "helicity index (^{1}H NMR)" available from vicinal coupling constants (Hz)

Compounds		^{1}H NMR data (CD_3OD)		Rotamer populations (%) (ϕ1 degree)			Helicity Index (^{1}H NMR) at sn-1,2 position		
		δ ppm ($^3J_{H1,H2}$ Hz)		gt (+60)	gg (-60)	tg (180)	sign	disparity [gt-gg] %	volume [gt+gg] %
No	X =	H1*proR*	H1*proS*						
2	β-D-Glc(Ac_4)-O-	4.60 (6.6)	4.70 (3.6)	55	37	8	+	18	92
3	β-L-Glc(Ac_4)-O-	4.53 (6.2)	4.70 (3.9)	50	39	11	+	11	89
4	H-	4.49 (7.0)	4.60 (3.3)	60	35	5	+	25	95
5	N=N=N-	4.57 (6.5)	4.71 (4.2)	51	34	15	+	17	85
6	$CH_3(CH_2)_5CH_2$-O-	4.59 (6.6)	4.70 (3.7)	54	37	9	+	17	91
7	CH_3COO-	4.60 (6.1)	4.70 (4.2)	47	38	15	+	9	85
8	$CH_3(CH_2)_{14}COO$-	4.60 (5.8)	4.70 (4.2)	44	41	15	+	3	85

Results of our ^{1}H NMR using the standard equation (**eq. B-1**) were summarized together with the helicity index (^{1}H NMR) in

Table 3-2. The population is given as time-averaged populations (%) of each rotamer which can interconvert each other much faster (order of 10^{-6}~10^{-9} second) than ^{1}H NMR time scale (order of 10^{-3} seconds) in solution states. “Helicity index (^{1}H NMR)” is composed of three stereochemical items (sign, intensity-2 and volume) useful for charactering helical property around the sn-1,2 position. The sign and intensity-2 are defined as difference in populations between gt-(+) and gg-(-) conformers: the sign becomes positive (+), and the intensity-2 becomes stronger as the right-handed helical conformer increases relative to the left-handed one. Obviously, these indexes should correspond to the helicity index (CD) which was discussed in preceding section. In the helicity index (^{1}H NMR), “volume” was added as a new index to characterize the helical property. The “volume” is defined as the sum of gt-(+) and gg-(-) population (%) which indicates the total volume of these two *gauche*-conformers in equilibrium.

^{1}H NMR data of compounds **2~8** gave a persistent relation of ^{3}JH1proR,H2 > JH1proS,H2 (Hz) and δH1proS > δH1proR (ppm), though there were some deviations in both chemical shifts and coupling constants among these compounds. The

conformer populations calculated with **eq. B-1** have shown that all compounds studied here favor gt-(+) conformer with right-handed helicity more than gg-(-) with left-handed helicity. Thus, the (+)-sign in the helicity index completely matched with the (+)-sign in CD indexes. Disparity (%) between the two helical conformers varied among the compounds similarly to the values in the CD intensity. The helical volume (%) was greater than 80% indicating that the two helical conformers (gt and gg) were predominant over tg-conformer.

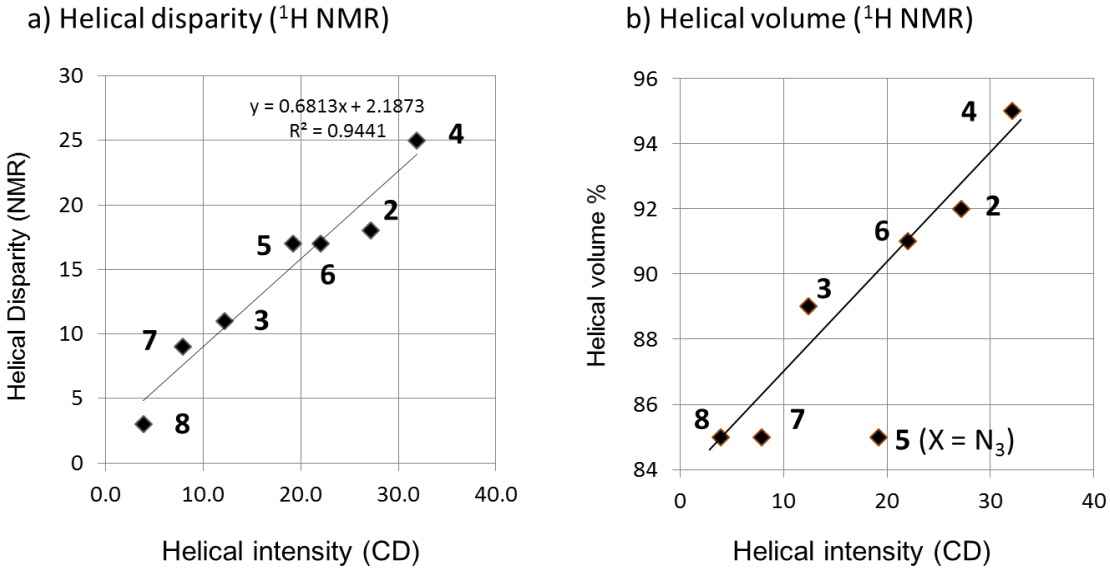

Figure 3-5 Correlation between helical intensity (CD) and ^{1}H NMR data: (a) helical intensity and (b) helical volume (%)

Here, it may be of interest to mention that compound **4**, which is the smallest chiral 1,2-diol derivative, can show the highest intensity in both ^{1}H NMR and CD indexes, while

compound **8** with a long fatty acid (C16) ester has shown the weakest helical property around the di-O-benzoates, Here, we plotted each value in intensity (CD) against those in the helical disparity (^{1}H NMR) for correlation between the two independent approaches. As shown in **Figure 3-5a**, it was found that the helical intensity (CD) holds a linear relation with the NMR index. It is obvious that the two independent approaches are in good agreement in analyses of helical property in the asymmetric 1,2-di-O-benzoyl-sn-glycerols.

Next, intensity (CD) values were plotted against the NMR helical volume. As shown in **Figure 3-5b**, values in the helical intensity (CD) is nearly proportional also to the NMR helical volume defined by sum of gt-(+) and gg-(-) conformers (%). This means that the degree of helical disparity between the two *gauche*-conformers is associated mainly with change in population of gt-(+) rather than that in gg-(-). Here, it was notable that compound **5** with azide group showed an exceptional behavior. Compounds **5** (-N=N=N) showed a behavior analogously to O-acyl derivatives **7** and **8** in the point that they have the lowest helical volume (85%). The helical property of **5** was, however, different obviously from those of **8**

(O-palmitate) which showed the lowest value in both helical intensity and volume among the model compounds studied here.

Table 3-3 . ^{1}H NMR analysis of helical properties of 1,2-di-O-benzoyl-sn-glycerols **2~8** in methanol

Comp	Rotamers % (ϕ1 degree)			Helicity Index (NMR) (eq. B-2)			Rotamers % (ϕ1 degree)			Helicity Index (NMR) (eq. B-3)		
	gt (+65)	gg (-65)	tg (180)	sign	disparity [gt-gg]%	volume [gt+gg]%	gt (+65)	gg (-65)	tg (185)	sign	disparity [gt-gg]%	volume [gt+gg]%
2	54	32	14	+	22	86	52	33	15	+	19	85
3	48	34	18	+	14	82	46	36	18	+	10	82
4	60	30	10	+	30	90	59	31	10	+	28	90
5	50	29	21	+	21	79	47	31	22	+	16	78
6	53	32	15	+	21	85	52	33	15	+	19	85
7	45	33	22	+	12	78	43	35	22	+	8	78
8	42	37	21	+	5	79	40	38	22	+	2	78

When **eq. B-2** and **eq. B-3** as listed in **equation 2** were employed instead of **eq. B-1**, some changes appeared in both helical intensity and volume (**Table 3-3**). But, we have noticed no critical change in these NMR data and also in the induced helical index by selection of these three equations. In general, the use of **eq. B-2** and **eq. B-3** tends to decrease the helical volume (%) and increase the population of anti-periplanar tg-conformer. This implies that the standard equation (**eq. B-1**)

may overestimate the helicity volume [gt-(+) and gg-(-)] in present analysis as well as "*gauche effects*" which are often argued not only in conformational analyses of sn-glycerols[7,8] but also in carbohydrates.[20-23] In fact, we had concluded previously that Mycoplasma α-glycosyl-sn-glycerols adopted such an ordered conformation as to adopt the two *gauche*-conformers near exclusively at the lipid tail.[7] It is also possible that **eq. B-2** may overestimate disparity the helical intensity in comparison with **eq. B-3**, while showing no significant difference in the helicity volume (%).

In the correlation processes between CD (**Table 3-1**) and NMR data (**Table 3- 3**), it has been found that the data by **eq. B-3** can hold a higher linearity ($y = 0.82x - 0.03$, $R^2 = 0.958$) with the CD intensity those by **eq. B-1** ($y = 0.68x + 2.17$, $R^2 = 0.945$) and **eq. B-2** ($y = 0.77x + 4.13$, $R^2 = 0.942$). Moreover, the correlation line by **eq. B-3** passed through the origin (**Figure 3-6**). On the other hand, the data by **eq. B-2** showed larger deviation than those by **eq. B-1**. Other than these results, we have collected several reasons why **eq. B-3** can be recommended in the stereochemical study of sn-glycerols including phospholipids and glycolipids (Mengfei and Nishida, unpublished).

3-4 Conclusion

We have described about variable helical properties in compounds **2~8** as models of 1,2-di-O-acyl-sn-glycerols. The independent analyses undertaken with circular dichroic (CD) and ^{1}H NMR spectroscopies were in good agreements: all these 1,2-di-*O*-benzoyl-sn-glycerols possessed right-handed helicity around the sn-1,2 di-O-benzoates regardless of their sn-3 substituting groups. The gt-(+) conformer was predominated in constant over gg-(-) and tg conformers. On the other hand, disparity between gt-(+) and gg-(-) conformers was variable among these compounds due to notable effects of the sn-3 substituting groups. The effects can be expressed with the correlation line passing thought the origin (**Figure 3-6**), which has been induced in the present study owing to the CD di-benzoate chirality method of Nakanishi and Harada,[16] the general Karplus equation by Haasnoot et al.[15] and the chirally deuterium-labelling methodology of Ohrui and Meguro et al.[24,25]

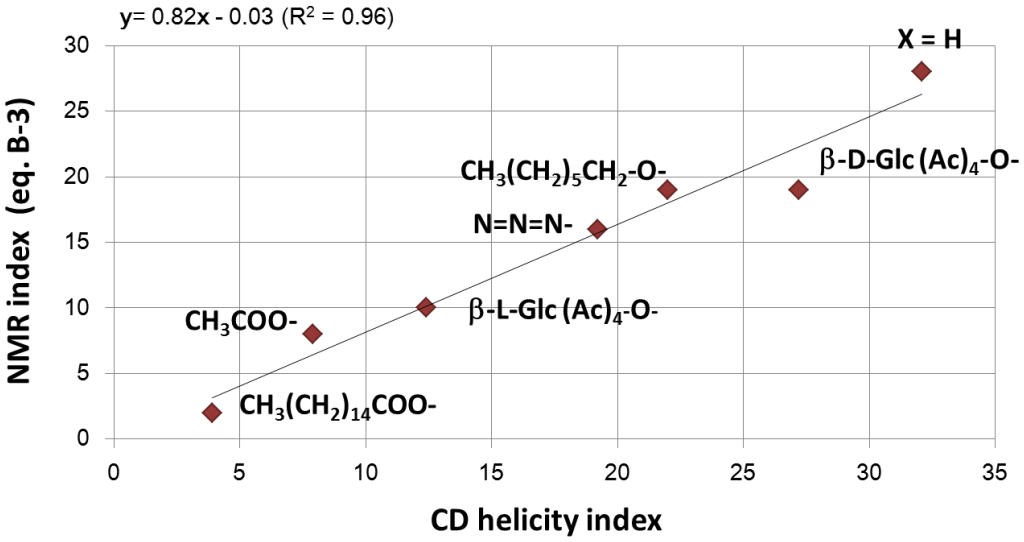

Figure 3-6

As can be seen also in **Figure 3-4**, helical property around the sn-1,2 di-O-benzoates varied largely by the nearby sn-3 groups. The compound **4** (**X** = H) without oxygen atom at sn-3 showed the strongest helical intensity meaning that the sn-3 oxygen atom in sn-glycerols has a notable effect to average disparity between gt-(+) and gg-(-) conformers at sn-1,2 position. The sn-3 O-acyl groups in **7** and **8** strongly reduced the helical disparity, while keeping the rule of gg-(+) > gg (-). Effects of sn-3 O-glycoside linkages were changeable by stereochemistry in the head sugar groups. Effect of sn-3 azide (-N=N=N) group looked very similar to those of O-alkyl groups but could be differentiated in the correlation between CD intensity and ^{1}H

NMR helicity volume as was shown in **Figure 3-5b**.

It should be mentioned at the end of this summary that effects of these sn-3 substituting groups are associated closely with the homologous solution state in methanol. The obtained effects will be changed widely by the solvents used and other surrounding conditions. Our recent interests are focused on roles of sn-3 O-glycosyl groups at the head in 1,2-di-O-acyl-sn-glycerols which possess a strong self-assembling property analogously phospholipids. Though situations will become more complicated than the present case, the approach undertaken here will work effectively towards solution of stereochemistry in these biomembrane forming 1,2-di-O-acyl-sn-glycerols.

3-5 References and Notes

1. "Nomenclature of Lipids", IUPAC-IUB Commission on Biochemical Nomenclature (CBN) (www.chem.qmul.ac.uk/iupac/lipid).
2. Awai, K., Ohta, H., Sato, N., *Proc. Natl. Acad. Sci. USA*, **2014**, 111(37), 3571-13575. And see the related references cited therein.
3. Nishida, Y.; Tamakoshi, H.; Kobayashi, K.; Thiem, J. *Org Lett.*, **2001**, *3*, 1-3.
4. Uzawa, H.; Nishida, Y.; Hanada, S.; Ohrui, H.; Meguro, H. *Chem. Commun*. **1989**, 862-863.
5. Nishida, Y.; Uzawa, H.; Hanada, S.; Ohrui, H.; Meguro, H. *Agric. Biol. Chem.* **1989**, 53, 2319-2323.
6. Uzawa, H.; Nishida, Y.; Ohrui, H.; Meguro, H. *J. Org. Chem.* **1990**, *55*, 116-122.
7. Nishida, Y.; Shingu, Y.; Mengfei, Y.; Fukuda, K.; Dohi, H.; Matsuda, S.; Matsuda, K. *Beilstein J. Org. Chem*., **2012**, *8*, 629-639.
8. Hauser, H.; Pascher, I.; Pearson, R.H.; Sundell, S. *Biochim. Biophys. Acta,* **1981**, 650, 21-51.
9. Hauser, H.; Radloff, C.; Ernst, R. R.; Sundell, S.; Pascher, I. *J. Am. Chem. Soc*., **1988**, *110*, 1054.

10. Hong, M.; Schmidt-Rohr, K.; Zimmermann, H. *Biochemistry*, **1996**, *35*, 8355-8341. (Phospholipid analysis by 2D NMR).
11. Feller, S.; MacKerell, Jr., A. D. *J. Phys. Chem. B*., **2000**, *104*, 7510-7515.
12. Krishnamurty, S.; Stefanov, M.; Mineva, T.; Begu, S.; Devoissell, J. M.; Goursot, A.; Zhu, R.; Salahub, D. R. J. Phys. Chem. B, **2008**, *112*, 13433.
13. Hauser, H.; Pascher, H.; Sundell, S. *Biochemistry*, **1988**, *27*, 9166-9174.
14. Uzawa, H.; Nishida, Y.; Ohrui, H.; Meguro, H. *Agric. Biol. Chem.*, **1989**, *53*, 2327.
15. Haasnoot, C. A. G.; de Leeuw, F. A. A. M.; Altona, C. *Tetrahedron* **1980**, *36*, 2783-2790.
16. Harada, N.; Nakanishi, K. *Circular Dichroic Spectroscopy Exciton Coupling in Organic Stereochemistry*; University Science Books: California, 1983.
17. Wiesler, W.; Nakanishi, K. *J. Am. Chem. Soc.*, **1989**, *111*, 3446.
18. Nishida, Y.; Hori, H.; Ohrui, H.; Meguro, H. *J. Carbohydr. Chem*. **1988**, *7*, 239-250.
19. Marchessault, R. H.; Peretz, S. *Biopolymers*, **1979**, *18*, 2369.
20. Wolfe, S. *Acc. Chem. Res.*, **1972**, *5*, 102.

21. Duin, J.; Baas, J. M. A.; Graaf, B. *J. Org. Chem*., **1986**, *51*, 1298.

22. Rockwell, G. D.; Grindley, T. B. *J. Am. Chem. Soc*., **1998**, *120*, 10953-10963.

23. Woods, R. J.; Kirschner, K. *Proc. Natl. Acad. Sci. USA*, **2001**, *98(19)*, 10541-10545.

24. Ohrui, H.; Horiki, H.; Kishi, H.; Meguro, H. *Aric. Biol. Chem*. **1983**, *47*, 1750.

25. Ohrui, H.; Nishida, Higuchi, H.; Hori, H. Meguro, H. *Can. J. Chem.*, **1987**, *65*, 1145.

Chapter 4

Stereochemical profiles of *M. pneumoniae* glycolipid (β-DGGLs) and the relating cell-membrane phospholipids and glycolipids

4-1 Introdution

α. *sn*-Glycerol as prochiral compound

Glycerol (1,2,3-propan-triol) is a symmetric three-carbon compound, and the prochiral positions are defined with *sn*-1 and *sn*-3 numbering according to the IUPAC rule of stereospecific numbering [1]. S*n*-glycerol can be understood in the term of a "prochiral compound."[2] This means that when either the sn-1 or sn-3 position is chemically modified, the symmetric glycerol derivative turns to a chiral compound having an asymmetric center at the C-2 position. Actually in nature, the two *sn*-positions are discriminated by both synthetic and degrading enzymes, and thus, most of naturally occurring glycerol derivatives are optically active chiral compounds.

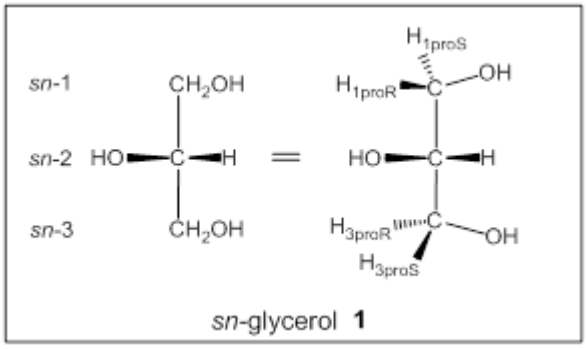

Figure 4-1. S*n*-glycerol as "prochiral compound."

b. Chiral 1,2-di-*O*-acyl-*sn*-glycerols in nature

Cell-membrane phospholipids such as DPPC are also chiral lipids, possessing an asymmetric center at the sn-glycerol

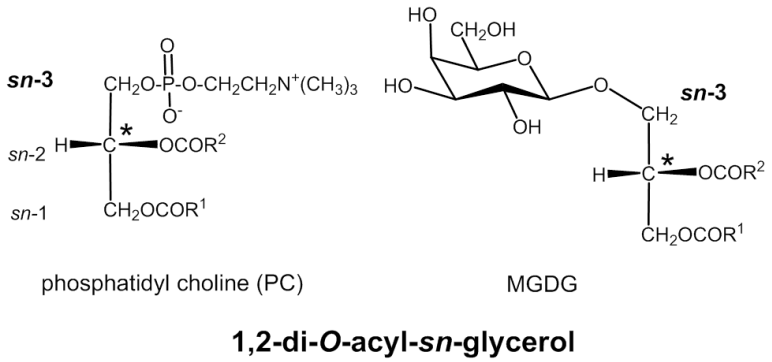

Figure 4-2. Chiral 1,2-di-*O*-acyl-*sn*-glycerols in nature

C-2 position. In both eukaryote and prokaryote biosynthetic systems, 1,2-di-O-acyl-sn-glycerol provides a basic asymmetric backbone in sn-glycerol phospholipids and glycolipids. The sn-1,2 positions are replaced with either *O*-acyl (ester) or *O*-alkyl (ether) groups. This can be explained in the term of "biological homochirality"[3] which expresses that only one of two enantiomers is utilized in our life system.

The biological homo-chirality is being kept in chlorophile photosynthetic systems, Both mono-β-D-galactopyranosyl -sn-glycerolipids (MGDG) and di-galactosyl-sn-glycerolipids

(DGDG) are major components of photosynthetic cells, namely, thylakoid and believed to play major roles in photosynthesis.[4,5] Irrespective of natural sources, the β-D-galactopyranosyl linkage is attached at the glycerol *sn*-3 position.[4-7] Obviously, the enantiomer selectivity in enzymatic trans-glycosylation conforms to the rule of the "biological homo-chirality" .

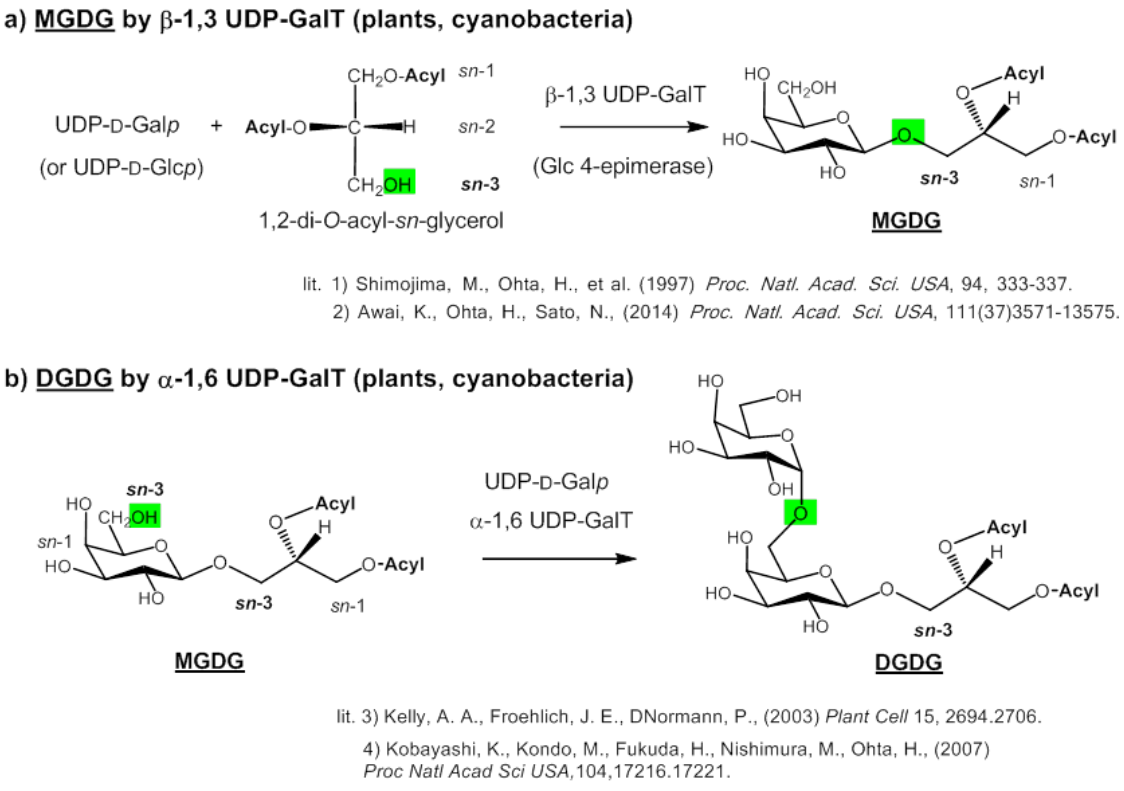

Figure 4-3. Synthesis of MGDG and DGDG

a) Absolute structures of *M. pneumoniae* cell-membrane glycolipids (β-DGGLs)

It has long been suggested that *M. pneumonia* may possess antigenic peptides or other membrane-bound lipids which specifically occur in this microbe.[8] Our research group had identified a set of glycolipids (**β-DGGLs, Figure 4-4**) in *M. pneumonia* which serve as the specific antigen.[9,10] They were isomers having an identical molecular weight (Mw) each other, and their absolute structures were elucidated by chemical syntheses of each isomer.[10] In **β-DGGLs**, a β-D-galactopyranosyl linkage is attached at the glycerol sn-3 position, and they have another β-D-glucosyl (Glc-type) or β-D-galactosyl (Gal-type) linkage at the galactose O-6 (primary) position.

Figure 4-4. **Cell-membrane lipid-anitigens of *Mycoplasam pneumonia* (β-DGGLs)**

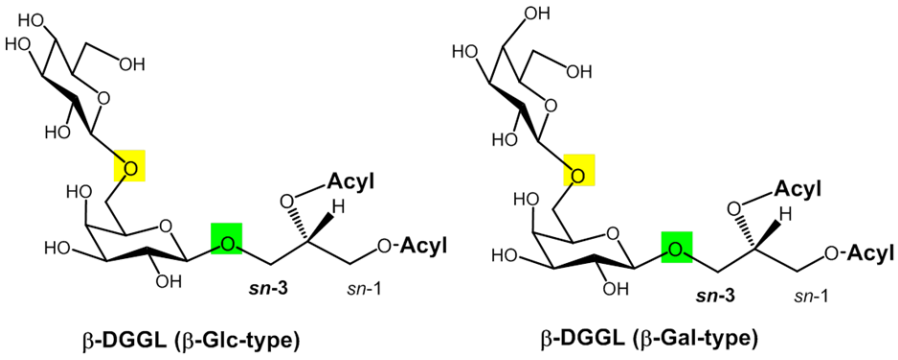

The overall chemical structures of β-**DGGLs** are very close to plant DGDG except for the fact that the non-reducing glycoside is bound with β-(1→6)-linkage, and the sn-glycerol 1,2-di-O-acyl groups are replaced with saturated fatty acid esters (C_{16} and C_{18}).

The genome size of *M. pneumonia* is 816kb with 688 open reading frames (ORFs) [11,12] which corresponds to less than 20% (ca. 18%) of *E. coli* genome size. The ORFs coding β-glycosl enzymes (MPM483) have been identified to be in a group of CAZy GT-family 2, which utilizes either UDP-Gal or UDP-Glc as the glycosyl donor for the biosynthesis of sn-glycerol β-galactolipids.[13]

b) Conformational property of chiral 1,2-di-O- acyl- *sn*-glycerols

The C-C single bonds in the 1,2-di-O-acyl-sn-glycerol give rise to rotational conformers, gg (gauche-gauche), gt (gauche-trans) and tg (trans-gauche). The molecular conformational flexibility as well as the molecular asymmetry seems characteristic of both phospholipids and glycolipids made of the acyclic *sn*-glycerol. It can be also considered that a fluid membrane property is

ascribable to self-assemble of these surface active compounds (amphiphiles). On the other hand, the rotational property along each of the glycerol sn-1,2 and sn-2,3 single bonds has rarely been studied in the past [14,15] and yet not fully understood.

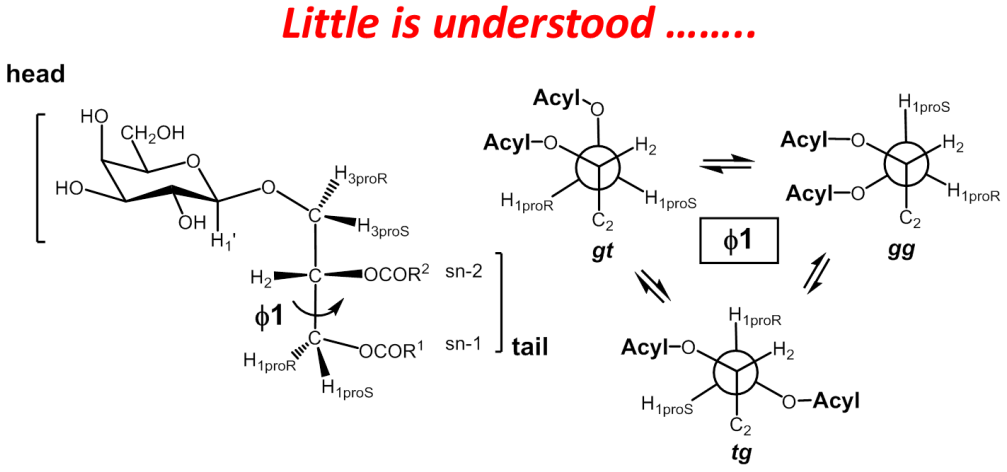

Figure 4-5. Conformational property around the acyclic sn-glycerol moiety

Since these amphiphilic compounds make self-assembled structures, a major part of conformational studies have been directed to their liquid crystalline (LC) and gel properties. This holds true for the conformational studies on phospholipids which constitute self-assembled lamellar structures in LC and gel phases depending on surrounding temperatures.[16,17,18]

For studies on the conformational property of organic

compounds, ^{1}H-NMR spectroscopy has provided powerful tools and methodologies. By coupling this advanced spectroscopic technology with synthetic carbohydrate chemistry, our group has analyzed conformational properties of mono-, di- and oligosaccharides.[19,20] In the analyses of *sn*-glycerols (**Figure 4-6**), many analyses have been hampered by the presence of four diastereomeric protons at sn-1 and sn-3 positions which make ^{1}H NMR signals highly complicated.

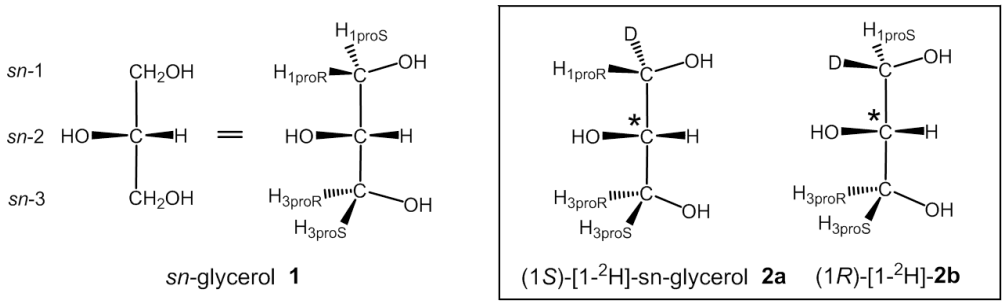

Figure 4-6. The structure of sn-glycerol 1 and 2a .2b

We have solved this problem by developing the technology of stereoselective deuterium labeling to produce **2a** and **2b** and thereby analyzed conformations in solutions [2,21,22]. Large ^{1}H NMR data have been collected by our approach and led to formulation of some empirical ^{1}H NMR rules very useful for discrimination of the diastereomeric protons, HproR and HproS in chiral molecules [22].

4-2 Aim of this study

In the preceding chapter (see **Chapter 2**), our conformation analysis was performed for the *M. fermentans* α-glycolipid antigen (GGPL-I).[22] There, we have seen that GGPL-I and the relating α-glycolipids are able to construct a self-assembled bilayer membrane together with ubiquitous phospholipids without stereochemical stress. This conclusion was based on the results that the rotational property of the *M. fermentans* glycolipid (GGPL-I) is very close to that of phospholipids having an identical sn-configuration with 1,2-di-*O*-palmitate structure.

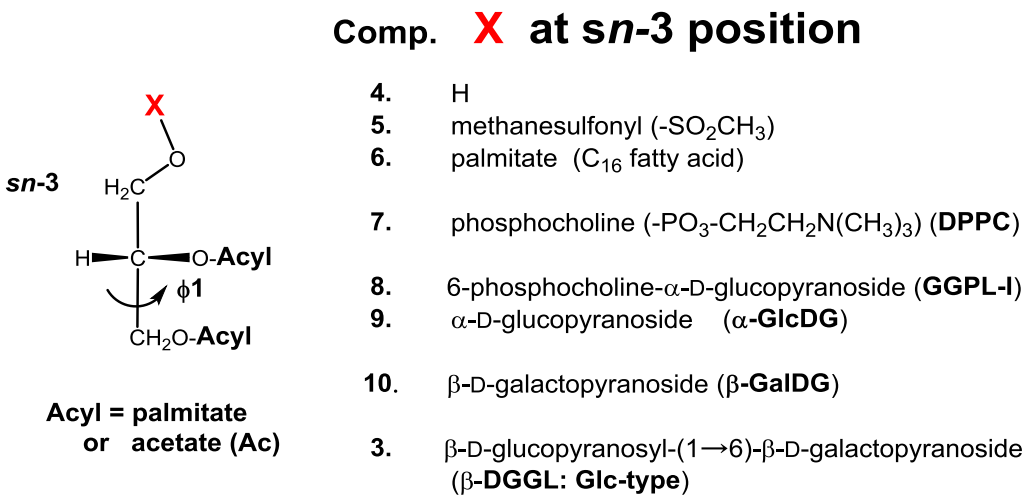

Figure 4-7. series of 3-substited 1,2-di-O-acyl-sn-glycerols (compounds 3~10) including the *M. pneumoniae* β-DGGL

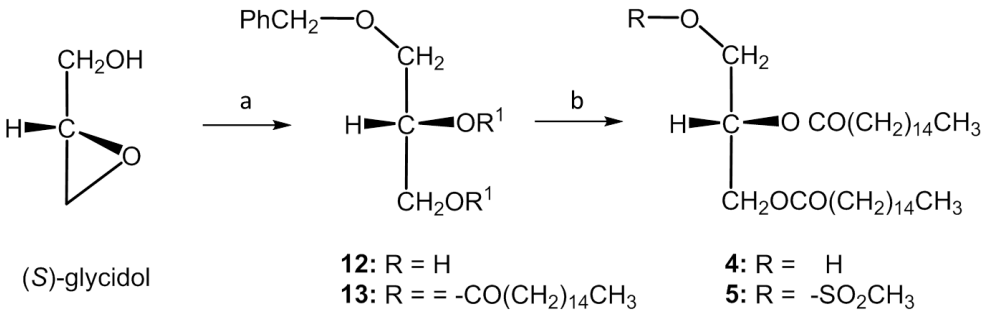

(*S*)-glycidol

12: R = H
13: R = = -$CO(CH_2)_{14}CH_3$

4: R = H
5: R = -SO_2CH_3

a) Reagents: i) BnCl, NaH/DMF, ii) TFA, Ac_2O, iii) K_2CO_3 in MeOH , iv) Palmitoyl chloride in pyridine (65% yields)
b) Reagents: i) H_2, $Pd(OH)_2$ in 2-propanol, ii) CH_3SO_2Cl in pyridine (72% yields)

Scheme 4-1. Synthesis of compounds **4** and **5**

In the present study, the study was extended to the conformation analysis for a series of 3-substited 1,2-di-O-acyl-sn-glycerols (compounds **3~10**)(**Figure4-7**) including the *M. pneumoniae* β-DGGL (compound 3). As reference compounds, the author analyzed also the 1,2-di-O-acetyl derivatives of **3** (β-Gal) and **10** (β-GGGL) which were soluble not only in a mixture of organic solvents ($CDCl_3$ and CD_3OD) but also in pure water (D_2O).

4-3 Materials and Methods

a. **Preparation of 1,2-di-*O*-acyl-sn-glycerols**: Synthesis of compounds **4** and **5** were carried out in a manner as outlined in **Scheme 4-1**. The glycolipids (**3**, **8-10**) were prepared in our established way [10,22]. Other compounds were purposed from Tokyo Kasei Kogyo Co. Ltd., (TOKYO)

and used without purification.

b. **^{1}H NMR measurement**: NMR was measured on JEOL-JNM -LAs-500 (500 MHZ) at 25~30℃ in several solvent systems, *i.e.*, $CDCl_3$, a mixture of $CDCl_3$ and CD_3OD (1:1~1:10) and D_2O. Concentrations were set at ca. 10mM solution in each solvent.

c, **Karplus equations for analysis around the sn-1,2- C-C single bond**: Each of single C-C single bonds in the sn-glycerol moiety can afford three staggered conformers of *gg* (*gauche-gauche*), *gt* (*gauche-trans*) and *tg* (*trans-gauche*). In solution and also in self-contacting liquid crystalline (LC) states, transition between conformers occurs more quickly (within $1.0x10^{-12}$~$1.0x10^{-10}$ sec) than NMR time scale (order of $1x10^{-6}$ sec). This means that NMR singles reflect the position of rotational equilibrium among the three conformers. The position of the equilibration can be estimated with ^{1}H-1H coupling constants of ^{1}H NMR spectroscopy with assist of a general Karplus equation of Haasnoot et al. [23].

Equation-(1)

$^{3}J_{H,H}(Hz) = 13.22\cos^{2}\Phi - 0.99\cos\Phi + R$

$R = \mathrm{Sum}\{\Delta Xi[0.87 - 2.46\cos^{2}(r\Phi + 19.9\mathrm{ABS}(\Delta Xi))]\}$ (r = +1 or -1).

$^{3}J_{H,H}$ (Hz)is a vicinal 1H-1H coupling constant (Hz). R is the sum of effects of each electron negative substituent in neighbor to the coupling protons

Table 4-1. Parameters for optimization of Karplus equation

Basic Karplus equation	$^{3}J_{H,H}$= 13.22cos^2Φ -0.99cosΦ + R (effects of electron negative substituents)							
	R = Sum ΔXi[0.87-2.46cos^2(rΦ+19.9ABS(ΔXi))] (r = +1 or -1)							
Parameters		**electron negativity (ΔXi)**			**Dihedral angles**	*gg*	*gt*	*tg*
	X1=C3	0.4	0.4	0.08	Φ (O2,O3)	-60	60	180
	X2=O2	1.3	1.3	1.22				
	X3=O1	1.3	1.3	1.22				
Dihedral angles	Dihedral angles	*gg*	*gt*	*tg*	Ref : 1) Haasnoot, C. A. G.; de Leeuw, F. A. A. M.; Altona, C., Tetrahedron, (1980), 36, 2783-2790. 2) Y. Nishida et al, J. Carbohydrate Chem., (1988), 7 (1) 239-250.			
	Φ (H2,H1proS)	-60	60	180				
	Φ (H2,H1proR)	60	180	300				
RESULTS								
Contribution of Φ	JH2,H1proS (Factor of Φ)	2.81	2.81	14.21				
	JH2,H1proR (Factor of Φ)	2.81	14.21	2.81				
		JH2,H1proS			JH2,H1proR			
		gg	*gt*	*tg*	*gg*	*gt*	*tg*	
Contribution of R	R1 (C3)	-0.02	0.21	-0.62	0.21	-0.62	-0.02	
	R2 (O2)	1.11	-1.06	-1.46	-1.06	-1.46	1.11	
	R3 (O1)	-1.06	1.11	-1.46	-1.06	-1.46	1.11	
	R = SUM(R1,R2,R3)	0.03	0.26	-3.53	-1.91	-3.53	2.20	
Induced Karplus relations		***gg***	***gt***	***tg***				
	JH2,H1proS =	**2.8**	**3.1**	**10.7**				
	JH2,H1proR =	**0.9**	**10.7**	**5.0**				

A three-simultaneous Equation- (2) was induced from the general Karplus equation-(1). This is optimized for the analysis of acyclic 1,2-di-O-acyl-sn-glycerols, in which every electron negative substituent in

each of the three staggering conformers was taken into accounts.

Equation-(2)

$$2.8gg + 3.1gt + 10.7tg = {}^{3}J_{H2,H1S} \quad (\text{or } {}^{3}J_{H2,H3R})$$

$$0.9gg + 10.7gt + 5.0tg = {}^{3}J_{H2,H1R} \quad (\text{or } {}^{3}J_{H2,H3S})$$

$$gg + gt + tg = 1$$

In the equation-(2), a perfect staggering (ϕ1 and ϕ2 = +60, -60 or 180 degree) is assumed for every rotamer. This equation can be modulated by changing the dihedral angle from those in perfect staggering when it is considered necessary[20] .The optimization process by changing the electron negativity and the dihedral angles can be performed with a PC software (free software in Microsoft Excel, Nishida & Yuan, Chiba University, 2015, **Table 4-1**).

4-4 Results and Discussion

a) Conformational property of 1,2-di-O-palmitoyl-sn-glycerols with a hydrophobic substituting group at the sn-3 position

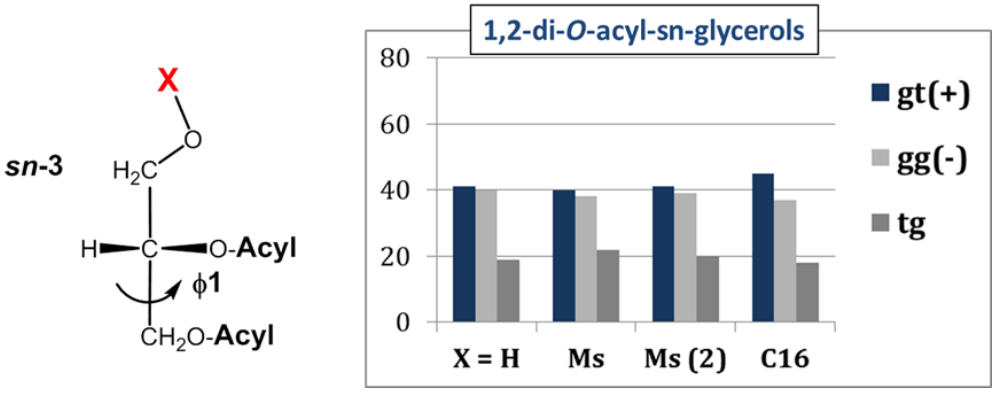

Figure 4-8. Conformational property of 1,2-di-O-palmitoyl-sn-glycerols

Solvent systems: Every compound was dissolved in a homologous medium of $CDCl_3$. In the case of the methanesulfonyl derivative (Ms), a mixture of $CDCl_3$ and CD_3OD (10:1) was also tested to give the result in Ms(2). **Abbreviation:** Acyl = palmitate (C16), Ms = 3-O-methanesulfonyl derivative, C16 = 3-O-palmitoyl derivative.

In solution states as undertaken in the present ^1H NMR study, the titled 1,2-di-O-palimitoy-sn-glycerols were found to show a conformational behavior very similar to each other. The rotamers equilibrium was constant among them keeping the approximate ratio of *gt* (40-45%), *gg* (40%) and *tg* (20%), (**Figure 4-8**) When the result of compounds **4** (X=H) is compared with those of **5** (X=Ms and Ms(2)) or **6** (X=C16, palmitate), we can know the substituent effect by these hydrophobic group at the sn-3 position. These hydrophobic groups have induced no apparent change along the tail sn-1,2 conformation. It is notable that the *gauche*-conformers (gt and gg) are more favored than the *trans*-conformer (tg). This is consistent in any acyclic compounds we gave so far examined and has been rationalized with the term of "gauche-effect".

b. Conformational property of GGPL-I and DPPC with a polar substituting group at the sn-3 position

The amphiphilic DPPC favors the *gt*-conformer strongly around the tail sn-1,2 position [ϕ1 along the C(1)-C2(2) bond] disfavoring the *tg*-conformer in an approximate ratio of *gt* (60%), *gg* (35%) and *tg* (5%, **Figure 4-9**). The difference of DPPC from the previous hydrophobic sn-glycerols is obvious, especially in the point that the sn-3 phosphocholine group can induce a significant change in the conformational property along the acyclic tail moiety. It is notable also that the clockwise helicity is pronounced by the increasing gt(+)-conformer versus the anticlockwise gg(-) one along the asymmetric 1,2-di-O-acyl-sn-glycerol backbone .

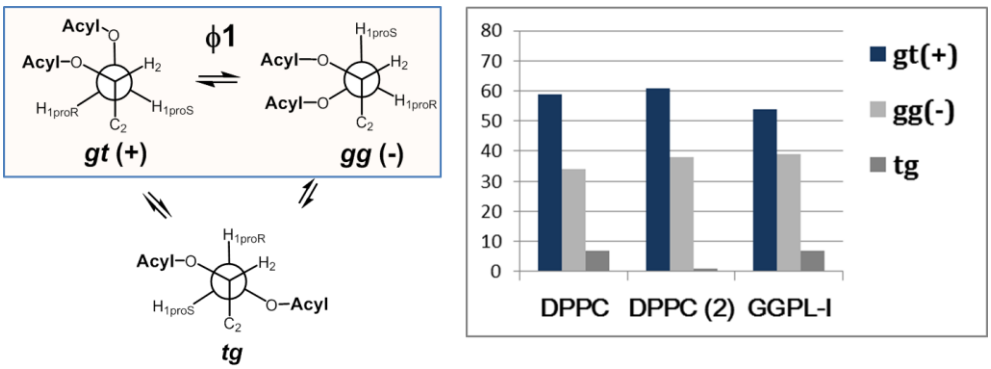

Figure 4-9. Conformational property of GGPL-I and DPPC

Solvent systems: A mixture of $CDCl_3$ and CD_3OD (10:1). In the case of DPPC (2), an alternative solvent system, i.e., a mixture of $CDCl_3$ and CD_3OD (2:1) was used.

Abbreviations: DPPC = 1,2-O-dipalmitoyl-sn-phosphatidylcholine,

GGPL-I: One of major glycolipid antigens of *M. fermentans* and can be characterized by the presence of phosphocholine group at the α-Glc-6-OH position [22].

M. fermentans α-D-glucopyranosyl-*sn*-glycerolipids (GGPL-I) showed a similar tendency in the conformational property though the increment of the gt(+)-conformer was smaller than the case of DPPC. Both DPPPC and GGPL-I take the two *gauche*-conformers near exclusively at the tail position. This seems very unique to the amphiphilic 1,2-di-O-acyl-sn-glycerols and also significant in the event of forming a plasma membrane. We have observed also that the GGPL-I head moiety around the sn-2,3 position adapts a random conformation taking every gt, gg, and tg-conformers in averaged ratio (1:1:1). Probably, these amphiphilic chiral sn-glycerols can cooperate well in forming a lamellar structure without separating from each other and without giving stereochemical stress to each other.

c. Conformational property of *Mycplasma pneumoniae* β-MGDG and β-DGGL

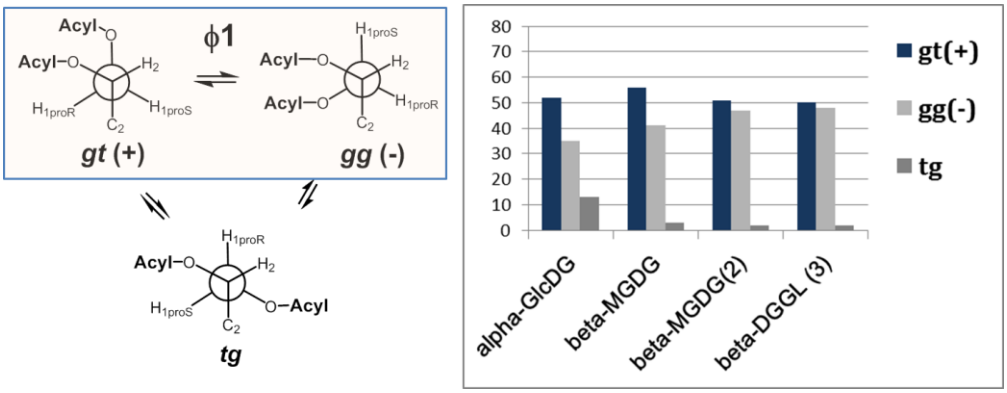

Figure 4-10. Conformational property of *Mycplasma pneumoniae* β-MGDG and β-DGGL

Solvent systems: For beta-GlcDG□[1,2-di-O-palmitoyl-3-O- (β-D-glucopyranosyl)-sn-glycerol] and its β–D-galactopyranosyl isomer (beta-MGDG), a mixture of $CDCl_3$ and CD_3OD (10:1) was used as solvent. For beta-MGDG(2), a mixture of $CDCl_3$ and CD_3OD (1:1), for beta-DGGL(3), a mixture of $CDCl_3$ and CD_3OD (2:1) was used.

Mycoplasma pneumonia possesses mono-β-Gal glycerolipid (β-MGDG in **Figure 4-10**) which serves as a key intermediate for bio-syntheses of β-DGGLs (β-Glc- and β-Gal-types, in **Figure 4-4**). The present study examined the conformational property of both β-MGDG and β-DGGL (β-Glc-type) and compared their behaviours with DPPC, GGPL-I and its synthetic precursor, α-GlcDG [24,25].

The results in **Figure 4-10** indicate that these β-Gal glycerolipids tended to exclude the *trans*-conformer (tg) more strongly than α–GlcDG. In comparison with DPPC and GGPL-I (**Figure 4-9**), they took the anticlockwise gg(-) more strongly. This tendency was enhanced in the methanol-rich solvent [β-MGDG(2)] and also in the *M. pneumonia*

β-DGGL. There, time-averaged populations of the three rotamers was gt:gg:tg = ca. 50:50:0, indicating that the tail sn-1,2 position adapts the two *gauche*-conformers having a reversing helicity each other. The conformational behaviour of β–MGDG was changed by solvents, and there was notable difference in conformational behaviours between α-gluco-lipid (α–GlcDG) and the *M. pneumonia* β-glycolipids (β-MGDG and β-DGGL).

d. Effects of acyl groups and solvents on the conformational property along the tail sn-1,2 position

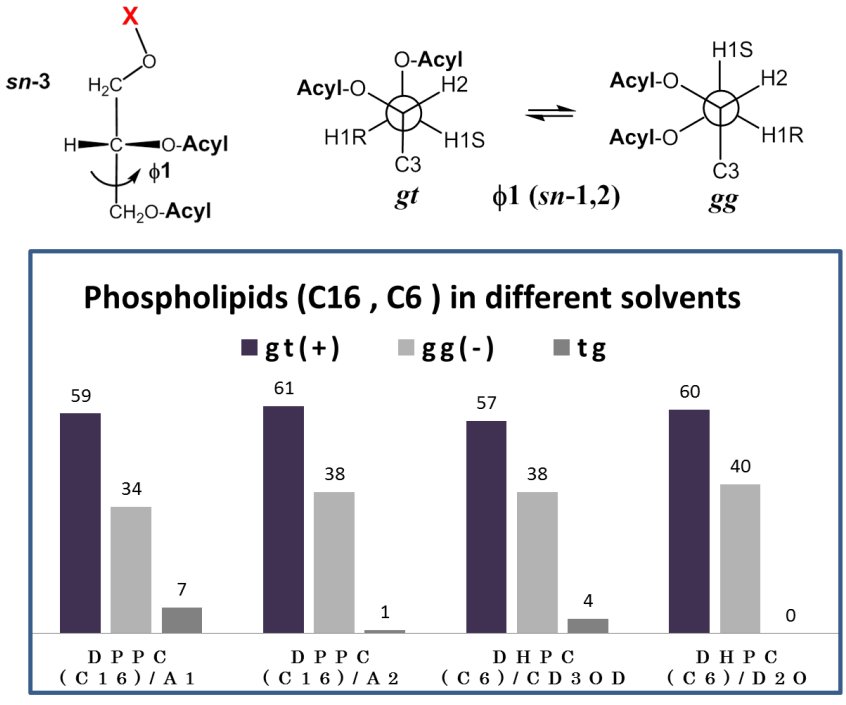

Figure 4-11. conformational property of Phospholipids in different solvents

Solvent systems: A1: $CDCl_3$+CD_3OD (10:1), **A2**: $CDCl_3$+CD_3OD (2:1), **CD3OD** = CD_3OD (>99.5%), **D2O** = D_2O (>99.5%).

Next, the author wish to discuss on the possible effect of acyl groups by referring the NMR data of DPPC and its n-hexanoate (C6) derivative (DHPC: 1,2-di-*O*-hexanoyl-sn-phosphtidyl choline), which were reported by Hauser et al [14,15] and analyzed in our way (**Figure 4-11**). As shown in this figure, the basic conformational property of DPPC is affected neither by the acyl groups nor by the solvents dissolved. The strong gt(+) and gg(-) preference to the tg conformer is not ascribable to a possible hydrophobic interaction between the long C16 acyl groups at the tail sn-1,2 position. Also strong hydration around the head moiety does not seem to affect the conformation property at the tail, and the overall conformation behavior of DPPC looks stable under different solvent conditions.

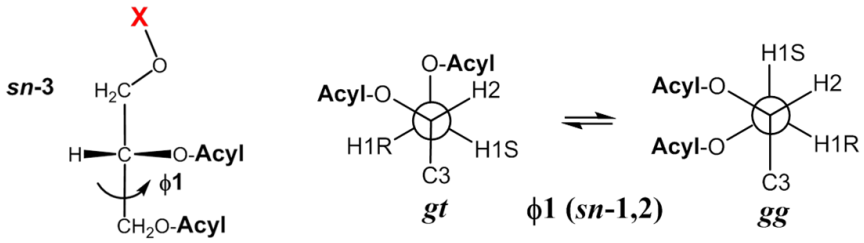

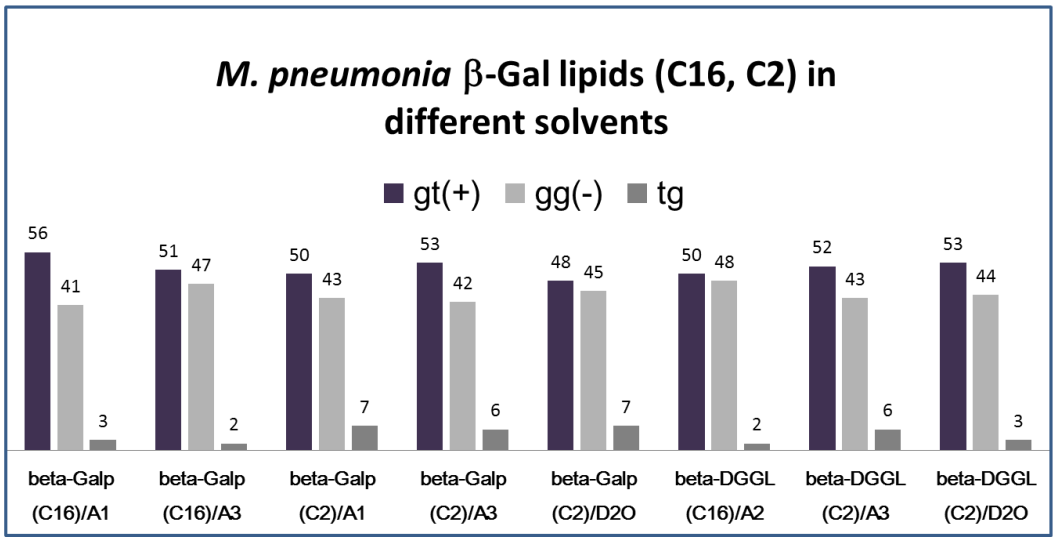

Figure 4-12. Conformational property of *M. pneumonia* β-Gal-lipids in different solvents

Solvent systems: **A1**: $CDCl_3$+CD_3OD (10:1), **A2**: $CDCl_3$+CD_3OD (2:1), **A3**: $CDCl_3$ and CD_3OD (1:1), **D2O** = D_2O.

In case of the *M. pneumonia* β-Gal-lipids, acetyl (C_2) homologues were prepared in our research group (R. Matsunaga, K. Fukuda, H. Dohi & Y. Nishida, unpublished result) and listed in **Figure 4-12** as beta-Galp (C_2) and beta-DGGL (C_2). These acetyl homologues are of highly utility not only in biological studies but also for the present conformational study. This is because they are soluble in water. Otherwise, β-Gal-lipids can be hardly dissolved in aqueous solvents. Therefore, a mixture of chloroform and methanol has been generally used as solvent for making solutions of

glycolipids, despite these organic solvents are unusual in biological systems.

The conformational behavior along the tail sn-1,2 position was very stable in the point that the tg conformer was the most disfavored. Obviously, the observed gt(+)- and gg(-) preference is not associated with hydrophobic interactions, and this result well matched the preceding conclusion in the study on the phospholipids. The population of the anticlockwise-helical gg(-) tended to decrease, while the tg-conformer increased to some extents when the long C16 group was replaced with the acetyl group. However, the relative order of gt(+) ≥ gg(-) >> tg was maintained among all of the *M. pneumonia* β-Gal lipid homologue examined here, and their rotational properties long the sn-1,2 position was substantially different from what we have seen in the phospholipid homologues in the point that the clockwise-helical gt (+) conformer is more strongly favored in the order as gt(+) > gg(-) >> tg.

d. Conformational property of *M. pneumonia* β-Gal lipids around the head moiety

To elucidate the three dimensional (3D) structures of the M. pneumonia β–Gal lipids (β-MGDG and β-DGGL), ^{1}H NMR analysis was extended to the glycerol sn-2,3 position. A definitive assignment was performed for

the diastereomeric protons (H-3proR and H-3proS) at the sn-3 position by adapting our preceding ^{1}H NMR rule for β-(1→6)-linked disaccharides [19]. Briefly, the β-glycoside linkage at the hexose O-6 position causes a significant downfield shift for H-6proS signal (ca. 0.2-0.3 ppm), while the α-glycoside linkage causes the downfield shift for H6proR signal (ca. 0.2~0.3 ppm). In the ^{1}H NMR spectrum of 1,2-*O*-dipalmitoy-sn-glycerol (compound **4** in **Figures 4-8** and, the two H-3 protons appeared at a region very close to each other (δ ppm = 3.72~3.73) in a typical AB-X coupling pattern. In the β-Gal-linkage caused the downfield shift to H-3proS (3.93 ppm) relative to H-3proR (3.7 ppm) by ca. 0.2 ppm. Definitive assignment was carried out also for the two H-6 protons (H-6proR and H-6proS) of each glycoside residue according to our preceding data of (*6S*)-[6-^{2}H]-D-hexoses [20]. Thus, every ^{1}H-signal has been assigned for the conformational analysis at the head group in the M. pneumonia β-Gal glycerolipids (**Tables 4-2** and **4-3**).

Table 4-2 Complete ^{1}H-NMR assignments of *M. pneumonia* β-MGDG homologues in solution states.

Comp	Solv	^{1}H signals (Chemical shift ppm / J HZ)						
	sn-Glycerol	H1proR	H1proS	H2	H3proR	H3proS		
beta-MGDG (C16)	CDCl3/CD3OD= 1/1 (v/v)	4.18	4.37	5.22	3.69	3.93		
		6.0	3.1	m	5.7	5.2		
		11.7	11.7		10.7	10.7		
	Gal	H-1'	H-2'	H-3'	H-4'	H-5'	H-6'proR	H-6'proS
		4.19	3.46	3.46	3.83	ca 3.5	ca. 3.7	3.75
		7.8	m	m	br	overlap	br	m
	CDCl3/CD3OD=	H1proR	H1proS	H2	H3proR	H3proS	(d ppm / J HZ)	
	1 0 /1 (v/v)	4.14	4.27	5.19	3.62	3.85		
		6.5	3.2	m	6	5.5		
		12.1	12.1		11	11		
	Gal	H-1'	H-2'	H-3'	H-4'	H-5'	H-6'proR	H-6'proS
		4.14	3.4-3.7	3.4-3.7	3.82	3.4-3.7	3.67	3.76
		7.5	overlap	overlap	0.4	m	5.2	6.5
beta-MGDG (C2)	CDCl3/CD3OD= 1/1 (v/v)	H1proR	H1proS	H2	H3proR	H3proS		
		4.18	4.33	5.2	3.7	3.94		
		6.3	3.4	m	5.5	5.4		
		11.9	11.9		11.01	11.01		
	Gal	H-1'	H-2'	H-3'	H-4'	H-5'	H-6'proR	H-6'proS
		4.19	3.49	3.45	3.83	3.46	3.7	3.75
		8.0	10.0	3.0	0.4	bt	5.9,11.0	6.7
	the second order analysis						3.7	3.75
							5.4	6.6

For the conformational analysis, some of the diastereomeric protons at the D-galactose residue appeared in a close region to afford an ABX coupling pattern. In this case, chemical shift and coupling constants were collected with the second order analysis in an established way.[26] Solvents effects were examined for the water soluble β-Gal-lipids since it is thought that hydration can provide a major factor for determining a conformational property of carbohydrate molecules.[27]

Table 4-3 Complete ^{1}H-NMR assignment of *M. pneumonia* β-DGGL homologues in solution states.

MGDG-OH	D2O	**H1proR**	**H1proS**	**H2**	**H3proR**	**H3proS**		
		3.49	3.57	3.8	3.65	3.8		
		6.0	4.0	m	m	m		
		12.01	12.01					
	Gal	**H-1'**	**H-2'**	**H-3'**	**H-4'**	**H-5'**	**H-6'proR**	**H-6'proS**
		4.29	3.43	3.54	3.8	3.46	3.68	3.63
		8.0	10.0	3.5	0.4	m	9.0, 11.5	4
	the second order analysis						3.68	3.64
							8.4, 11.6	4
beta-DGGL (C16)	CDCl3:CD3OD = 2/1 (v/v)	**H1proR**	**H1proS**	**H2**	**H3proR**	**H3proS**		
		4.18	4.35	5.22	3.69	3.91		
		5.9	3.1	m	5.8	5.5		
		12.01	12.01		11.01	11.01		
	Gal	**H-1'**	**H-2'**	**H-3'**	**H-4'**	**H-5'**	**H-6'proR**	**H-6'proS**
		4.18	3.48	3.43	3.9	3.62	3.8	3.97
		7.7	9.5, 7.7	3.3	3.3	bt	6.2	6.8
								10.5
	Glc	**H-1"**	**H-2"**	**H-3"**	**H-4"**	**H-5"**	**H-6proR"**	**H-6proS"**
		4.3	3.19	ca. 3.3	ca. 3.4	ca. 3.5	3.64	3.84
							5.4	2
								12
beta-DGGL (Ac)	CDCl3:CD3OD = 1/1 (v/v)	**H1proR**	**H1proS**	**H2**	**H3proR**	**H3proS**	Ac1	Ac2
		4.23	4.39	5.25	3.77	3.98	2.09	2.08
		6.2	3.4	m	5.5	5.6		
		12.01	12.01		11.01	11.01		
	Gal	**H-1'**	**H-2'**	**H-3'**	**H-4'**	**H-5'**	**H-6'proR**	**H-6'proS**
		4.24	3.54	3.49	3.94	3.69	3.86	4.02
		7.3	7.4, 9.5	3.3, 9.7	3.3	bt	6.4	6.4
	Glc	**H-1"**	**H-2"**	**H-3"**	**H-4"**	**H-5"**	**H-6proR"**	**H-6proS"**
		4.36	3.25	3.4	~3.34	~3.34	3.7	3.9
		7.9	8.0, 9.0	9.0, 9.0		m	5.5	2
	D2O	**H1proR**	**H1proS**	**H2**	**H3proR**	**H3proS**	Ac1	Ac2
		4.21	4.3	5.2	~3.82	~3.99	2.04	2.02
		6.2	3.2	m	~4.9±0.3	6		
		12.01	12.01		11.5	11.5		
	Gal	**H-1'**	**H-2'**	**H-3'**	**H-4'**	**H-5'**	**H-6'proR**	**H-6'proS**
		4.32	3.42	3.56	3.86	~3.78	3.82	3.95
		7.9	8.0, 9.9	3.3, 10.0	3.3	bdd	~8.0	3.5, 10.6
	Glc	**H-1"**	**H-2"**	**H-3"**	**H-4"**	**H-5"**	**H-6proR"**	**H-6proS"**
		4.43	3.199	3.4	3.9	3.37	3.625	3.83
		8.0	8.0,9.0	8.9, 9.0	9.0, 9.0	ddd	6.0, 12.3	2.3

The conformational behaviour along the sn-2,3 position was compared with 1,2-di-O-palmitoyl-sn-glycerol (1,2-di-palmitin in **Figure 4-13** or compound 4 in **Figures 4-7and Scheme 4-1**), in which sn-3 OH group is free from glycoside linkage. The rotamer distribution along the sn-2,3 bond was analogous to the conformation along the tail sn-1,2 position, favouring the

two *gauche*-conformers of gt(+) and gg(-).

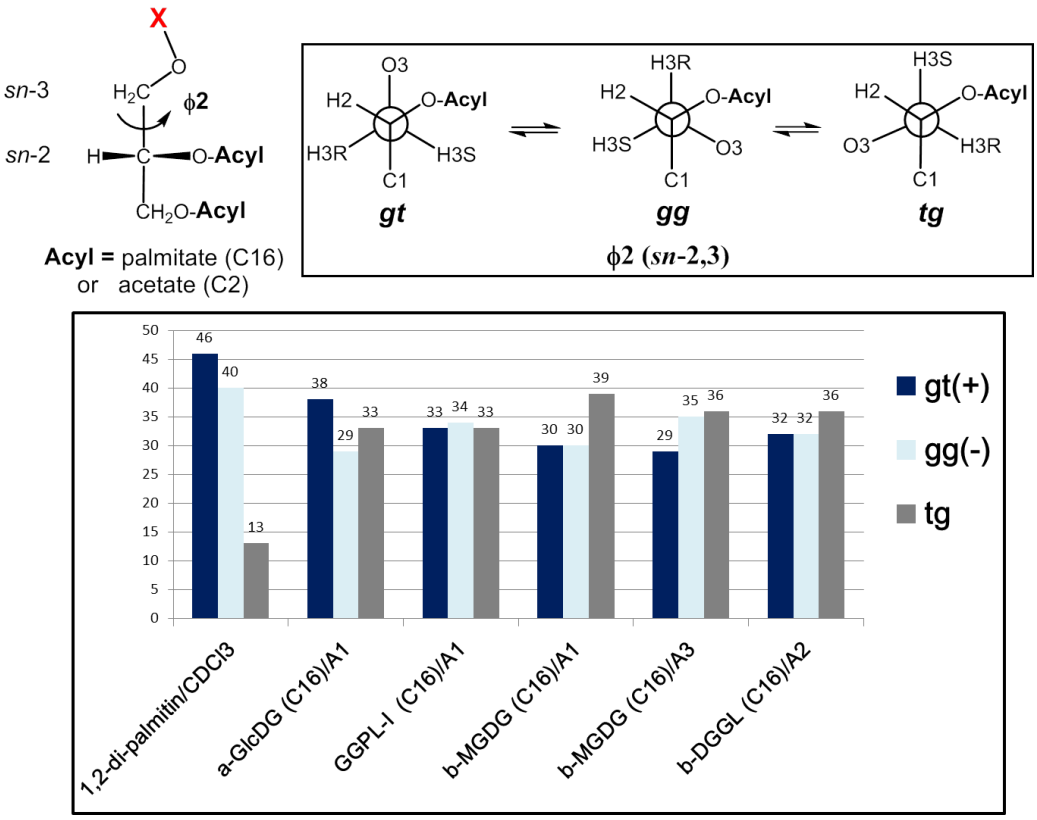

Figure 4-13. Conformational property of compounds above around the head moiety

Solvent systems: A1: $CDCl_3$+CD_3OD (10:1), A2: $CDCl_3$+CD_3OD (2:1), A3: $CDCl_3$ and CD_3OD (1:1), CDCl3 = $CDCl_3$ (chloroform-d).

The observed conformation property was significantly changed when the sn-3 OH was modified with glycoside linkage irrespective of α- and β-linkages. The M. fermentans GGPL-I and the relating a-Glc lipid adapt the three conformers in an averaged extents, *i.e.*, gt:gg:tg = 1:1:1. It should be of high interest to see the trans-tg conformer was favoured in the *M. pneumonia* β-Gal lipids. This is because it is widely accepted that

gauche-conformers become predominant in these acyclic 1,2-diol organic compounds because of "*gauche*-effects".

It is also known that the gauche-effect is enhanced in polar solvents rather than in less polar ones.[2,28,29] Here, the author examined possible effect of solvents by using the C2 (Ac) homologues of β-MGDG and β-DGGL, which were soluble in water. The results as shown in **Figure 4-16** have indicated that the C16 and C2 isomers give rise to no significant difference in the conformational preference along the head sn-2,3 bond in a mixture of $CDCl_3$ and CD_3OD (A1~A3), while the conformational behaviour changed significantly in water their solutions. There, the tg-conformer decreased and the clockwise-helical gt(+) increased. Such a change has never been observed along the tail sn-1,2 bond, and this seem characteristic to the conformation at the head position in these β–Gal glycerolipids.

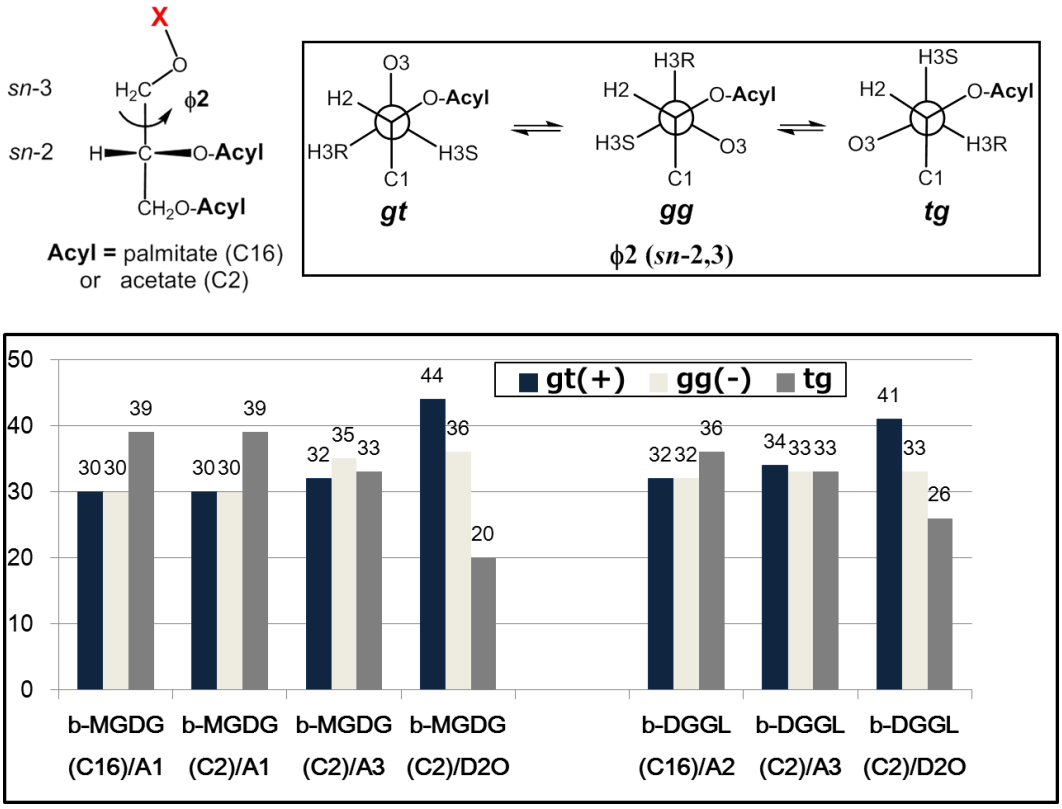

Figure 4-14. Conformational property of compounds above around the head moiety

Solvent systems: **A1**: $CDCl_3$+CD_3OD (10:1), **A2**: $CDCl_3$+CD_3OD (2:1), **A3**: $CDCl_3$ and CD_3OD (1:1), D2O = D_2O.

The results in Figure 4-16 showed also that the gt(+)-conformer along the sn-2,3 bond increased with the polarity of solvents increased. This tendency accorded with the preceding studies regarding the "gauche-effects" and may be associated some electron static effect around the vicinal oxygen atoms. It is also possible that hydration around the sugar surface, which is often called "glyco-layer," plays a major role in the notable conformational change.

e. Conformational property of *M. pneumonia* β-Gal lipids around the D-galactose C5-C6 bond.

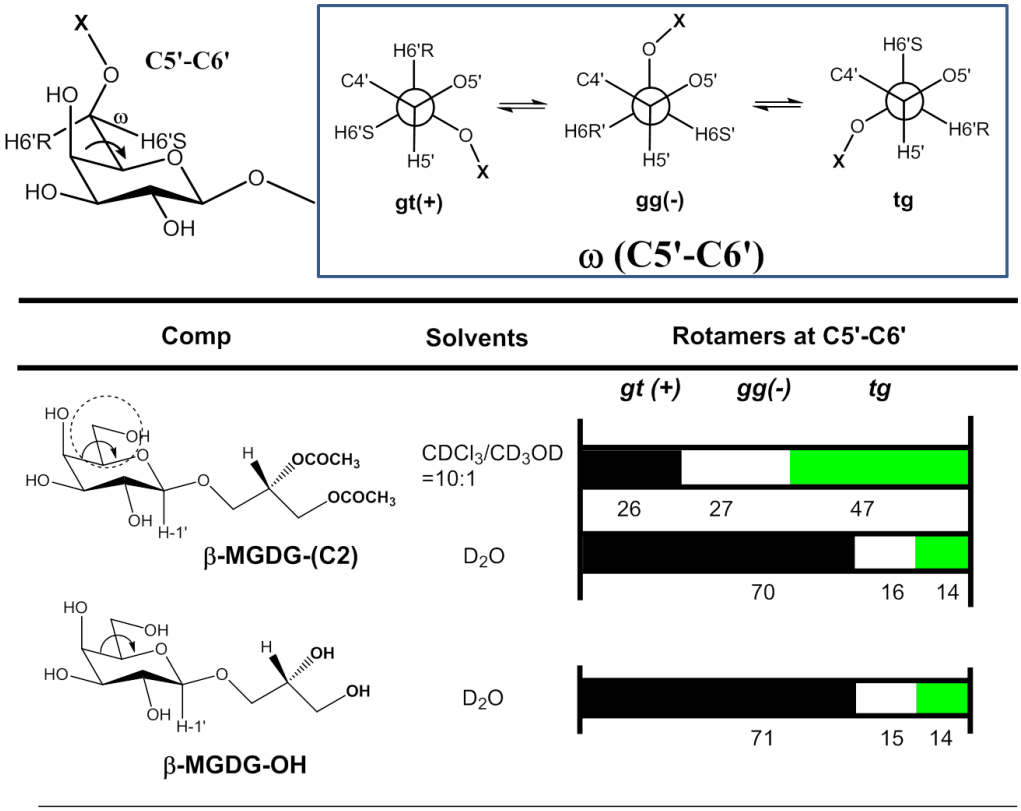

Figure 4-15. Conformational property of *M. pneumonia* β-Gal lipids around the D-galactose C5-C6 bond.

Also D-hexose C5-C6 bond gives rise to three staggering conformers. The conformational analysis around the exocyclic position has extensively been performed since Nishida et al.[20,30,] determined the preferred conformation of monosaccharides in solutions with an unequivocal evidence by deuterium labelling

and ^{1}H NMR spectroscopic analysis. In this study, the conformational property was examined for the *M. pneumonia* β-Gal lipids by using the water soluble C2 (Ac) homologues.

The analysis was performed in the same way as has just been cited above and was based on the ^{1}H NMR data being given in **Tables 4-2** and **4-3**. The prochiral H-6proR and H-6proS signals in D-galactose residue were discriminated unequivocally with (6S)-[6-2H]-D-galactose derivatives. [31,32]

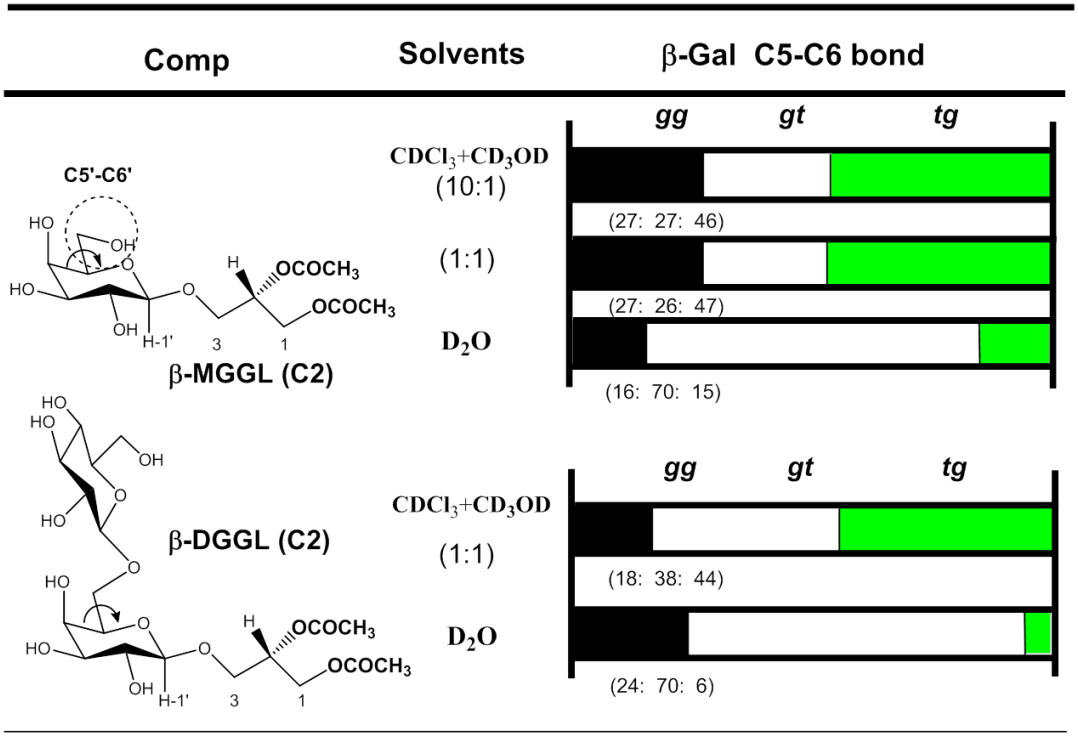

Figure 4-16. ^{1}H-NMR analysis of the *M. pneumonia* β-DGGL (Glc-type)

In a mixture of $CDCl_3$ and CD_3OD 10:1), the C5-C6 bond

favored the tg-conformation, while the conformational preference changed into gt(+) in wate solution. The drastic change is the same as what we have been in both D-galactose and D-GalNAc derivatives. A similar phenomenon was observed also in the ^{1}H-NMR analysis of the *M. pneumonia* β-DGGL (Glc-type, **Figure 4-16**). The β(1→6)-linkage strongly favored the clockwise-helical gt (+) (70%) rather than the other two conformers, gg(-) (25%) and tg (5%) in water (D_2O) solution.

The above conformational property has disclosed also such a unique 3D-structure of β-DGGL (Glc-type), in which the terminal D-Glc residue is folded back to the reducing end terminal (Figure 18) by adapting the clockwise-helical gt(+) conformation around the D-Gal C5-C6 bond.

4-5 Conclusion and Perspectives

The author has described a conformational analysis for a series of *Mycoplasma* glycolipids, whose absolute structures had been elucidated in our research group. *M. fermentans* GGPLs and *M. pneumonia* β-DGGLs.

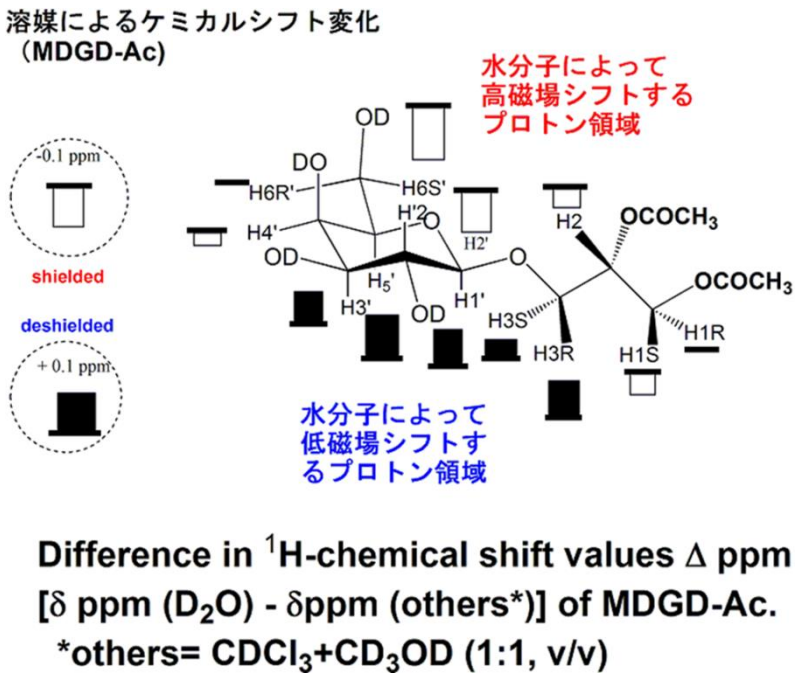

Figure 4-17. Difference in ^{1}H-chemical shift values of MDGD-Ac.

They have a common conformational property at the acyclic glycerol moiety; the lipid tail moiety prefer two *gauche*-conformations (*gg* and *gt*) in the order as *gt* > *gg* >> *tg*, while the sugar head moiety takes three conformers near equally (*gg* = *gt* = *tg*). At the tail position, *gt*-conformer with clock-wise helicity is predominated over anti-clockwise *gg*-conformer. The observed conformation was very close to what we have seen in DPPC. The coincidence allows us to assume that the Mycoplasma GGPLs may be able to constitute cytoplasm membranes in good cooperation with other phospholipids without affording any stereochemical stresses.

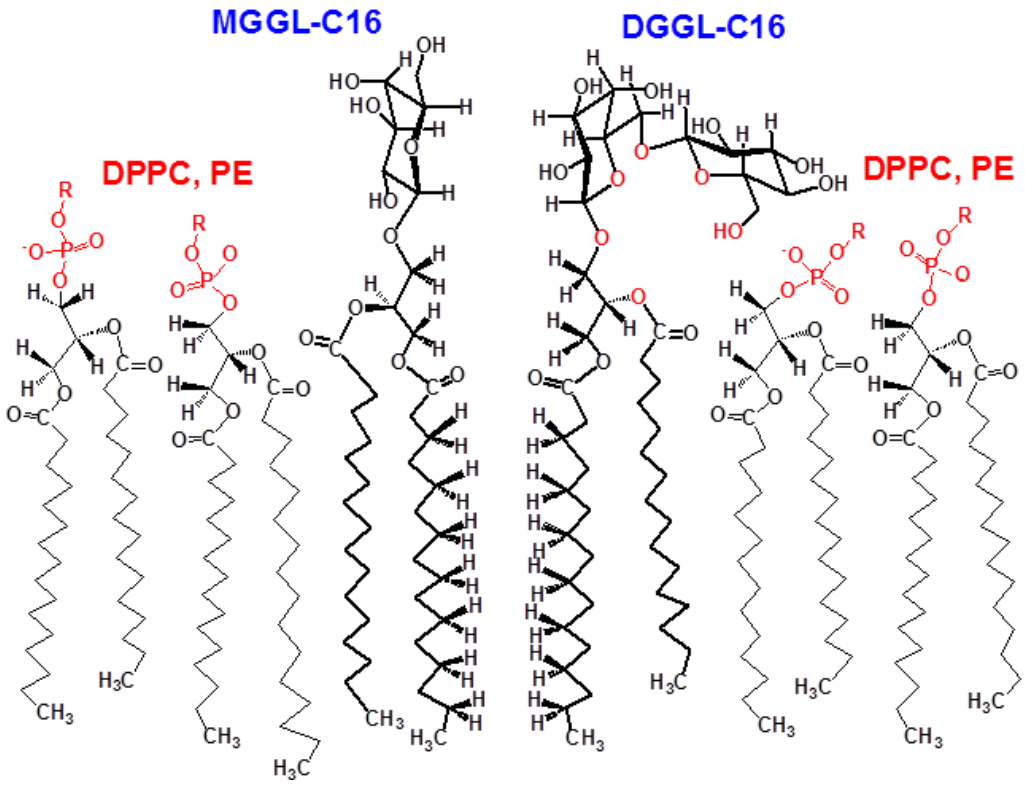

Figure 4-18. A possible role of GGLs in the *M. pneumonia* cytoplasm membrane.Molecular dynamic analysis with NMR spectroscopy supports that *M. pneumonia* GGLs can make a self-assembled micro-domain (raft) in cytoplasm membrane and construct "hydrophobic lipid pore" in it.

4-6 Experimental section (in preparation)

General Methods

Infrared (IR) spectra were recorded on a JASCO FT/IR-230 Fourier transform infrared spectrometer on the form of KBr disks. All ^{1}H NMR (500 MHz) spectra were recorded using Varian INOVA-500 or Varian Gemini 200. ^{1}H chemical shifts are expressed in parts per million (δ ppm) by using an internal standard of tetramethylsilane (TMS = 0.000 ppm). Mass spectra were recorded with a JEOL JMS 700 spectrometer for fast atom bombardment (FAB) spectra. Silica gel column chromatography was performed on silica gel 60 (Merck 0.063-0.200 mm and 0.040-0.063 mm). For purification of synthetic products, a column chromatography on Iatrobeads (IATRON LABORATORIES. INC., 6RS-8060) was applied. For thin layer chromatography (TLC) analysis, Merck pre-coated TLC plates (silica gel 60 F_{254}, layer thickness 0.25mm) and Merck TLC aluminum roles (silica gel 60 F_{254}, layer thickness 0.2mm) were used. All other chemicals were purchased from Tokyo Kasei Kogyo Co., Ltd., Kishida Chemical Co., Ltd., and Sigma - Aldrich Chemical Company Co, Int., and were used without further purification.

4-7 References and Notes

1. “Nomenclature of Lipids”, IUPAC-IUB Commision on Biochemical Nomenclature(CBN) (www.chem.qmul.ac.uk/iupac/lipid)

2. (a) Nishida, Y.; Uzawa, H.; Hanada, S.; Ohrui, H.; Meguro, H. Agric. Biol. Chem. 1989, 53, 2319-2323.

(b) Uzawa, H.; Nishida, Y.; Hanada, S.; Ohrui, H.; Meguro, H. Chem. Commun. 1989,862.

(c) Uzawa, H.; Nishida, Y.; Ohrui, H.; Meguro, H. J. Org. Chem. 1990, 55, 116-122.

3. Carrol, J. D., Chirality, 2009, 21, 354-358. “A new definition of life”.

4. Shimojima, M., Ohta, H., et al. Proc. Natl. Acad. Sci. USA, 1997, 94, 333-337.

5. Kelly, A. A., Froehlich, J. E., D¨ormann, P., Plant Cell, 2003, 15, 2694-2706.

6. Kobayashi, K., Kondo, M., Fukuda, H., Nishimura, M., Ohta, H., Proc Natl Acad Sci USA, 2007, 104,17216-17221.

7. Awai, K., Ohta, H., Sato, N., Proc. Natl. Acad. Sci. USA, 2014, 111(37), 3571-13575.

8. (a) Rottem, S. Biochem. Biophys. Acta 1980, 604, 65-90.

(b) Boggs, I. M. Biochim. Biophys. Acta 1987, 906, 353-404.

(c) Rawadi, G. Microbes and infection, 2000, 2, 955-964.

(d) Shimizu, T.; Kida, Y.; Kuwano, K. Immunology, 2004, 113, 121-129.

(e) Francisco, R.; Encarnacion, M.; Alfonso, R.-B.; Maria, J.-V. Current Microbiol. 2004, 48, 237-239.

9. Matsuda, K.; Tadano-Aritomi, K.; Ide-Tanaka, N.; Tomiyama, T.; Harasawa, R.; Shingu, Y.; Morita, D.; Kusunoki, S., Japanese J. Mycoplasmol., 2007, 34, 45-46.

10. Miyachi, A.; Miyazaki, A.; Shingu, Y.; Matsuda, K.; Dohi, H.; Nishida, Y. Carbohydr. Res., 2009, 344, 36-43.

11. Himmelreich, R.; Hibert, H.; Plagens, H.; Pirkl, E.; Li, B-C, Hermann, R. Nucl. Acids Res., 1996, 24, 4420-4449.

12. Dandekmar, T.; Huynen, M.; Regula, J. T.; Ueberle, B.; Zimmermann, C. U.; Andrade, M. A. et al., Nucl. Acids Res., 2000, 28, 3278-3288.

13. Klement, M. L. R.; Ojemyr, L.; Tagscherer, K. E.; Widmalm, G.; Wieslander, A., Molecular Microbiol., 2007, 65(6), 14444-1457.

14.(a) Hauser, H.; Guyer, W.; Levine, B.; Skrabal, P.; Williams, R.

J. P., Biochim. Biophys. Acta, 1978, 508, 450-463.

(b) Hauser, H.; Pascher, I.; Pearson, R.H.; Sundell, S. Biochim. Biophys. Acta, 1981, 650, 21-51.

15. Hauser, H.; Pascher, H.; Sundell, S., Biochemistry, 1988, 27, 9166-9174.

16. Koynova, R. D.; Kuttenreich, H. L.; Tenchov, B. G.; Hinz, H. J. Biochemistry 1988, 27, 4612–4619.

17. Mannock, D. A.; Lewis, R. N.; McElhaney, R. N. Chem. Phys. Lipids 1990, 55, 309-321.

18. Mannock, D. A.; Lewis, R. N.; McElhaney, R. N.; Akiyama, M.; Yamada, H.; Turner, D. C.; Gruner, S. M. Biophys J. 1992, 63, 1355–1368.

19. Ohrui, H.; Nishida, Y.; Watanabe, M.; Hori, H.; Meguro, H. (a) Tetrahedron Lett. 1985, 26, 3251-3254.

(b) Nishida, Y.; Hori, H.; Ohrui, H.; Meguro, H.; Uzawa, J.; Reimer, D.; Sinnwell, V.; Paulsen, H. Tetrahedron Lett. 1988, 29, 4461-4464.

(c)Hori, H.; Nishida, Y.; Ohrui, H.; Meguro, H.; Uzawa, J. Tetrahedron Lett. 1988, 29, 4457-4460.

20. Nishida, Y.; Hori, H.; Ohrui, H.; Meguro, H. J. Carbohydr. Chem. 1988, 7, 239-250.

21. Nishida, Y.; Tamakoshi,H.; Kobayashi,K.; Thiem, J. Org Lett., 2001, 3, 1-3.

22. Nishida, Y.; Shingu, Y.; Mengfei, Y.; Fukuda, K.; Dohi, H.; Matsuda, S.; Matsuda, K. Beilstein J. Org. Chem., 2012, 8, 629-639.

23. Haasnoot, C. A. G.; de Leeuw, F. A. A. M.; Altona, C., Tetrahedron 1980, 36, 2783-2790.

24. Ishida, N.; Irikura, D.; Matsuda, K.; Sato,S.; Sone, T.; Tanaka, M.; Asano, K. Curr. Microbiol. 2009, 58, 535-540.

25. Ishida, N.; Irikura, D.; Matsuda, K.; Sato, S.; Sono, T.; Tanaka, M.; Asano, K. J. Biosci. Bioeng. 2010, 109,341-345.

26. (a) Garbish Jr., E. W., J. Chem. Edu., 1968, 45 (5), 311.

(b) Stevenson, P. J. Org. Biomol. Chem., 2011, 9, 2078-2084.

27. Rockwell, G. D.; Grindley, T. B. J. Am. Chem. Soc., 1998, 120 (42), 10953-10963 “Effect of solvation on the rotation of hydroxymethyl groups in carbohydrates”

28. Wolfe, S. Acc. Chem. Res., 1972, 5, 102.

29. Duin,J.; Baas, J. M. A.; Graaf, B. J. Org. Chem., 1986, 51, 1298.

30. Nishida, Y.; Ohrui, H.; Meguro, H. Tetrahedron Lett., 1984, 25, 1575-1578.

31.Ohrui, H.; Nishida, Y.; Higuchi, H.; Hori, H.; Meguro, H. Can. J. Chem., 1987, 65, 1145.

32.(a) Nishida, Y.; Ohtaki, E.; Ohrui,H.; Meguro, H. J. Carbohydr. Chem.,1990,9,287.

(b) Ohrui,H.; Nishida, Y.; Itoh, H.; Meguro, H. J. Org. Chem., 1991, 56, 1726

Chapter 5

Concluding Remarks

Concluding Remarks

It is confusing and difficult to identify the mycoplasma-infected patient among those of incurable diseases. There is no straightforward method that is valid at an early stage in infection and appearance of MIDs symptoms. Glycolipid-antigen presentation (cellular immunity) specific characteristics, it is expected that synthetic lipid-antigens could be used as diangostic kits and Vaccines.

In chapter 2, the author described a practical synthetic pathway to GGPL-I homologue (C16:0) and its diastereomer, in which our one-pot α-glycosylation method was effectively applied. The synthetic GGPL-I isomers were characterized with 1H NMR spectroscopy to determine equilib ium among the three conformers (gg, gt, tg) at the acyclic glycerol moiety. The natural GGPL-I isomer was found to prefer gt (54 %) and gg (39 %) conformers around the lipid tail, while adopting all of the three conformers equally around the sugar position. This property was very close to what we have observed in the conformation of phosphatidylcholine (DPPC), suggesting that the Mycoplasma glycolipids GGPLs may constitute the cytoplasm fluid

membrane together with ubiquitous phospholipids without inducing stereochemical stress.

In Chapter 3, the author found that effects of sn-3 substituting groups are associated closely with the homologous solution state in methanol. The obtained effects will be changed widely by the solvents used and other surrounding conditions. The author recent interests are focused on roles of sn-3 O-glycosyl groups at the head in 1,2-di-O-acyl-sn-glycerols which possess a strong self-assembling property analogously phospholipids. Though situations will become more complicated than the present case, the approach undertaken here will work effectively towards solution of stereochemistry in these biomembrane forming 1,2-di-O-acyl-sn-glycerols.

In Chapter 4, the author describesd 1H-NMR analysis for a series of 1,2-di-O-palmitoyl-sn-glycerols carrying different functional groups at the sn-3 position. The functional group involved phosphocholine in DPPC and α- and ß-D-gluco or galactopyranosides in M. fermentans GGPL-I and M. pneumoniae β-DGGLs.

In the present NMR analysis, all of the methylene protons, i.e, HproR and HproS, at the sn-1 position was assigned

unequivocally on the basis of our previous 1H-NMR studies on chirally deuterium-labelled sn-glycerols and then used for the present conformational analysis. Time-averaged populations of three staggered conformers (gg, gt, and tg) were determined around the sn-1,2 bond. To examine an effect of acyl groups and solvents, we used also some acetyl-homologues in which the sn-1,2 palmitate was replaced with acetate (Ac) group.

The NMR analysis has shown that 1,2-dipalmitoyl-sn-glycerols adapt a conformation equilibrium between the two gauche-conformers of gt (40-60%) and gg (30-40%) around the 1,2-diacyl moiety.

Phospholipids adapted the clockwise-helical gt(+) more than the anti-clockwise gg(-) conformer. This tendency was kept in the M. fermentans α-glycolipids (GGPL-I) and the relating α-glucolipids, supporting our previous conclusion that the M. fermentans GGPL-I is able to construct a bio-membrane together with ubiquitous phospholipids.

The conformational property of the M. pneumonia β-galactolipids (β-DGGL) was apparently different from these phospholipids, suggesting that they may make a self-assembled

micro-domain being separated from phospholipid-based bilayer membranes.

In water solutions, the M. pneoumoniae ß-glycolipids showed a drastic change in preferred conformation at the head sn-2,3 position as well as the sugar C5'-C6' bond. The clockwise gt(+)-conformation was strongly preferred (>70%), and thus making such an ordered conformation in which a continuous hydrophobic region is expanding from the lipid tail into the sugar C5'-C6' terminal.

Publications

1） Mengfei Yuan, Hirofumi Dohi, Hirotaka Uzawa, and Yoshihiro Nishida. **Comparative analyses of helical property in asymmetric 1,2-di-O-acyl-sn-glycerols by means of ^{1}H NMR and circular dichroic (CD) spectroscopy: Notable effects of substituting groups at sn-3 position.** Tetrahedron: Asymmetry.(Accept)

2） Mengfei Yuan, Kazuo Fukuda, Hirofumi Dohi, and Yoshihiro Nishida.**^{1}H NMR spectroscopic analysis of helical property around lipid tail in 1,2-di-O-palmitoyl- sn- glycerols: Strong effects of solvents and sn-3 phosphate groups on inducement of right-handed (+)-helicity.**(In preparation)

3 ） Yoshihiro Nishida, Yuko Shingu, Yuan Mengfei, Kazuo Fukuda, Hirofumi Dohi, Sachie Matsuda and Kazuhiro Matsuda. **An easy α-glycosylation methodology for the synthesis and stereochemistry of mycoplasma α-glycolipid antigens.** *Beilstein J Org Chem*. 2012; 8:629-39.

4 ） Kazuhiro Matsuda, Mengfei Yuan, Kazuo Fukuda, Sachie

Matsuda, Yoshihiro Nishida. **Mycoplasma Lipid-antigens are Allergen or Vaccine?** (In preparation)

International Conferences

1）Mengfei Yuan, Ryoko Matsunaga, Hirofumi Dohi, Sachie Matsuda, Kazuhiro Matsuda, Yoshihiro Nishida.

Conformational properties of alpha- and beta- glycolipids as Mycoplasma cytoplasmic-membrane components

International symposium on Glycoconjugates（Glyco22）

2）Mengfei Yuan，Sachie Matsuda, Kazuhiro Matsuda, Yoshihiro Nishida. New Mycoplasma detection.

13th Conference On International Exchange Of Professionals，China

3）Mengfei Yuan，Kazuo Fukuda ,Yoshihiro Nishida, Sachie Matsuda，Kazuhiro Matsuda.

Synthetic glycolipid antigens (GGPLs and GGLs) for diagnosis of Mycoplasma infectious dieases

The 34th Japanese Carbohydrate Symposium, Tokyo

Acknowledgements

First of all, I would like to express my deepest gratitude to Professor Yoshihiro Nishida for helpful suggestions, continuous guidance and encouragement through this study.

I would like to express my sincere appreciation to Dr. Kazuhiro Matsuda (M. Biotech Inc.) for his helpful advises.

I greatly appreciate Assist. Professor Hirofumi Dohi for his helpful advises and kind guidance of analysis of NMR data.

I thank all the members of the Organic chemistry Laboratory for their kind help in supporting this research.

Finally, I would like to extend my great appreciation to my parents, Shudong Yuan and Lingli Wang for their continuous encouragement and spiritual supports through my research life.

July 2015